IAEA HUMAN HEALTH SERIES

No. 24

Dosimetry in Diagnostic Radiology for Paediatric Patients

IAEA
International Atomic Energy Agency

IAEA HUMAN HEALTH SERIES PUBLICATIONS

The mandate of the IAEA human health programme originates from Article II of its Statute, which states that the "Agency shall seek to accelerate and enlarge the contribution of atomic energy to peace, health and prosperity throughout the world". The main objective of the human health programme is to enhance the capabilities of IAEA Member States in addressing issues related to the prevention, diagnosis and treatment of health problems through the development and application of nuclear techniques, within a framework of quality assurance.

Publications in the IAEA Human Health Series provide information in the areas of: radiation medicine, including diagnostic radiology, diagnostic and therapeutic nuclear medicine, and radiation therapy; dosimetry and medical radiation physics; and stable isotope techniques and other nuclear applications in nutrition. The publications have a broad readership and are aimed at medical practitioners, researchers and other professionals. International experts assist the IAEA Secretariat in drafting and reviewing these publications. Some of the publications in this series may also be endorsed or co-sponsored by international organizations and professional societies active in the relevant fields.

There are two categories of publications in this series:

IAEA HUMAN HEALTH SERIES

Publications in this category present analyses or provide information of an advisory nature, for example guidelines, codes and standards of practice, and quality assurance manuals. Monographs and high level educational material, such as graduate texts, are also published in this series.

IAEA HUMAN HEALTH REPORTS

Human Health Reports complement information published in the IAEA Human Health Series in areas of radiation medicine, dosimetry and medical radiation physics, and nutrition. These publications include reports of technical meetings, the results of IAEA coordinated research projects, interim reports on IAEA projects, and educational material compiled for IAEA training courses dealing with human health related subjects. In some cases, these reports may provide supporting material relating to publications issued in the IAEA Human Health Series.

All of these publications can be downloaded cost free from the IAEA web site:

http://www.iaea.org/Publications/index.html

Further information is available from:

Marketing and Sales Unit
International Atomic Energy Agency
Vienna International Centre
PO Box 100
1400 Vienna, Austria

Readers are invited to provide their impressions on these publications. Information may be provided via the IAEA web site, by mail at the address given above, or by email to:

Official.Mail@iaea.org.

DOSIMETRY IN DIAGNOSTIC RADIOLOGY FOR PAEDIATRIC PATIENTS

The following States are Members of the International Atomic Energy Agency:

AFGHANISTAN
ALBANIA
ALGERIA
ANGOLA
ARGENTINA
ARMENIA
AUSTRALIA
AUSTRIA
AZERBAIJAN
BAHAMAS
BAHRAIN
BANGLADESH
BELARUS
BELGIUM
BELIZE
BENIN
BOLIVIA
BOSNIA AND HERZEGOVINA
BOTSWANA
BRAZIL
BRUNEI DARUSSALAM
BULGARIA
BURKINA FASO
BURUNDI
CAMBODIA
CAMEROON
CANADA
CENTRAL AFRICAN REPUBLIC
CHAD
CHILE
CHINA
COLOMBIA
CONGO
COSTA RICA
CÔTE D'IVOIRE
CROATIA
CUBA
CYPRUS
CZECH REPUBLIC
DEMOCRATIC REPUBLIC OF THE CONGO
DENMARK
DOMINICA
DOMINICAN REPUBLIC
ECUADOR
EGYPT
EL SALVADOR
ERITREA
ESTONIA
ETHIOPIA
FIJI
FINLAND
FRANCE
GABON
GEORGIA
GERMANY
GHANA
GREECE
GUATEMALA
HAITI
HOLY SEE
HONDURAS
HUNGARY
ICELAND
INDIA
INDONESIA
IRAN, ISLAMIC REPUBLIC OF
IRAQ
IRELAND
ISRAEL
ITALY
JAMAICA
JAPAN
JORDAN
KAZAKHSTAN
KENYA
KOREA, REPUBLIC OF
KUWAIT
KYRGYZSTAN
LAO PEOPLE'S DEMOCRATIC REPUBLIC
LATVIA
LEBANON
LESOTHO
LIBERIA
LIBYA
LIECHTENSTEIN
LITHUANIA
LUXEMBOURG
MADAGASCAR
MALAWI
MALAYSIA
MALI
MALTA
MARSHALL ISLANDS
MAURITANIA
MAURITIUS
MEXICO
MONACO
MONGOLIA
MONTENEGRO
MOROCCO
MOZAMBIQUE
MYANMAR
NAMIBIA
NEPAL
NETHERLANDS
NEW ZEALAND
NICARAGUA
NIGER
NIGERIA
NORWAY
OMAN
PAKISTAN
PALAU
PANAMA
PAPUA NEW GUINEA
PARAGUAY
PERU
PHILIPPINES
POLAND
PORTUGAL
QATAR
REPUBLIC OF MOLDOVA
ROMANIA
RUSSIAN FEDERATION
RWANDA
SAN MARINO
SAUDI ARABIA
SENEGAL
SERBIA
SEYCHELLES
SIERRA LEONE
SINGAPORE
SLOVAKIA
SLOVENIA
SOUTH AFRICA
SPAIN
SRI LANKA
SUDAN
SWAZILAND
SWEDEN
SWITZERLAND
SYRIAN ARAB REPUBLIC
TAJIKISTAN
THAILAND
THE FORMER YUGOSLAV REPUBLIC OF MACEDONIA
TOGO
TRINIDAD AND TOBAGO
TUNISIA
TURKEY
UGANDA
UKRAINE
UNITED ARAB EMIRATES
UNITED KINGDOM OF GREAT BRITAIN AND NORTHERN IRELAND
UNITED REPUBLIC OF TANZANIA
UNITED STATES OF AMERICA
URUGUAY
UZBEKISTAN
VENEZUELA
VIET NAM
YEMEN
ZAMBIA
ZIMBABWE

The Agency's Statute was approved on 23 October 1956 by the Conference on the Statute of the IAEA held at United Nations Headquarters, New York; it entered into force on 29 July 1957. The Headquarters of the Agency are situated in Vienna. Its principal objective is "to accelerate and enlarge the contribution of atomic energy to peace, health and prosperity throughout the world''.

IAEA HUMAN HEALTH SERIES No. 24

DOSIMETRY IN DIAGNOSTIC RADIOLOGY FOR PAEDIATRIC PATIENTS

INTERNATIONAL ATOMIC ENERGY AGENCY
VIENNA, 2013

COPYRIGHT NOTICE

Marketing and Sales Unit, Publishing Section
International Atomic Energy Agency
Vienna International Centre
PO Box 100
1400 Vienna, Austria
fax: +43 1 2600 29302
tel.: +43 1 2600 22417
email: sales.publications@iaea.org
http://www.iaea.org/books

Printed by the IAEA in Austria
December 2013
STI/PUB/1609

IAEA Library Cataloguing in Publication Data

Dosimetry in diagnostic radiology for paediatric patients. — Vienna : International Atomic Energy Agency, 2013.
p. ; 24 cm. — (IAEA human health series, ISSN 2075–3772; no. 24)
STI/PUB/1609
ISBN 978–92–0–141910–1
Includes bibliographical references.

1. Radiation dosimetry. 2. Pediatric diagnostic imaging. 3. Diagnostic imaging — Health aspects. I. International Atomic Energy Agency. II. Series.

IAEAL 13–00847

FOREWORD

Concern about the radiation dose to children from diagnostic radiology examinations has recently been popularly expressed, particularly as related to computed tomography (CT) procedures. This involves the observation that children can receive doses far in excess of those delivered to adults, in part due to the digital nature of the image receptors that may give no warning to the operator of the dose to the patient. Concern for CT examinations should be extended to the broad range of paediatric diagnostic radiological procedures responsible for radiation doses in children, especially as factors, such as increased radiosensitivity and the longer life expectancy of children, increase the associated radiation risk. In all cases, owing to the added paediatric radiological examination factor of patient size and its associated impact on equipment selection, clinical examination protocol and dosimetric audit, the determination of paediatric dose requires a distinct approach from adult dosimetry associated with diagnostic radiological examinations.

In response to this, there is a need to inform health professionals about standardized methodologies used to determine paediatric dose for all major modalities such as general radiography, fluoroscopy and CT. Methodologies for standardizing the conduct of dose audits and their use for the derivation and application of diagnostic reference levels for patient populations, that vary in size, are also required. In addition, a review is needed of the current knowledge on risks specific to non-adults from radiation, and also an analysis of the management of factors contributing to dose from paediatric radiological examinations.

In 2007, the IAEA published a code of practice, Dosimetry in Diagnostic Radiology: An International Code of Practice, as Technical Reports Series No. 457 (TRS 457). TRS 457 recommends procedures for dosimetric measurement and calibration for the attainment of standardized dosimetry, and addresses requirements both in standards dosimetry laboratories and clinical centres for radiology, as found in most hospitals. A coordinated research project was established in order to provide practical guidance to professionals at the Secondary Standards Dosimetry Laboratories (SSDLs) and to clinical medical physicists on the implementation of TRS 457, including the establishment of dosimetric measurement processes in clinical settings. Among the recommendations from the coordinated research project (see IAEA Human Health Reports No. 4, published in 2011) was the need for guidance on dosimetric standards and methodologies related to dosimetry for paediatric patients undergoing diagnostic radiology.

Following the recommendations of the advisory committee of the IAEA/World Health Organization SSDL network, known as the SSDL Scientific

Committee, a drafting group, consisting of P. Homolka (Austria), A. Fransson (Sweden), C.-L. Chapple (United Kingdom) and K. Strauss (United States of America), was appointed in 2010 to develop this publication to complement TRS 457. The contribution of the drafting group to writing this publication is gratefully acknowledged.

The IAEA officers responsible for this publication were H. Delis, I.D. McLean and W. van der Putten of the Division of Human Health.

CONTENTS

1. INTRODUCTION

1.1. FROM GENERAL TO SPECIFIC DOSIMETRY: PAEDIATRIC RADIOLOGY

The dosimetry for paediatric patients undergoing diagnostic radiology requires special consideration in addition to the general dosimetric methodologies used for adult patients. The reasons why paediatric dosimetry needs to be addressed as a specific area of study include:

— The importance of dosimetry for this patient group is more acute than for adults given their:
  • Longer life expectancy;
  • Higher risk from radiation: This increased risk is complex and is expressed through the relative radiosensitivity of various body tissues which vary with sex and age [1] (see Section 5).
— Data collection and analysis are complex, fundamentally due to the wide and continuous range of patient sizes present in the paediatric population.
— Paediatric patient examinations differ from adult examinations in many ways including:
  • Different technique factors, beam quality and ideally different radiological equipment;
  • Type of examinations performed;
  • The skill set of the staff necessary to perform these procedures successfully.
— Paediatric dosimetry requires different specialized phantoms and, in some cases, radiation measurement equipment, e.g. more sensitive air kerma area product (KAP) meters.
— There is relatively little dosimetric information available clinically on radiation doses and risks for common paediatric examinations, making decisions on risk assessment, which is essential for justification of examinations and consideration of alternative examinations, difficult.
— There is, generally, a marked lack of optimization of protection in paediatric radiographic examination procedures and the use of accurate, and reliable dosimetric information is an important prerequisite to successful optimization.

1.2. THE ROLE OF MEDICAL PHYSICISTS IN PAEDIATRIC DOSIMETRY

Compared to adult radiology, there are fewer paediatric radiology facilities worldwide (either in dedicated paediatric hospitals or in specific examination rooms in the general X ray department), so currently most paediatric radiology is performed in a mixed environment with adult radiology.

There is a general lack of medical physicists specialized in diagnostic radiology. Such medical physicists should have an understanding of the clinical examinations [2], which enables them to make the necessary measurements and interpretations for paediatric dose determination.

Paediatric dose levels have been shown to vary significantly for the same examination from facility to facility. This can be seen from the generation and analysis of dose audit data. Awareness arising from the results of such audits may lead to the modification of examination procedures and, in some cases, of equipment, to allow dose reduction.

Reduced paediatric radiation dose may be more difficult to achieve without a dedicated 'in-house' medical physicist due to the limited time that a consultant medical physicist may be contracted to be on site. The work of a dedicated medical physicist should include assessment of patient dosimetry and the optimization processes, in conjunction with radiologists and radiographers. This is necessary to manage radiation dose and to provide diagnostic image quality [3–5]. Managing dosimetry effectively is more involved than simple quality control measurements and should lead to a better knowledge of institutional patient dose values.

1.3. DOSIMETRY FORMALISM

The dosimetry formalism follows the general concepts introduced in Technical Reports Series No. 457 (TRS 457) [3] published by the IAEA. In general, measured air kerma is used as the basis for directly measured application specific quantities such as air kerma area product P_{KA} and entrance surface air kerma (ESAK) K_e. All other quantities are derived from these measured quantities using conversion coefficients with procedures described further in this section. The general equation for converting a reading M_Q of the dosimeter at a beam quality Q into an application specific dosimetric quantity K_Q is:

$$K_Q = M_Q N_{K,Q_0} \Pi k_i \tag{1}$$

where

N_{K,Q_0} is the calibration coefficient of the dosimeter at the reference beam quality Q_0;

and Πk_i is the product of the correction factors by means of which deviations between reference conditions and conditions of measurement are taken into account.

Every dosimetry measurement must consider accuracy. This is normally done through an uncertainty budget. This assesses the contributions from various components to the total uncertainty in the dose measurement. This is examined in some detail in Ref. [3], especially with respect to the instrumentation involved in measurement. Consideration should be given to both the clinical scenario for an individual dose determination and additional uncertainties involved in the determination of dose averages for typical clinical procedures, such as those arising from size variations and small sample sizes.

1.4. DOSIMETRY INSTRUMENTATION

Dosimeters may be either ionization chambers or semiconductor detectors conforming to the International Electrotechnical Commission (IEC) 61674 [6] specification with a traceable calibration under appropriate calibration conditions [7]. It is important to use a calibration coefficient appropriate for the clinical beam quality. Increasingly, beam qualities used for radiological examinations include filtrations that are not covered by IEC beam quality standards, particularly for equipment specifically used or designed for paediatric applications. Additional care should be taken when making measurements in beam qualities using dosimeters that have not been specifically calibrated for those qualities. As a first step, interpolation of the calibration factors with regard to half-value layer (HVL) can improve accuracy, especially for ion chambers. The situation for semiconductor detectors is more complex as these detectors have a much higher inherent energy dependence [8]. For this reason, it is important to measure the HVL of the radiation beams typically used in paediatric radiology for each X ray device. This may be done as part of routine quality assurance procedures, but the user should be aware of possible differences between beams used for paediatric and adult patients. The former may use significantly lower tube voltages and/or greater beam filtrations, depending on the type of equipment and local protocols. Advice should be sought, where necessary, from the calibration laboratory regarding interpolation of calibration factors to clinical

beam qualities, and appropriate contributions made to the associated uncertainty budget for the measurements.

The usefulness and limitations of different measurement devices are discussed in more detail in Section 2.

1.5. DOSIMETRY THROUGH DIGITAL IMAGING AND COMMUNICATIONS IN MEDICINE STRUCTURES

Increasingly, X ray equipment can supply parameters related to dose, that are usually displayed on the equipment console and also stored in Digital Imaging and Communications in Medicine (DICOM) structures. Examples of these include an estimation of air kerma area product P_{KA} that is not directly measured, similarly the interventional reference point kerma [9], that is related to an estimate of the entrance surface air kerma K_e, and computed tomography (CT) dose quantities, such as the volume CT dose index C_{VOL} and air kerma length product P_{KL}. Great care should be taken before these estimated parameters can be safely used to describe patient dose. Each parameter should be verified through independent direct measurement, where possible. This would normally occur during the commissioning of new equipment and would ideally be subject to follow-up verification periodically, particularly with software upgrades. Once the veracity of these parameters has been established, indicative dosimetric data could be used for dose audit purposes, provided they can either be identified within the DICOM header and access successfully gained through an automated data collection system, or recorded by clinical staff. In the future, patient dose should be provided through the Integrated Healthcare Enterprise radiation exposure monitoring profile[1].

1.6. CHARACTERIZATION OF PAEDIATRIC SIZE

In order to make meaningful comparisons of paediatric dosimetry information, it is important to compare patients of similar size using standard size ranges or a series of common reference sizes. This requires a commonly accepted and easily measurable metric. Most commonly used are a series of standard age groups or a small number of standard ages. However, these provide only a very broad indication of actual patient size, due to the large variations in

[1] DICOM Standard PS 3.16 (2009), http://wiki.ihe.net/index.php?title=Radiation_Exposure_Monitoring

both growth rate and obesity levels. In addition, average patient sizes might be expected to show significant variation between different countries, giving rise to a systematic bias in results. Other size metrics include directly measured patient parameters, such as weight, height or body thickness, and derived parameters, such as body mass index or equivalent diameter. These metrics are discussed in detail in Appendix I, along with the most commonly used paediatric age bands and reference ages.

Once a suitable metric has been determined, a method for analysing the data needs to be developed that enables data to be presented in a meaningful form and compared with other datasets. This is particularly important for the determination of, and comparison with, diagnostic reference levels (DRLs). For the establishment and use of DRLs, a sufficient number of patients at several discrete age or size groups is needed and this may not always be practical; a continuous 'DRL curve' can, in some cases, provide a more accurate and convenient solution [10]. Paediatric data analysis and interpretation are discussed in Section 4.

1.7. DOSE AUDIT AND ANALYSIS

Possibly the main reason for developing a knowledge of dosimetry for paediatric patients is for its application in the process of optimizing protection in the clinical environment. Since the dose to individual patients is subject to considerable variation, it is advisable to consider the dose to a population of similar patients. This process is called a dose audit and is discussed in detail in Section 3. The dose audit is more complex for paediatric radiology compared to adults, since the number of variables, especially those due to patient size, is greater. The results of an audit need to be analysed in such a way that useful information is provided to the user. One useful statistic is the distribution of dose values within one examination room or between different examination rooms or between different institutions. An extension of this analysis is to compare the results of a dose audit to recognized bench mark dose levels, such as DRLs[2] [11, 12] (see Section 4.2). While for many paediatric examinations it is true that existing DRL values are limited, it must be considered that the amount of DRL data is growing rapidly, and that other indicators, such as achievable doses[3] [13], are being developed. Another reason for undertaking a dose audit is to make a

[2] DRLs are typically based on the 75th percentile of a distribution of measured doses.

[3] The achievable dose may be set at the median (50th percentile) of the survey dose distribution.

determination of the risk of a procedure, perhaps in comparison to an alternative procedure. Section 5 deals with this question.

1.8. DOSE AND RISK FOR DIFFERENT MODALITIES OF IONIZING RADIATION

A recent study revealed that approximately 15% of all imaging studies performed in the United States of America (USA) involving ionizing radiation (interventional fluoroscopy, CT and cardiac nuclear medicine) deliver 85% of the total radiation dose delivered to patients, while other imaging studies (i.e. radiography and general fluoroscopy) deliver the remaining 15% [14]. This suggests that while the optimization principle should be applied to all examinations of paediatric patients, priority should be given to those examinations that deliver high doses. A study should concentrate not just on radiation dose but also on diagnostic outcome. This is discussed further in Section 6.

1.9. SCOPE OF PUBLICATION

This publication covers the material needed by medical physicists specialized in diagnostic radiology to provide an effective service to a radiology department involved in the radiological examination of paediatric patients. The material includes necessary information on dosimetric processes as well as a discussion on optimization strategies and organ dose, and the resulting risk. The introduction is followed by Section 2 on the formalism of dosimetry as applied specifically to paediatric patients. This section supplements Ref. [3] and, thus, follows the flow and terminology in that publication. Section 3 examines the process of taking a dose audit, while Section 4 addresses approaches to the analysis of audit data and particularly its relationship to patient size. The effect of size on DRL measurement and comparisons is also discussed, as are the size related dosimetric quantities for CT. Section 5 examines the steps involved in moving from simple dosimetric measurements to organ dose and the associated risk estimate that can be inferred from such processes. Section 6 discusses the equipment and optimization processes that need to be considered for optimal diagnostic outcome at reduced dose levels.

2. CLINICAL PAEDIATRIC DOSIMETRY MEASUREMENTS

2.1. INTRODUCTION

This section builds on the general dosimetric principles and methodologies found in TRS 457 [3] and extends this publication's application to paediatric patients, focusing on three key modalities. Despite dental radiology being an important area for paediatric dosimetry, due to the high frequency of paediatric dental X ray examinations, it is not considered in detail here as no additional comment on the methodology is needed to that described for adults in Ref. [3].

For each modality, the procedures for conducting phantom measurements are described first, followed by methodologies for measurements with patients. While a summary of basic dosimetry methodologies, as described in Ref. [3], is included here, particular attention is focused on areas of difference for paediatric dosimetry as outlined in Section 1. Worked examples and an analysis of experimental uncertainties are included for each modality, with appropriate work-sheets given in the Annex.

2.2. GENERAL CONSIDERATIONS

2.2.1. Types of dosimetric measurement

The recommendations of TRS 457 [3] are that dose measurements or determinations be made wherever possible, both with phantoms and patients. The use of a phantom enables repeatable, standardized measurements to be made, with a rapid evaluation of results. This is particularly useful for serial measurements on one piece of equipment (as in quality assurance tests) and also for making comparisons between different systems. Results are most meaningful when measurements are carried out under full or partial[4] automatic exposure control[5] (AEC) using clinical settings. To enable comparisons between centres, it is important that standardized phantoms are used. The adult phantoms described

[4] In some cases, the clinical protocol may require that the tube voltage be specified while still under AEC.

[5] AEC systems may also be known as 'automatic dose control', 'automatic dose rate control' and 'automatic brightness control'. The latter is often used for fluoroscopic examinations.

in Ref. [3] are inappropriate for dose assessment in paediatric radiology. The following sections make recommendations on suitable paediatric phantoms for each modality. A compromise has to be made between simulation of a wide range of patient sizes and keeping the number of measurements required within reasonable limits. A further balance has to be kept between good anatomical simulation and the simplicity and reproducibility of phantoms.

Since dose assessments on a phantom may not result in an accurate estimate of average dose for a specific patient group or indication of dose variations within the one examination observed in clinical practice, it is important to complement these with measurements and determination of dose for patients. Clinical measurements may also be made with solid state devices such as thermoluminescent dosimeters (TLDs) or optically stimulated luminescence (OSL) dosimeters. The main problem with TLDs is that there is typically a 0.1 mGy minimum absorbed dose to produce a reasonably accurate result. This is above most paediatric entrance surface air kerma K_e values. Thus, although such solid state detectors can be useful in phantom measurements, the use of these devices in paediatric dosimetry is not discussed in detail here. The interested reader is referred to Refs [6, 15] for a detailed discussion of TLD and OSL dosimetry.

The recommended dose quantities for patient dose are either incident air kerma, ESAK, air kerma area product or air kerma length product. A primary purpose of these measurements is to allow a clinical facility to compare patient dose measurements against a benchmark such as DRLs. The decision as to which dose quantity is most appropriate should be made according to the availability of the required measurement equipment and DRL values. Patient dose audit in paediatric radiology can be complex (see Section 3).

2.2.2. Kerma area product meters

KAP meters are among the most useful tools to measure patient dose. Their usefulness, of course, depends on accurate calibration. KAP meters should be calibrated in situ [15] and particular care must be taken to establish calibration factors at the appropriate clinical beam qualities, which usually vary with patient size. KAP meters exhibit significant energy dependence, and the effect of differences between the calibration and clinical beams must be included in the uncertainty budget. It is important to include the precision of the KAP meter in this budget, as individual KAP readings may be low for paediatric patients.

In practice, it is desirable to use a KAP meter with a digital resolution of 0.1 μGy·m^2 or better[6].

When calibrating a KAP meter in the field, care should be taken to specify the irradiation geometry, so that reproducible geometry can be used for subsequent calibrations. It should be noted that the recorded room temperature and pressure at the time of calibration can be used as a benchmark for temperature and pressure correction for future calibrations and measurement[7].

2.3. GENERAL RADIOGRAPHY

The principal dosimetric quantities for use in general radiography are incident air kerma, entrance surface air kerma and air kerma area product. Incident air kerma is measured for phantoms and is determined using recorded exposure parameters for patients. For patients, ESAK is typically determined from the incident air kerma with the application of the appropriate backscatter factor (BSF)[8], but may also be measured directly with a TLD [3] or derived from the P_{KA} measured using a KAP meter.

2.3.1. Phantom measurements

TRS 457 [3] recommends the use of CDRH (Centre for Devices and Radiological Health) phantoms for simulation of adult chest and abdomen [3]. These are inappropriate for the simulation of paediatric patients, and it is recommended that a number of phantoms varying in size be used instead as a basis for paediatric dosimetry. Simple phantoms of either polymethyl methacrylate (PMMA) or water are most easily obtained or manufactured, and the thickness can be adjusted to simulate patients of varying sizes. Suggested phantom dimensions and corresponding size equivalents are given in Table 1. These are abdominal equivalent phantoms, and no specific chest phantoms are recommended for paediatric dosimetry.

---

[6] It should be noted that care is needed when reading different KAP meters as the units in use are not standardized.

[7] The use of 'typical' temperature and pressure for a room is often the only practical way to make this required correction. The effect of this approach should be reflected in the budget of uncertainties.

[8] The BSF is generally smaller for paediatric rather than adult dosimetry, due primarily to the smaller field sizes used (see Appendix III).

TABLE 1. DETAILS OF RECOMMENDED PHANTOMS FOR PAEDIATRIC DOSIMETRY

Phantom dimensions		Corresponding patient demographics		
Approximate tissue thickness[a] (cm)	Polymethyl methacrylate thickness (cm)	Approximate weight (kg)	Approximate height (cm)	Approximate age (USA)
5	5	[b]	[b]	Preterm
10	10	4.7	56	Newborn
15	15	31	138	10 years

[a] 60–70 kV with varying filtrations.

[b] Not possible to quantify.

The same equipment used for measurement of incident air kerma, as given in Ref. [3] for adults, is used with paediatric phantoms. The diagnostic dosimeter should be calibrated for paediatric general radiography beam qualities and the phantom positioning and radiographic technique parameters should mimic clinical practice for the appropriate size of the patient. If clinical practice is to use AEC, care should be taken that the AEC detector is exposed appropriately.[9] Measurements should be carried out for abdomen protocols for each standard size. In the case of chest examinations, the AEC is usually only used for larger children, thus allowing the use of the central AEC detector. In this case, the abdominal phantoms (Table 1) can be used. If the central AEC detector is not used, phantom measurements are not recommended and patient based dosimetry should rather be used, as described in Section 2.3.2.

The following critical points should also be considered:

— For each phantom size and examination type, the phantom must be positioned according to the clinical protocol for that patient group, using a vertical or table Bucky as appropriate.
— Other factors that require care to ensure clinical accuracy are: the use of a grid, choice of filtration where adjustable, choice of focus to detector distance, and use of AEC detectors.
— The X ray field size for phantom measurements should be similar to the typical field size during clinical practice.

[9] It should be noted that the position of AEC detectors should be different for paediatric set-ups to account for the smaller size of the patient.

— The dosimeter must be placed at a sufficient distance from the phantom to avoid inclusion of backscatter, and should be positioned so as to avoid shadowing the AEC detector if possible. If the dosimeter needs to be moved off centre for this purpose, it should be shifted along a line perpendicular to the tube anode–cathode axis (which minimizes the contribution of the heel effect). The position of the dosimeter and phantom with respect to the tube focus must be recorded accurately (see fig. 3.2 of Ref. [3]).
— Exposures must represent clinical practice as far as possible, including use of AEC and/or pre-programmed factors. Where factors are selected manually, the equivalent size guide in Table 1 should be used to aid selection for exposure of the phantom.
— To avoid large uncertainties arising from the measurement of low dose levels, it may be appropriate to make three consecutive measurements without re-setting the dosimeter, and dividing by three to give the mean measured value for a single exposure.
— When using an ionization chamber, account of temperature and pressure conditions is necessary.

The HVL of each clinically used beam should be measured, taking care to ensure any variable filtration is accounted for. The methodology for HVL measurement is detailed in Ref. [3].

The air kerma $K(d)$ at the measurement point d is given by:

$$K(d) = \bar{M} N_{K,Q_0} k_Q k_{\mathrm{TP}} \tag{2}$$

where

$\bar{M}$ is the mean value of the dosimeter readings;
N_{K,Q_0} is the calibration factor of the dosimeter at beam quality Q_0;
k_Q is the correction factor for dosimeter response at the clinical beam quality Q compared to Q_0;

and k_{TP} is the correction factor (for ionization chamber dosimeters only) for temperature and pressure, as given by:

$$k_{\mathrm{TP}} = \left(\frac{273.2 + T}{273.2 + T_0}\right)\left(\frac{P_0}{P}\right) \tag{3}$$

Work-sheets for paediatric phantom measurements in general radiography are given in the Annex.

2.3.2. Patient dosimetry

For each patient, the incident air kerma K_i can be determined by calculation from recorded exposure parameters and the measured tube output. If the X ray machine is equipped with a suitable KAP meter, the air kerma area product P_{KA} can be recorded. As discussed in Section 2.2.1, the selection of K_i or P_{KA} as the dosimetry quantity is especially important in paediatric dosimetry. Assuming that a KAP meter is installed, the availability, reliability and currency of the appropriate DRL should be considered for the examination to be evaluated. Other factors that should be considered include the quantization error from the KAP reading[10], and the importance of identifying poor collimation practice that is possible from careful P_{KA} dosimetric analysis. The consideration of collimation requires great care. This is true for adult radiography, but is particularly so in paediatrics, where collimation is often much more difficult. The methodology for air kerma area product measurements is given in Section 2.4. The methodology for measuring tube output is given in Ref. [3].

For paediatric dosimetry, particular care is required in the collection of exposure factors and other technique data. Recommendations on types of examination, numbers of patients and required data are given and discussed in Section 3. It should be noted here, however, that an accurate measurement of focus skin distance (FSD), or otherwise both patient thickness and tube focus to patient support distance, should be made for each patient. If measurements are not an option, however, typical patient diameters can be obtained from height and weight (see Appendix I).

The incident air kerma is calculated from:

$$K_i = Y(d) P_{It} \left(\frac{d}{d_{FSD}} \right)^2 \quad (4)$$

where

$Y(d)$ is the X ray tube output measured at a distance d from the tube focus, for the particular tube voltage and filtration used for the patient exposure;

P_{It} is the tube loading (mAs)[11] for the patient exposure;

---

[10] Procedures, especially for young patients, that generate little KAP signal should be carefully evaluated.

[11] The 'tube loading' is the tube current–exposure time product (mAs) (i.e. the product of the X ray tube current (mA) and the exposure time (s)) that applies during a particular exposure.

and d_{FSD} is the tube focus to patient surface distance, which may be calculated from:

$$d_{FSD} = d_{FTD} - t_p \quad (5)$$

where

d_{FTD} is the tube focus to patient support distance;

and t_p is the thickness of the patient.

ESAK may be calculated from the incident air kerma by applying the appropriate BSF (see Appendix III):

$$K_e = K_i B \quad (6)$$

An example of the determination of uncertainties for typical entrance surface dose measurements is given in Table 2.

Work-sheets for paediatric patient measurements in general radiography are given in the Annex, including both standard work-sheets in the format from Ref. [3], and a 'clinical' work-sheet that may be used by radiographic staff collecting patient data.

2.4. FLUOROSCOPY

The principal dosimetric quantities for use in fluoroscopy are the ESAK rate and the P_{KA}. Some fluoroscopy equipment will also display cumulative air kerma (in grays) which is an estimate of cumulative skin dose [15]. This quantity is relevant to deterministic skin damage. This is not expected to be of major concern in paediatrics and will not be further discussed. The ESAK rate is measured with phantoms, while for patients, the P_{KA} is measured using a calibrated KAP meter. The X ray equipment may also have a computational method to determine P_{KA}, when its calibration should be verified by measurements with a calibrated KAP meter (or, as before TRS 457 [3], with a calibrated ion chamber).

2.4.1. Phantom measurements

The ESAK rate can be measured using the same PMMA phantoms of varying thicknesses, as described above for paediatric general radiography (Table 1). This is analogous to the PMMA phantoms recommended for adult

TABLE 2. UNCERTAINTIES FOR GENERAL RADIOGRAPHY MEASUREMENTS

	Scenario A	Scenario B	Scenario C
Description of scenario	Determination of K_i using dose output measurements, corrections applied	Practical method; as in scenario A, no manual corrections applied	Measurement of P_{KA} during patient exposure, no corrections applied
Uncertainty (k = 2) in dosimetric quantity due to:			
Intrinsic error of dosimeter	3.2%	3.2%	>3.2%[a] [3]
Calibration coefficient N_{K,Q_0}	1.6%	1.6%	1.6%
Long term stability of dosimeter reading	1%	1%	1%
Difference in beam qualities between calibration and clinical use	1%	5%	>20% [3]
In situ calibration of P_{KA} chamber	N/A	N/A	7.5%
Field size/field inhomogeneity	2%	2%	5%
Focus skin distance	4%	10%	—
Focus detector distance and scatter influence at dose output measurement	3%	3%	—
X ray output accuracy: Patient exposure Output measurement (three exposures)	5% 2.9%	5% 2.9%	—
Air density correction: Pressure Temperature	0.2% 0.5%	2% 2%	2% 5% [3]
Electromagnetic compatibility and humidity; other uncertainties estimated <1% each	2%	2%	2%
Combined expanded (2σ) uncertainty in K_i or P_{KA}	9%	14%	>23%
	Determination of K_e		
Backscatter factor	5%	20%	
Expanded (2σ) uncertainty in K_e	10%	24%	

[a] This could be as high as 50% for measuring low values on a KAP meter with low digital resolution, and should be individually assessed for each situation.

fluoroscopy in Ref. [3]. If the detector does not respond to backscattered radiation (e.g. semiconductor detectors with shielding on the exit surface), the entrance air kerma rate must be determined by applying an appropriate BSF to the measured incident air kerma rates.

The equipment used for measurement of entrance air kerma rates for adults, as given in Ref. [3], is also suitable for paediatric phantoms. The diagnostic dosimeter should be calibrated for clinical paediatric fluoroscopic beam qualities and the selected protocol should mimic clinical practice for the appropriate size of patient. Adjustable parameters could include the AEC setting, intensifier field size, fluoroscopic pulse width and/or pulse rate, and air kerma rate to the image receptor. The following points, in particular, should be noted:

— The dosimeter must be placed in contact with the phantom, at the X ray beam entrance surface, with the set-up appropriate for the beam geometry in use clinically (over couch/under couch/lateral). The tube focus to image receptor and focus to dosimeter distances must be measured accurately.
— Exposures must represent clinical practice as far as possible, including use of AEC, and the use of a grid and/or pre-programmed technique factors. Where some factors (e.g. tube voltage) are selected manually, the equivalent size guide in Table 1 should be used to aid selection for exposure of the phantom.
— The field size used should mimic that used clinically for the appropriate patient size. Typical values are given in Section 3, Table 7 on p. 28.
— It should be ensured that the AEC system has stabilized before making a measurement, and measurements should be repeated to give a total of three values.
— When using an ionization chamber, readings should be taken of temperature and pressure.

The ESAK rate is given by:

$$\dot{K}_{\mathrm{e}} = \overline{\dot{M}} N_{K,Q_0} k_Q k_{\mathrm{TP}} \tag{7}$$

where

$\overline{\dot{M}}$ is the mean value of the dosimeter readings;
N_{K,Q_0} is the calibration factor of the dosimeter at beam quality Q_0;
k_Q is the correction factor for dosimeter response at the clinical beam quality Q compared to Q_0;

and k_{TP} is the correction factor (for ionization chamber dosimeters only) for temperature and pressure, as given by:

$$k_{TP} = \left(\frac{273.2+T}{273.2+T_0}\right)\left(\frac{P_0}{P}\right) \tag{8}$$

If PMMA phantoms are used, an additional correction needs to be made to allow for the difference in BSF between water and PMMA. In this instance, the equation for the ESAK rate becomes:

$$\dot{K}_e = \bar{\dot{M}} N_{K,Q_0} k_Q k_{TP} \frac{B_w}{B_{PMMA}} \tag{9}$$

where B_w and B_{PMMA} are the BSFs for water and PMMA, respectively, under the measurement conditions.

It can be shown that B_w/B_{PMMA} is reasonably independent of energy with a slight field size dependence. A general value of 0.93 can be assumed with an error over the field size and energy of about 2%, with a value of 0.94 for a 10 cm^2 field, falling to 0.92 for a 25 cm^2 field. It is appreciated that the error involved in the measurement of the ESAK rate would be significantly in excess of the error due to the backscatter correction for material.

Work-sheets for paediatric phantom measurements in fluoroscopy are given in the Annex.

2.4.2. Patient measurements

Measurement of P_{KA} using a transmission ionization chamber (KAP meter) is recommended for monitoring patient exposures for examinations involving fluoroscopy (see Section 2.2.2). KAP readings, along with patient and examination details, should be taken for a series of paediatric patients for each examination type under investigation. Recommendations for patient and examination selection are given in Section 3. The air kerma area product is calculated for each patient as:

$$P_{KA} = M N_{P_{KA},Q_0} k_Q k_{TP} \tag{10}$$

where

M is the KAP meter reading;

N_{P_{KA},Q_0} is the calibration factor of the dosimeter at beam quality Q_0;
k_Q is the correction factor for dosimeter response at the clinical beam quality Q compared to Q_0;

and k_{TP} is the correction factor for temperature and pressure (see Section 2.2.2).

$$k_{TP} = \left(\frac{273.2 + T}{273.2 + T_0}\right)\left(\frac{P_0}{P}\right) \tag{11}$$

Work-sheets for paediatric patient measurements in general fluoroscopy are given in the Annex, including both standard work-sheets in the format from Ref. [3] and a 'clinical' work-sheet that may be used by radiographic staff collecting patient data.

An example of the determination of uncertainties for typical fluoroscopy dose measurements is given in Table 3.

2.5. COMPUTED TOMOGRAPHY

The principal dosimetric quantities for use in CT are the CT air kerma indices $C_{a,100}$[12] and C_W ($CTDI_W$). A further CT air kerma index C_{VOL} ($CTDI_{VOL}$) is derived from C_W for particular patient scan parameters. Patient doses for a complete examination are described in terms of the CT air kerma length product $P_{KL,CT}$ (dose length product (DLP) in IEC terminology) (see Table 4 for comparison of IAEA and IEC definitions[13]). For paediatric dosimetry, the use of a displayed computed tomography dose index (CTDI) will most probably underestimate the dose to the patient when compared to the case for adults. This is because the display (console value) of the CT scanner is usually calibrated with measurements in a 32 cm diameter phantom, except for head CT. If specific paediatric protocols are available, the calibration of the console can be either with a 32 cm diameter phantom or (more usually) with a 16 cm diameter phantom, but even the latter will lead to underestimation for very small children [16]. This critical point is further discussed in Section 4.4.1.

[12] It should be noted that $C_{a,100}$ is not used in standard CT dosimetry but has application in the determination of organ doses and quality control processes.

[13] IEC definitions of CTDI are based on the use of an ionization chamber with a dose integration length of 100 mm [16]. The CTDI is a dose index and should not be interpreted as a patient dose.

TABLE 3. UNCERTAINTIES FOR FLUOROSCOPY MEASUREMENTS

Uncertainty ($k = 2$) in dosimetric quantity due to:	Scenario 1 Determination of entrance surface air kerma rate $\dot{K}_e$ using a phantom, applying air density and beam quality correction	Scenario 2 Determination of entrance surface air kerma rate $\dot{K}_e$ using a phantom, no manual corrections applied	Scenario 3 Measurement of P_{KA} during patient fluoroscopy, P_{KA} chamber calibrated in situ
Description of scenario			
Intrinsic error of dosimeter	3.2%	3.2%	>3.2%
Calibration coefficient N_{K,Q_0}	1.6%	1.6%	1.6%
Long term stability of dosimeter reading	1%	1%	1%
Difference in beam qualities between calibration and clinical use	3%	6%	>20%
Field size/field inhomogeneity	2%	2%	5%
Distance measurements and correction	4%	4%	—
Scatter radiation	3%	3%	—
Kerma rate[a]	5%	5%	5% or greater
In situ calibration of P_{KA} chamber	N/A	N/A	7.5%
Difference in table attenuation compared to in situ calibration point due to varying beam hardness (under couch systems)	N/A	N/A	15%
Air density correction: Pressure Temperature	0.2% 0.5%	2% 2%	2% 5%
Electromagnetic compatibility and humidity; other uncertainties estimated <1% each	2%	2%	2%
Backscatter factors	5%	5%	N/A
Combined expanded (2σ) uncertainty in K_e or P_{KA}	10%	12%	24%

[a] Instruments should be checked for the range of dose rates over which their calibration is valid, and an appropriate uncertainty determined.

TABLE 4. COMPARISON OF IAEA AND INTERNATIONAL ELECTROTECHNICAL COMMISSION DOSIMETRY TERMINOLOGY USED IN COMPUTED TOMOGRAPHY

Quantity	IAEA	International Electrotechnical Commission
Measured free-in-air:		
Computed tomography air kerma index	$C_{a,100} = \frac{1}{N \cdot T} \int_{-50}^{+50} K(z)\, dz$	$CTDI_{air} = \frac{1}{N \cdot T} \int_{-\infty}^{+\infty} K_a(z)\, dz$
Measured in standard phantom:		
Weighted computed tomography air kerma index	$C_W = \frac{1}{3}(C_{PMMA,100,c} + 2C_{PMMA,100,p})$	$CTDI_W = 1/3 CTDI_{100,c} + 2/3 CTDI_{100,p}$
Normalized weighted computed tomography air kerma index	${}_nC_W$	${}_nCTDI_W$
Volume computed tomography air kerma index	C_{VOL}	$CTDI_{VOL}$
Computed tomography air kerma length product	$P_{KL,CT} = \sum_j {}_n C_{VOL_j} l_j P_{It_j}$	$DLP = CTDI_{VOL} L$

It is also essential that the CTDI or DLP[14] definition be consistent with the definition used for the relevant DRL (see Sections 4.2 and 4.4).

2.5.1. Phantom and free-in-air measurements

CT air kerma indices $C_{a,100}$ and C_W are measured with a calibrated pencil ionization chamber. The chamber should be calibrated for the tube voltage used clinically for paediatric patients (this may routinely be lower than 120 kV in some centres). $C_{a,100}$ is measured free-in-air, and C_W, to simulate a paediatric

[14] DLP is the preferred indicator for examinations as it accounts for the scan length, over scanning and the number of series in an examination.

body, should be measured in the standard CT head phantom[15] (16 cm diameter). It is recognized that even this phantom size may be significantly larger than some paediatric patients, and a methodology for converting measurements to values in a different size phantom is discussed in Section 4. The measurement protocol is detailed in Refs [3, 16] and should be followed with the following points noted:

— Care needs to be taken to make measurements for clinically relevant paediatric settings (tube voltage, slice widths, field of view (FOV), focal spot size[16], etc.).
— If the pencil chamber is calibrated in terms of milligrays rather than milligray centimetres (mGy·cm), the value of the dosimeter reading must be multiplied by a factor of 10 cm (corresponding to the length of the chamber). Measurements must be made for a single rotation of the X ray tube with no couch movement. The ease with which this may be done depends on the particular type of scanner. If engineers' mode can be accessed, this may prove most convenient; otherwise, an axial/sequential protocol must be selected. All scanners will have a high resolution chest protocol using sequential mode, and usually sequential head and abdomen protocols; the number of slices must be set to one and the increment or couch movement to zero. It should be pointed out that, depending on scanner type, the set-up and use of single axial slices can be difficult, especially as most clinical protocols are spiral (helical) scans.
— Ionization chamber readings must be corrected for temperature and pressure.

The air kerma indices are calculated according to the following equations. For measurements in air:

$$C_{\mathrm{a},100} = \frac{1}{N \cdot T} \bar{M} N_{P_{\mathrm{KL}},Q_0} k_Q k_{\mathrm{TP}} \tag{12}$$

[15] A 10 cm diameter phantom for the paediatric head is used by some workers; however, at this stage, the 16 cm phantom is recommended for consistency with existing dosimetry data.

[16] $\mathrm{CTDI}_{\mathrm{air}}$ can change fairly significantly with focal spot size for some scanners. As focal spot size is automatically selected, according to the FOV and tube current, there may be a requirement to make measurements at both focal spot sizes and record this parameter with clinical data.

and the normalized value:

$$ {}_{\mathrm{n}}C_{\mathrm{a},100} = \frac{C_{\mathrm{a},100}}{P_{\mathrm{It}}} \tag{13} $$

where

$\bar{M}$ is the mean value of the dosimeter readings for a single rotation of the X ray tube;
$N{\cdot}T$ is the nominal beam width in a single rotation with $N = 1$ for single slice scanners;
P_{It} is the tube loading (mAs) for that single rotation;
N_{P_{KL},Q_0} is the calibration factor of the dosimeter at beam quality Q_0;
k_Q is the correction factor for dosimeter response at the clinical beam quality Q compared to Q_0;

and k_{TP} is the correction factor (for ionization chamber dosimeters only) for temperature and pressure, as given by:

$$ k_{\mathrm{TP}} = \left(\frac{273.2+T}{273.2+T_0}\right)\left(\frac{P_0}{P}\right) \tag{14} $$

For measurements made in the head phantom, central and peripheral values are calculated and combined as follows to give C_{W} and the normalized ${}_{\mathrm{n}}C_{\mathrm{W}}$:

$$ C_{\mathrm{PMMA},100,\mathrm{c}} = \frac{1}{N\cdot T}\bar{M}_{\mathrm{c}}N_{P_{\mathrm{KL}},Q_0}k_Q k_{\mathrm{TP}} \tag{15} $$

$$ C_{\mathrm{PMMA},100,\mathrm{p}} = \frac{1}{N\cdot T}\bar{M}_{\mathrm{p}}N_{P_{\mathrm{KL}},Q_0}k_Q k_{\mathrm{TP}} \tag{16} $$

$$ C_{\mathrm{W}} = \frac{1}{3}\left(C_{\mathrm{PMMA},100,\mathrm{c}} + 2C_{\mathrm{PMMA},100,\mathrm{p}}\right) \tag{17} $$

where subscripts c and p denote measurements in the centre and periphery of the phantom, respectively.

$$ {}_{\mathrm{n}}C_{\mathrm{W}} = \frac{C_{\mathrm{W}}}{P_{\mathrm{It}}} \tag{18} $$

It has been demonstrated that the above CT kerma quantities, such as C_{W}, based on the use of a 100 mm pencil chamber and a 15 cm CT dose phantom,

lose viability for nominal beam widths that exceed 40 mm. In this case, C_W can be determined using the following formulation[17]:

$$C_{W,N\cdot T} = C_{W,Ref} \times \frac{C_{a,100,N\cdot T}}{C_{a,100,Ref}} \quad (19)$$

where

$C_{W,N\cdot T}$ is the weighted CT air kerma index for a nominal beam width of $N\cdot T$ mm (if $N\cdot T$ is >40 mm);

$C_{W,Ref}$ is the weighted CT air kerma index for a reference beam width of 20 mm (or closest possible value below 20 mm);

$C_{a,100,N\cdot T}$ is the CT air kerma index measured free-in-air for a beam width of $N\cdot T$ mm;

and $C_{a,100,Ref}$ is a similar quantity at the reference beam width.

The methodology used to measure $C_{a,100,N\cdot T}$ can be found in recent publications [16].

Work-sheets for paediatric phantom measurements in CT are given in the Annex. An example of the determination of uncertainties for CT dose measurements in CT is given in Table 5.

2.5.2. Patient dosimetric data assessment

No direct measurements are made on patients for CT examinations, but two further dose quantities, C_{VOL} and air kerma length product $P_{KL,CT}$, are derived from the air kerma indices described above and technique data for individual patients. Technique data that should be collected are detailed in Table 6, as different interpretations for some parameters are used for different scanner types.

C_{VOL} is given by:

$$C_{VOL} = {}_nC_W P_{It} \frac{N\cdot T}{L} \quad (20)$$

[17] Measurements of C_W using a 100 mm pencil chamber do not capture the extended scatter dose tails within or external to the phantom [17–19] that are independent of the nominal beam width and can exceed 20%. These are not addressed by the correction factors shown in Eq. (19).

or

$$C_{\mathrm{VOL}} = {}_{\mathrm{n}}C_{\mathrm{W}}P_{\mathrm{It,eff}} \tag{21}$$

where $P_{\mathrm{It,eff}}$ (effective mAs) is given.

TABLE 5. UNCERTAINTIES FOR COMPUTED TOMOGRAPHY MEASUREMENTS

Influence quantity	Uncertainty (%) $k = 1$
Intrinsic error $N_{K,Q}$	3.2
Radiation quality	0.5 (higher for solid state dosimeters)
Kerma rate	0.5
Direction of radiation incidence	1.0
Air pressure	0.5
Temperature and humidity	0.5
Electromagnetic compatibility	1.5
Field size/field homogeneity	1.0
Operating voltage	1.2
Long term stability of user's instrument	0.5
Precision of reading	0.6
Precision of tube loading indication	1.0
Precision of chamber/phantom positioning in the centre of the gantry	0.3
Uncertainty of 1 mm in phantom diameter and 0.5 mm in depth of measurement bores	0.35
Uncertainty in chamber response for in-phantom measurements (C_{W} only)	3.0
Relative combined standard uncertainty ($k = 1$) for $C_{\mathrm{a,100}}$	3.5
Relative expanded uncertainty ($k = 2$) for $C_{\mathrm{a,100}}$	7.0
Relative combined standard uncertainty ($k = 1$) for C_{W}	4.6
Relative expanded uncertainty ($k = 2$) for C_{W}	9.2
Displayed values of C_{VOL} and dose length product P_{KL}	20% if not calibrated

TABLE 6. PARAMETERS TO BE RECORDED FOR ASSESSMENT OF PATIENT DOSE IN COMPUTED TOMOGRAPHY

Parameter to be recorded	Notes on interpretation of parameter
Tube voltage (kV)	
P_{It} (mAs)/rotation or $P_{\mathrm{It,eff}}$ (effective mAs)	Effective mAs incorporates pitch.
Couch increment l or helical pitch	Manufacturers can use varying definitions of pitch. For dosimetry, pitch is defined as the distance moved by the couch divided by nominal slice width. The parameter is not required if effective mAs is recorded.
Acquisition slice width setting $N \cdot T$	For example, a four slice scanner $N \cdot T$ could be 4 × 1 mm or 4 × 5 mm, etc. This should not be confused with the reconstructed slice width which may be different.
Total tube loading (mAs) $P_{\mathrm{It,tot}}$ is the total mAs for each series	Should not include scan projection radiograph mAs, but should be actual rather than maximum or projected mAs where possible. This is not supplied by all scanner types, so may need to be calculated from total scan time or scan length.

Air kerma length product is given most simply by:

$$P_{\mathrm{KL,CT}} = {}_{\mathrm{n}}C_{\mathrm{W}} P_{\mathrm{It,tot}} N \cdot T \tag{22}$$

or, where total mAs is not given, by:

$$P_{\mathrm{KL,CT}} = {}_{\mathrm{n}}C_{\mathrm{W}} P_{\mathrm{It,eff}} L \tag{23}$$

where L is the total scan length including over-ranging.

Collected patient data should be recorded using the appropriate work-sheets in the Annex.

Displayed values of C_{VOL} ($\mathrm{CTDI}_{\mathrm{VOL}}$) and $P_{\mathrm{KL,CT}}$ (DLP) may usefully be recorded and should be compared to calculated values to ensure correct evaluation, especially in conjunction with tube current modulation. In this case, post-scan values must be used. However, these displayed quantities (which are based on internal machine calculations) must not be collected in isolation unless their calibration has been checked across the full range of clinical protocols.

3. PAEDIATRIC DOSE AUDIT

3.1. AIM OF PAEDIATRIC DOSE AUDITS

There are a number of reasons for carrying out a paediatric dose audit that may include the following:

— The IAEA Basic Safety Standards [4] have the inherent requirement that patient dosimetry be performed.
— To determine the distribution of dose values for a particular examination.
— To assess the appropriate usage of equipment with respect to defined protocols[18].
— To provide input to and comparison with local or national DRLs (see Section 4.2) or, where these do not exist, international values.
— To set local DRLs: The intention should be to gather enough data to provide representative dose values for a number of typical examinations and for a range of patient sizes, appropriate to the department in question.
— To determine the radiation risk of a certain procedure when compared to an alternative procedure.

3.2. GENERAL CONSIDERATIONS

It is important to use appropriately calibrated instruments. If these are not available, the dose audit will only be able to supply comparative data between different techniques at the same establishment. If a dose audit is carried out over a period of several months using a KAP meter, the calibration of the KAP meters should be confirmed at the beginning and end of the study period and, preferably, at appropriate intervals in between. The calibration of the displayed $CTDI_{VOL}$ and DLP on CT scanners should also be measured at the previously described intervals.

Before an audit is undertaken, the following points should be considered:

— That appropriate periodic quality assurance tests on equipment have been carried out to rule out equipment problems.

[18] In this case, a more limited number of patients may be sufficient for a protocol check rather than a full audit.

— The skill profile of the radiographic staff: Are any staff members highly trained paediatric radiographers? Do staff rotation patterns in the area cause the skill profile to vary, e.g. normal working hours versus nights, weekends or holidays?
— Whether examination protocols for all possible age groups are in existence for the examinations that need to be performed; and whether these protocols are routinely used by staff.
— A dose audit will only be successful if carried out with the full cooperation of clinical and technical staff. Staff operating the equipment, and those responsible for clinical governance in the area, should be included in planning discussions, and should receive the results of the dose audit.
— The maximum recommended period of time for data collection is 3–6 months. (This does not prevent a further extension of the audit being carried out at a later date, following analysis of the initial data.) Motivation will be lost if the time period is too long. Too short a measurement period will not result in an adequate amount of data.
— Generic work-sheets (examples are provided in the Annex) should be adapted for local equipment and protocols. It is essential that staff completing work-sheets understand fully what is required and what the varying parameter descriptors mean[19]. It should be noted that examination names and other terminology vary from country to country.
— The collection of dosimetric data from DICOM structured reports associated with a patient examination is very appealing as it provides a rapid method of collecting data. However, additional knowledge may be necessary to convert the DICOM data to established dosimetric forms, and not all manufacturers currently make full use of the available DICOM structures. Required patient data, if restricted to the age of the patient, may limit the analysis of such data in the paediatric setting. In this case, supplementary patient size data (such as height and weight) may need to be gathered manually. As new DICOM data fields become available, this process will be simplified.
— A paediatric dose audit can be a complex and lengthy task that covers a wide range of parameters in order to be valid. It is not always possible to be completely prescriptive in outlining audit techniques, as these may be influenced by local factors.

[19] In practice, it may be advisable to convert some of the standard nomenclature used here to more common local terms, e.g. mAs instead of P_{It}, as has been done in the 'clinical' forms in the Annex.

3.3. SELECTION OF PATIENTS

Reference [3] makes no recommendations regarding the number or various sizes of patients required for data collection. However, the sample size should be large enough to avoid statistical fluctuations caused by a small number of patients. Variation in measured doses can be particularly large if the sample contains a wide range of patient sizes. For paediatric dosimetry data collection, the sample size may well be limited by the available number of paediatric examinations. There are at least two data collection approaches that can be used to assist in this situation:

(a) Using defined age bands to allow the averaging of dose data within each band;
(b) Analysing the data as a function of patient size or age (see Section 4.3.5).

A combination of these approaches may also be employed.

If data are being collected for defined age bands, a minimum of 20 patients per age group is recommended for a full audit. When patients are not grouped, ideally the patient sizes should be equally distributed with a sample size sufficient to provide a good statistical analysis of the patient dose with respect to patient age or size. For more complex examinations, or if there are no standard paediatric protocols in place[20], there are likely to be large fluctuations in dose, even for patients that are nominally the same size. In this case, patient sample size should be increased to 40–50 patients per age group if possible.

3.4. SELECTION OF PATIENT EXAMINATIONS

Examinations that are commonly performed on paediatric patients may vary in different countries. It is important to audit those examinations that have the highest potential dose and/or frequency, based on the practice in the local radiology facility. The most common examinations may vary with patient age group. Examinations with standard protocols are preferred. Suggested examinations for inclusion in an audit are given in Table 7; however, this list should be supplemented by local procedures if alternative high frequency or high dose examinations are performed.

[20] Particularly when there is a high staff turnover.

TABLE 7. SUGGESTED EXAMINATIONS FOR PATIENT DOSE AUDIT

Modality	Examination	Typical field size[a] (cm × cm)		
		1 year old	5 year old	10 year old
General radiography	Chest AP (supine)	16 × 13	18 × 17	21 × 23
	Chest PA (erect)	17 × 14	20 × 19	23 × 26
	Abdomen AP	15 × 17	21 × 15	26 × 19
	Pelvis AP	15 × 10	21 × 15	26 × 19
Fluoroscopy	Voiding/micturating cystourethrogram	11 × 11	12 × 12	14 × 14
	Contrast swallow	9 × 13	11 × 15	12 × 17
	Contrast meal (upper gastrointestinal tract)	8 × 14	13 × 15	[b]
	Contrast enema (lower gastrointestinal tract)	[b]	[b]	[b]
Computed tomography[c]	Head (brain protocol)			
	Thorax			
	High resolution thorax	—	—	—
	Abdomen			
	Pelvis			

[a] Based on data from the Australia and United Kingdom. However, large individual variations from these values are common.

[b] No data available.

[c] Trunk examinations may be combined depending on local protocols. Clinical indications should always be recorded, as these may have given rise to large dose differences for examination of the same body area.

Note: AP: anteroposterior; PA: posteroanterior.

3.5. AFTER AN AUDIT

It is important that the audit loop be ‘closed’ after the collection of data. The results need to be analysed and reported to the audited department to allow optimization of protection for the examination to begin. This should be followed by a follow-up audit. An initial narrow scope for an audit, for example, analysis of doses for one particular examination or age group with a defined end point rather than all examinations, equipment and modalities at once, usually results in a more immediate improvement in radiation safety for the patient. An important caveat is that patient radiation dose cannot be considered in isolation, and an assessment of image quality should be included when interpreting the results of a dose audit.

4. PAEDIATRIC DATA ANALYSIS AND INTERPRETATION

4.1. INTRODUCTION

Paediatric dosimetry data may be utilized in two main ways:

(a) To derive, contribute to or compare with relevant DRLs;
(b) To estimate risk, or relative risk, for a specific patient.

For the first case, variations in dosimetric data arising from the variable sizes of the paediatric population being studied should be removed, to the extent possible, in order to either derive or compare doses at reference sizes or to analyse the doses as a function of patient size or age (Section 4.3.5). For the second case, individual patient size must be taken into account, through the use of size specific conversion factors, for a risk related dose quantity, as described in Section 5.

4.2. DIAGNOSTIC REFERENCE LEVELS

DRLs are defined by the International Commission on Radiological Protection (ICRP) [20] as a form of investigation level using easily measured dose quantities, such as incident air kerma or entrance air kerma, as used for either a simple standard phantom or a representative patient for typical diagnostic radiological examinations. The term 'reference value' may be used in some countries. The following points should be noted regarding the definition and use of DRLs:

— The use of DRLs is mandatory [4], but a given DRL value is not a dose limit. Specific DRLs are advisory, not regulatory, measures. They are not related to dose limits established for radiation workers and members of the public.
— DRLs are intended to identify high levels of radiation dose to patients.
— DRLs apply to common examinations[21]. Recent experience also suggests that, in some cases (e.g. in CT), the DRLs should be specified for a given indication of the examination [21, 22].

[21] The use of different equipment specific DRLs for an examination is not encouraged.

— Dose quantities and techniques should be easy to measure (e.g. entrance or incident air kerma).
— National DRL selection is by professional or governmental bodies, typically using a percentile point on the observed distribution for patients, and is specific to a country or region.
— As noted by the ICRP, the objective of a DRL "...is accomplished by comparison between the numerical value of the diagnostic reference level (derived from relevant regional, national or local data) and the mean or other appropriate value observed in practice for a suitable reference group of patients or a suitable reference phantom." [20]
— DRLs are not static, but can be expected to change over a period of time due to both technological advances and increased optimization. When referencing DRLs, the source, including the date of derivation, should always be included.

4.3. ANALYSIS OF AUDIT DOSE DATA AS A FUNCTION OF SIZE

4.3.1. Generalized dose as a function of size

There are many factors that affect patient dose, including the equipment used, the experience of staff, the protocols used, the complexity of the procedure and the size of the patient. This may be expressed such that the form of any given patient dose D can be given as:

$$D = D_0 f(x) f(c) \tag{24}$$

where

D is the value of a dose quantity (such as K_i or P_{KA});
D_0 is a constant;
$f(x)$ is a function relating to patient size;

and $f(c)$ is a function combining all of the other factors described above that behaves effectively as a random variable whose magnitude varies with the examination complexity and is assumed not to be correlated with patient size.

Various authors have demonstrated that the variation in patient dose, arising from size alone, is best described as an exponential relationship [23–26]. This may be written as:

$$f(x) = e^{mx} \tag{25}$$

where

x is the size-related parameter such as patient weight, thickness or equivalent diameter;

and m is a constant.

Equation (26), thus, shows patient dose as a two component function, one component predictably dependent on patient size and the other unpredictably attributed to other examination factors:

$$D = D_0 e^{mx} f(c) \tag{26}$$

Taking the logarithm of Eq. (26) gives:

$$\ln D = \ln D_0 + \ln f(c) + mx \tag{27}$$

For a dose study involving a relatively simple examination in a single room with well defined protocols, $f(c)$ may be close to constant, and a typical log plot of dose or dose descriptor against size is shown in Fig. 1.

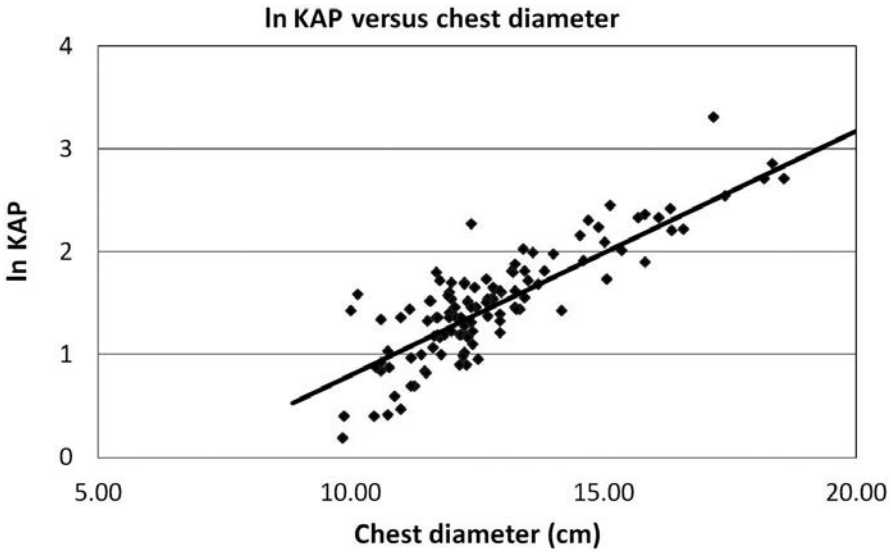

FIG. 1. ln P_{KA} for a simple examination (chest radiograph) as a function of chest diameter for a single X ray room.

For more complicated examinations, such as fluoroscopic procedures, the same plot will more typically be like Fig. 2. The function $f(c)$ gives rise to dose distributions with the form of a Gaussian with a high-dose tail.

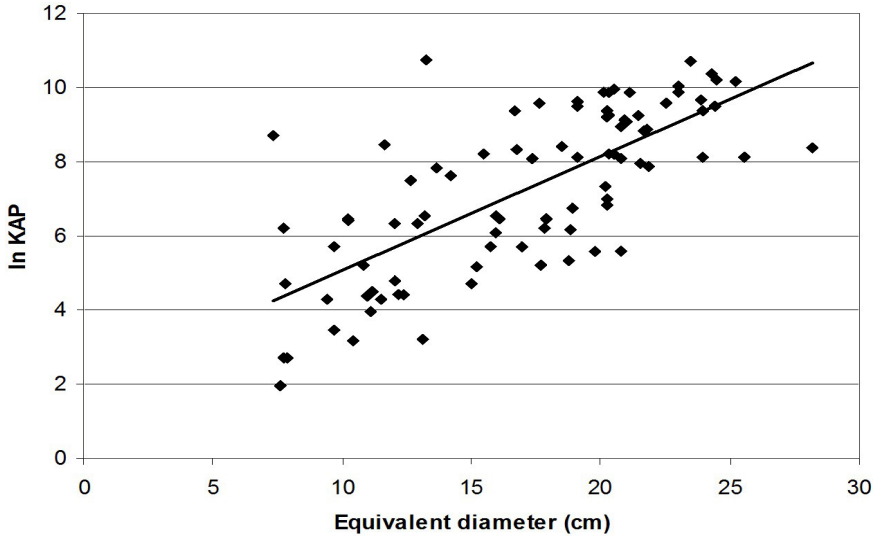

FIG. 2. Kerma area product data for a complex examination.

4.3.2. Normalization of patient dose to reference sizes

The patient reference dose value D_{ref} for a specific reference size x_{ref} is simply determined through the normalization of a patient dose value D from consideration of Eq. (24) to give:

$$D_{ref} = Df(x_{ref}) \tag{28}$$

as $f(c)$ is constant for a particular patient examination.

This implies that there is no substantial change in the conduct of the examination with the change in patient thickness, such as a change in tube voltage or of grid conditions[22]. In this case, Eq. (28) can be further simplified to give:

$$D_{ref} = De^{m(x_{ref}-x)} \tag{29}$$

[22] To ensure that this condition is met, it may be necessary to restrict the range of the thickness used in Eq. (28).

or

$$\ln D_{ref} = \ln D + m(x_{ref} - x) \quad (30)$$

thus, linearizing the size dependence in the logarithmic notation, allowing simple determination of D_{ref} using logarithmic averaging (see later).

In order to determine m, several authors have taken the approach of collecting large data samples and plotting the log of the dose variable D against an appropriate sized parameter x, followed by determination of the gradient of the resultant graph. This value is then used to determine a series of correction factors to convert dose data to a dose corresponding to the reference sizes/ages [23, 25]. This approach requires a reasonably large sample of data across a wide age/size range to obtain sufficient accuracy, as the data plotted contain the variables $f(x)$ and $f(c)$. The required sample size will depend on the magnitude of $f(c)$ and the required uncertainty acceptable for the survey. For small sample sizes, variations uncorrelated with size may obscure the effect of size, particularly for more complex procedures.

The above method enables each dose data point in a set of patient dose measurements to be adjusted to a dose at the reference patient size. The mean of these values is then taken to remove variations in the dose data as attributed to the complexity of the examination and other variables (summarized in $f(c)$). Analysis of this variation, however, will give a measure of the uncertainty of the dose estimation.

The approach of determining D_{ref} for a reference size x_{ref} can be used to:

— Calculate reference doses, defined for reference sizes, as part of a process to determine average dose values or DRLs;
— Adjust previously given reference dose values (average values to DRLs) to a size that is relevant for a particular study, as part of the analysis process.

4.3.3. Alternative methods for determining patient dose values for reference sizes

In addition to the method above, other approaches can be used to correct for size. In these approaches, it is usual that the collection of data be constrained in some way to limit sources of non-size-related variability and, hence, allow smaller sample sizes to be collected for the desired uncertainly of the audit. Some of these are described.

4.3.3.1. Use of effective attenuation coefficients

A National Radiological Protection Board (NRPB) publication [26] derives a theoretical exponential relationship between K_i and patient thickness, based on the assumption of a constant exit dose incident upon the image detector K_{id} and by incorporating an inverse square law correction into the linear attenuation coefficient of the patient to give:

$$K_{id} = k e^{\mu x} \tag{31}$$

where

μ is the effective attenuation factor, equivalent to m in earlier equations;
x is patient thickness;

and k is a constant.

Values for μ have been determined for a range of exposure conditions, from using both phantom measurements and Monte Carlo calculations, and these are tabulated according to field size and tube voltage. Values of the normalization factors required to convert patient dose data at specific thicknesses to D_{ref} are also given in the publication. A similar approach is used for KAP measurements, with an additional correction factor for changing field size. This approach requires access to the tabulated data and detailed knowledge of the tube voltage and field size used for each patient to correctly apply the data.

4.3.3.2. Utilization of a calibrated automatic exposure control response

Another approach for specific examinations, using the dose variable P_{KA} and performed under AEC, has the advantage that $f(x)$ can be determined under controlled conditions, thereby greatly reducing the magnitude of $f(c)$. In this case, phantom measurements are used to determine the increase in P_{KA} with changing patient thickness while under AEC [24]. A plot is made of the log of P_{KA} against phantom thickness x but, as measurements were made under fixed conditions, patient examination variability $f(c)$ is excluded as measurements are carried out with a fixed field size and fluoroscopy time for each phantom thickness. The relationship derived was:

$$\ln P_{KA} = kx + c \tag{32}$$

where

x is patient thickness[23];
k is equivalent to variable m (Section 4.3.2);

and c is a constant.

It has been found that many systems exhibit a very similar AEC response, and that k can be established from Eq. (32). The method allows normalization for size correction to be applied to any measurement dose. This method does not include any correction for field size variation with patient size.

4.3.4. Binning of data

Whatever approach is used to normalize data with respect to patient size, uncertainties will be reduced by minimizing the spread of sizes in any one data sample. This can be achieved by grouping or binning the data into a series of age or size ranges. In the simplest cases where no data normalization occurs, paediatric dose data should be binned with an averaging process applied to both the size and dose variables (see Section 4.3.4.1). The most commonly used reference ages and their associated sizes are given in Appendix I.

Data may be binned appropriately for any of the methods in Sections 4.3.1 and 4.3.2. If using the NRPB method (Section 4.3.3.1), it is suggested that binning be centred on the reference sizes rather than using the standard age bands. If the logarithmic method (Section 4.3.4.1) is applied to datasets spread evenly around a reference age/size, this will also yield dose values applicable to the reference size. It should be noted that adequate sample sizes for statistical significance must be maintained. Examples of each methodology are given below.

The simplest case is perhaps the collection of paediatric dosimetric data binned within specified age bands, with a simple arithmetic mean of these values within each bin to give a mean patient dose. One advantage of this system is that it can be applied to situations where few or no size data are collected with the dosimetric data. An extension to this is to take a log average of the data, as described in Section 4.3.4.1. Examples of the methods are given in Section 4.3.4.2.

---

[23] In some cases, it might be more convenient to derive the equivalent cylindrical diameter from measurements of patient height and weight (see Appendix I).

4.3.4.1. Mean logarithmic method

Given the exponential nature of input dose parameters with size, instead of using an arithmetic mean, an arguably better approach is to take the log average of the dose data from binned datasets. The calculated log average dose value may be interpreted as the dose expected to be received by a patient equal in size to the arithmetic mean size for the patient sample undergoing an examination of typical complexity for a particular facility. Using this technique, there is no requirement to normalize individual patient dose measurements to a reference size, thus speeding up the analysis of the data and reducing uncertainties for more complex examinations.

The data analysis steps are as follows:

Step 1: Each patient dose data point should be logarithmically transformed.
Step 2: Logarithmic dose data should be averaged in size intervals.
Step 3: Average data should be transformed back to give the dose indicator from the average of logarithms of the data points.
Step 4: An average should be taken of the patient size data points within each size interval. This gives the patient size value which corresponds to the log average dose value determined in step 3. If no size data are available, the typical average size for that age group should be used.

4.3.4.2. Examples of data analysis to give the log average dose for the mean size of the binned sample

Table 8 shows the results of the analysis of incident air kerma data collected for thorax examinations at a single X ray unit, where data have been binned according to age bands with between 19 and 150 patients in each age band. For each calculated value of K_i, the logarithm was calculated and then for each age band the mean logarithmic value of K_i calculated. The exponential of these mean logarithmic values gives the size average, or log mean, dose value.

For this dataset, the log mean dose values are very close to the simple arithmetic mean dose values, as the sample sizes are large and evenly distributed throughout the size range, thus giving a close to normal distribution of doses.

Tables 9 and 10 show analysis of data collected for micturating cystourethrograms for a single X ray unit, and for patients with equivalent cylindrical diameter (ECD) within ±2 cm of the European standard for a 1 year old. The mean patient parameters of the data sample are described in Table 9, in comparison with the standard parameters. Details of the mean P_{KA} calculated as described above, along with that calculated according to the alternative methods described in Section 4.3.3, are given in Table 10.

TABLE 8. DATA ANALYSIS FOR A LARGE SCALE SURVEY OF INCIDENT AIR KERMA AT THORAX EXAMINATION

Age band	Thickness range (cm)	Mean thickness (cm)	Arithmetic mean K_i (units)	Log mean K_i value[a] (units)
0–1 month	8.5–10	9.2	25.6	25.3
0–1 year	9.2–12.2	10.7	27.9	27.9
1–5 years	10.2–13.8	11.9	33.0	32.0
5–10 years	11.2–18.3	13.4	41.9	41.4

[a] Exponential of mean ln K_i.

TABLE 9. PATIENT PARAMETERS FOR A MICTURATING CYSTOURETHROGRAM STUDY

Patient sample (71 children)	Standard 1 year old
Mean age: 0.9 years	1 year
Mean weight: 9.0 kg	9.26 kg
Mean equivalent cylindrical diameter: 12.7 cm	13.0 cm

TABLE 10. ANALYSIS OF DOSE DATA FOR A MICTURATING CYSTOURETHROGRAM STUDY

Mean P_{KA} calculation method	Mean P_{KA} value (units)
Mean raw data value	48
Mean value using an automatic exposure control normalization factor	48
Mean value using tabulated normalization factors	51
Value using a mean logarithmic method	35

The above example demonstrates how in this case the log mean value of P_{KA} is considerably less than the mean raw data value or either size normalized value (all of which yield similar values), as the dose distribution is significantly non-Gaussian, as illustrated in Fig. 3. The data plot shows the typical shape of patient dosimetry data plots, in that it has a roughly Gaussian body with a long high-dose tail. The mean raw and exponentially corrected values lie towards the upper edge of the Gaussian part of the distribution, whereas the log mean value lies within the peak of the Gaussian part. For such distributions, the derived log mean value is a closer representation of the median value of the distribution, which may be considered to be a better descriptor of 'typical' dose for this piece of equipment than the mean value, as the latter will be heavily influenced by a small number of unusually high values.

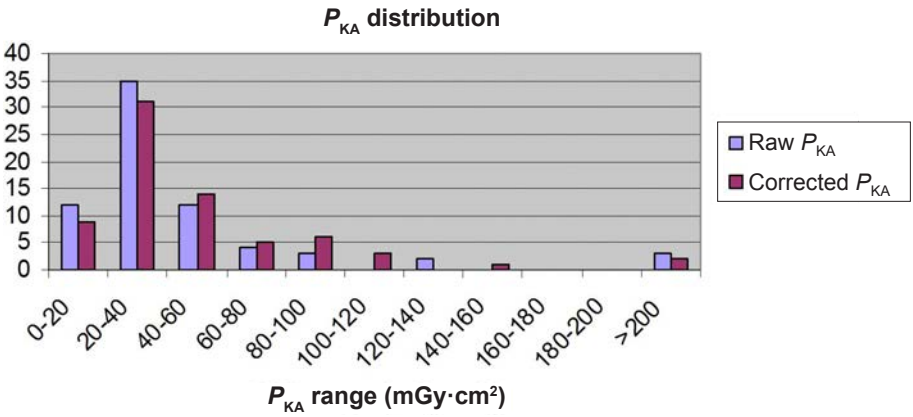

FIG. 3. Distribution of P_{KA} values in the micturating cystourethrogram study described in Tables 9 and 10.

4.3.5. Comparison of dose audit results to diagnostic reference levels

Once dose values have been established from a dose audit, these data should be checked against appropriate DRL values. Every effort should be made to have dose data for a standard patient size that match the size used for the DRL. If this is not possible, the audit data should be compared to the nearest (higher) DRL patient size. Dosimetry data should always be collated out in individual rooms and data should be analysed separately for each X ray unit in the first instance, as described above. This will have more impact on optimization than binning the data beforehand, as it may identify specific rooms where protocols have not been set up or used correctly.

In the thorax examination study example (Table 8) above, for the age band 1–5 years, the size averaged value of K_i is 32 μGy for a mean patient thickness of 11.9 cm which, for this data sample, is around the middle of the size range for this age band. The Austrian DRLs for this examination type are 60 μGy for 1 year olds and 70 μGy for 5 year olds; in this case, local dose values are well below national DRLs [23]. In general, the local value should be compared to the DRL for the age/size higher than that in the local survey, i.e. that for 5 year olds in this example. For greater accuracy, DRLs may be plotted as a function of size or age, and a DRL value deduced for the mean patient size [10, 21] in the local data sample.

4.3.6. Derivation of diagnostic reference levels from dose audit data

In the case of deriving DRL values, the generally accepted approach is to consider the spread of resultant mean dose values for each X ray facility and adopt the third quartile of the mean room doses as the DRL. In all cases, it is reasonable to round DRL values to one or, at most, two significant figures. For paediatric data, DRLs may also be plotted as a function of size or age in order to provide a relevant value for any particular patient group (as shown in Section 4.3.5). This may be particularly useful when the log-averaging method has been applied to a dataset where the mean patient size does not correspond to a specific reference size.

It should be recognized that if optimization is carried out for facilities with higher doses, the spread of doses should become progressively narrower and it may become inappropriate to use a third quartile value as the DRL. In this case, a more flexible pragmatic approach may be required, such as plotting the distribution of doses and finding the point at which the Gaussian part of the curve changes to a high-dose tail, or considering a number of standard deviations above the mean or median value.

4.4. INTERPRETATION OF COMPUTED TOMOGRAPHY DOSE INDICATORS

For radiography and fluoroscopy, the primary dose indicators (K_i and P_{KA}) are based on measures of tube output in air, whereas for CT the indicators (C_{VOL} and $P_{KL,CT}$) are based on both tube output and absorption in standard sized phantoms. These CT dose indicators quantify the amount of radiation generated by the CT scanner during a clinical examination. Since the standardized phantoms used for these measurements are not good models of patient attenuation for

patients of varying sizes, from an infant to large adult, C_{VOL} and $P_{KL,CT}$ should never be used as an estimate of patient dose during a CT examination.

4.4.1. C_{VOL}

C_{VOL} was defined in Ref. [27] to indicate the radiation output of a CT scanner measured in a specifically defined phantom. It is suitable for comparing radiation production of different scanners. As such, C_{VOL} is affected by many scan parameters: tube current, rotation time, pitch, tube voltage, location of the phantom relative to the scanner detector, X ray tube focal spot, and the shape, thickness and material of the bowtie filter inserted into the X ray beam. C_{VOL} may be considered a dose index of CT scanners [28].

Radiation dose in a clinical CT examination is determined by the amount of energy delivered to locations within the patient's body by the CT scanner. Thus, an estimation of patient dose can be determined by adjusting C_{VOL} (radiation output of the scanner) using a conversion factor that accounts for the attenuation of the patient's body, which is, in turn, a function of body size, in comparison with the attenuation properties of the standard CTDI phantom. Assuming that the scanner's displayed CTDI values for an abdominal scan are based on the 32 cm CTDI phantom, the estimated patient dose for an adult is similar to the displayed C_{VOL}. The small infant's estimated abdominal dose will be approximately three times greater than the C_{VOL}, while the abdominal dose to the largest adult abdomen will be approximately 70% of C_{VOL} [29]. In the event that the scanner displays C_{VOL} based on the 16 cm CTDI phantom, the estimated abdominal dose to the infant will only be 1.5 times greater than C_{VOL}. It is imperative that the operator know which of the two standard CTDI phantoms their scanner uses for each type of clinical examination when displaying C_{VOL}.

A set of conversion factors have been derived to convert C_{VOL} to a size specific dose estimate (SSDE) for children, small adults and large adults receiving CT scans [29]. These were derived using four independent methodologies to study the attenuation properties of patients. When the data from the four methodologies were combined, a logarithmic relationship between the effective diameter of the patient and the normalized conversion factor was found, giving a single set of conversion factors for all high voltage scan parameters between 80 and 140 kV [29]. The correction factors are currently limited to variations in patient size for the trunk of the body. The accuracy of the SSDE estimate as a function of patient size is believed to be within 20% [29]. The SSDE provides a patient dose estimate that can assist in assigning risks that result from CT paediatric scans as discussed in Section 5. This allows the radiologist and radiographer to use the SSDE to better manage the radiation dose delivered to paediatric patients, especially in institutions that scan paediatric patients a minority of

the time. Calculating SSDE is relatively simple with the use of look-up tables based on patient thickness. For example, if the electronic measurement of the scan projection image of the patient gives a lateral dimension of 12.3 cm, and the scanner displayed C_{VOL} is 5.4 mGy based on the 32 cm CTDI phantom, the correct look-up table [29] gives a correction factor of 2.5 for a 12 cm patient. The size specific dose estimated for the patient is given by Eq. (33):

$$SSDE = 5.4\ [mGy] \times 2.5 = 13\ [mGy] \quad (33)$$

It is important to note that the SSDE should not be used to compute a modified DLP nor to compute effective dose using currently available conversion factors (see Ref. [29]).

4.4.2. Dose length product

The concept of DLP incorporates both the mean C_{VOL} and the total distance scanned. It has often been considered to be the more useful of the two commonly used CT dose metrics, as it can be considered to be related more closely to risk. However, for paediatric dosimetry, in particular, it is important to understand both the drawbacks and the advantages of this quantity through a consideration of the factors affecting the total scan length:

— The size of the patient will have a large effect on the scan length for a single phase and the higher DLP resulting from scanning a taller patient will not necessarily correspond to higher organ doses.
— The choice of anatomical start and stop positions should normally be dictated by the clinical requirements of the examination but, for small children in particular, may have a critical effect on the dose to organs at the edge of the area of interest.
— The degree of over-ranging in helical scans, i.e. the additional scan volume either side of the region of interest, depends on the scanner type, nominal beam width setting and the pitch, as a specific type of scanner will usually use a set number of tube rotations before and after the selected range, and the distance this equates to in the z direction will vary with beam width and pitch. Over-ranging will result in additional dose to the patient, which is likely to be a greater percentage of the total dose as the patient size decreases.
— The number of phases of the examination will affect the total dose to organs within the scan volume, e.g. a two-phase scan could double the dose to scanned organs.
— One might be tempted to estimate the DLP of paediatric patients by substituting SSDE for C_{VOL}. While this might be helpful in some cases to

estimate risk, this cannot be done under any circumstance if the calculated paediatric DLP is going to be used with published effective dose conversion factors to estimate effective dose.

— Regarding CTDI values, it is important to know to which size phantom the displayed DLP values relate. This may be the head phantom for all paediatric protocols or may be the 32 cm phantom for body protocols. It may also depend on the FOV selected, rather than on head or body mode, e.g. selecting a small FOV on an abdomen protocol may use the head phantom value.

5. RADIATION RISK RELATED QUANTITIES

5.1. INTRODUCTION

The dose quantities described in earlier sections are relatively easy to measure or derive and, as such, are very suitable for use in setting, or comparisons with, DRLs. However, they are not, in general, directly related to the radiation risk to the patient for the following reasons:

— Generally, they do not specify the dose to radiosensitive organs or tissues[24].
— They do not take into account the radiosensitivity of the tissues being irradiated.
— They may not take into account the size of a particular patient, which affects the actual absorbed dose, and, hence, the risk.
— They do not specify the age and gender of the patient. These parameters also influence the risk.

Knowledge of the radiation risk associated with a specific examination, and particularly for a specific patient size and age, is important, especially when comparing alternative diagnostic examination types and, more generally, within the justification process.

This section reviews radiation effects in children that could result from diagnostic radiology examinations and discusses the steps involved in moving from dose information to suitable risk related quantities, with a discussion on specific computational methodologies for both projection and CT radiographic procedures.

5.2. RADIATION EFFECTS FOR PAEDIATRIC PATIENTS AT DIAGNOSTIC RADIOLOGY DOSE LEVELS

Radiation effects are divided into the categories of stochastic and tissue effects (deterministic) [20]. At dose levels commonly found in diagnostic radiology, the overwhelming effect in both adult and paediatric patients is believed to be an increased incidence and associated mortality from

[24] In the case of dose quantities, such as ESAK, however, there will be a relationship to deterministic effects on the skin.

stochastic effects [30]. At the dose levels which occur during complex interventional fluoroscopic procedures or CT examinations, the primary radiation risk differs for the small paediatric patient and large adult patient. The size of the adult patient results in larger dose rates to the entrance skin increasing the risk of tissue effects. At the same time, adult patients receiving interventional procedures tend to be older and sicker than the general population, making it less likely that they will survive long enough for stochastic effects to be expressed [30]. In contrast, the small paediatric patient receives smaller dose rates to the entrance skin, thus reducing the risk of tissue effects, while their greater sensitivity to the stochastic effects of radiation and their longer expected lifetime increase the likelihood of a stochastic effect [30]. Regarding larger paediatric patients, one should bear in mind that this group potentially has a similar risk of tissue effects as adult patients. The risk of stochastic injury, on the other hand, will not be different from that associated with other paediatric patients of the same age, gender and ethnicity [30].

5.2.1. Stochastic effects

5.2.1.1. Cancer induction

The major categories of paediatric cancer are leukaemia, brain tumours and lymphomas. They represent almost 70% of all paediatric cancers. In comparison, the most common forms of adult malignancies are of epithelial origin, such as in prostate, breast, lung and colon carcinomas. Baseline data on cancer induction during childhood are available through the International Classification of Childhood Cancer[25]. The cumulative induction risk to age 15 for the normal incidence of childhood cancer has been reported to lie in the range of 1.0–2.5 cases per thousand.

Cancer induction in children, and the risk of childhood malignancies from diagnostic radiological procedures based on epidemiological data in children, have been reviewed by Linet et al. [31]. The main concern for adverse health effects from radiation exposure in paediatric imaging is related to the increased risk of cancer incidence and mortality (stochastic effects). Linet et al. [31] conclude that the existing data and current knowledge are not sufficient to suggest a clear connection between early life diagnostic radiation exposure and the occurrence of paediatric cancer. Consequently, the need for nationwide surveys to estimate foetal and childhood radiation doses from common diagnostic procedures is emphasized (see chapter 3 of Ref. [31] for a discussion on paediatric dose audits).

[25] http://seer.cancer.gov/iccc/

A health risk assessment from exposure to low doses of ionizing radiation is summarized by the National Research Council of the National Academies. Data, including childhood cancer incidence and mortality from the BEIR VII Report [1], are summarized in Tables 11 and 12, as well as in Fig. 4. Compared to the population as a whole, the lifetime cancer risk from radiation exposure in childhood (both incidence and mortality) is generally higher for a given dose. The increased risk for a given dose for younger age groups reflects:

— The increased radiation organ sensitivity during development;
— The longer life expectancy of the child, during which time a cancer can become established and develop.

The increased risk of radiation effects in the paediatric population needs to be addressed in diagnostic radiation medicine. The task of ensuring that the radiation dose to children is the minimum needed to comply with the necessary image quality requirements of a diagnostic radiology examination is, therefore, of the utmost concern in paediatric imaging. As imaging smaller patients requires less radiation in general, paediatric examination protocols with reduced dose compared to corresponding adult protocols should always be available for such procedures. Strategies to achieve this through optimization of protection in paediatric diagnostic radiology procedures are discussed in Section 6.

TABLE 11. LIFETIME ATTRIBUTABLE CANCER INCIDENCE AND MORTALITY RISK FOR ALL CANCERS AS A FUNCTION OF AGE AT EXPOSURE *(number of incidence/mortality per 100 000 persons exposed to a single uniform whole body dose of 0.1 Gy: data from Ref. [1])*

Age (years)		0	5	10	15	20	30	40	50	60	70	80
Incidence	Male	2563	1816	1445	1182	977	686	648	591	489	343	174
	Female	4777	3377	2611	2064	1646	1065	886	740	586	409	214
Mortality	Male	1099	852	712	603	511	381	377	360	319	250	153
	Female	1770	1347	1104	914	762	542	507	469	409	317	190

TABLE 12. LIFETIME ATTRIBUTABLE CANCER INCIDENCE AND MORTALITY RISK FOR ALL CANCERS FOR PERSONS EXPOSED TO A SINGLE UNIFORM WHOLE BODY DOSE OF 0.1 Gy NORMALIZED TO THE AGE OF 70 YEARS *(data from Ref. [1])*

Age (years)		0	5	10	15	20	30	40	50	60	70	80
Normalized incidence	Male	7.47	5.29	4.21	3.45	2.85	2.00	1.89	1.72	1.43	1.00	0.51
	Female	11.68	8.26	6.38	5.05	4.02	2.60	2.17	1.81	1.43	1.00	0.52
Normalized mortality	Male	4.40	3.41	2.85	2.41	2.04	1.52	1.51	1.44	1.28	1.00	0.61
	Female	5.58	4.25	3.48	2.88	2.40	1.71	1.60	1.48	1.29	1.00	0.60

The increased radiation sensitivity of organs of children is seen from epidemiological data and is expressed in the BEIR VII Report as a decrease in cancer incidence and mortality with age [1]. Examination of these data shows that cancer incidence varies considerably between the different organs, with the lungs and female breast being the most radiosensitive at birth, and the thyroid and female breast showing the greatest decrease in radiosensitivity with age. It should also be noted that the sensitivity of different organs varies over time in specific ways. The risk of both cancer incidence and mortality is considerably higher for females.

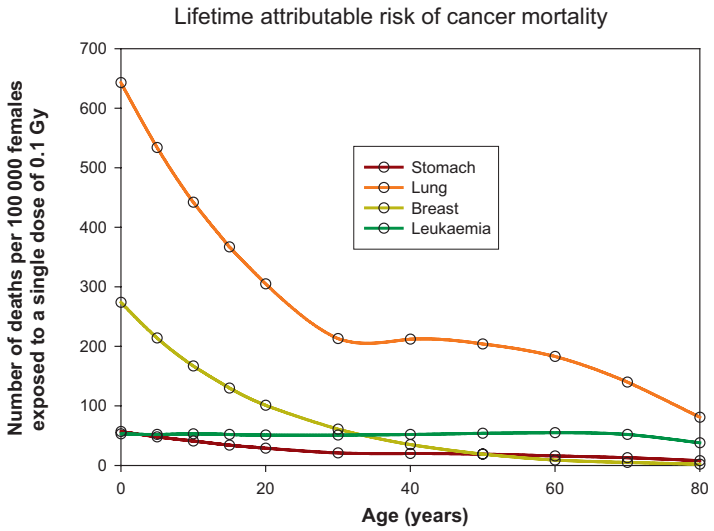

FIG. 4. Lifetime attributable risk of cancer mortality in females for irradiation of single selected organs (data from Ref. [1]).

5.2.1.2. Hereditary effects

Information on hereditary effects of radiation come almost entirely from animal experiments, combined with our current understanding of genetics. While it is a subject of much study [32], its importance in radiation detriment has been reduced as ICRP publication 103 [33] reduced the tissue weighting factor for the gonads from 0.2 to 0.08 (see Table 13 on p. 51).

5.2.2. Tissue effects

Tissue reactions, or deterministic effects, resulting from radiation exposure during a diagnostic radiology or interventional procedure can, in some circumstances, occur in heavily exposed tissue, usually the skin or the lens of the eye. Skin tissue reactions are infrequently experienced in paediatric X ray imaging, as the smaller size of paediatric patients requires lower skin doses during a typical procedure, compared to those needed for a similar adult procedure. Consequently, paediatric skin doses rarely reach the dose threshold required for deterministic effects to occur, provided there is not a serious problem with equipment and that adequate paediatric protocols are used.

It is, therefore, important to be vigilant in using optimized imaging protocols and procedures to prevent an unnecessarily high dose to sensitive organs and/or tissues especially prone to deterministic effects, such as the skin.

5.3. DOSE QUANTITIES AND RISK ASSESSMENT

Reference [31] includes a comprehensive summary of publications from the epidemiology literature relating risk of childhood cancers to early life post-natal medical radiation exposure. As no unified approach for dose metrics was observed, it was concluded in Ref. [31] that "differences in the radiologic dose units for different radiologic examinations complicate comparisons among procedures." In this section, the different dose units used to arrive at a risk related dose metric are summarized. Special attention is given to the concepts of 'effective dose' and 'equivalent organ dose'. Although effective dose has been the most commonly used dose metric when reporting the risk related to a given type of procedure, there is growing demand to replace or, at least, complement this metric with information on the equivalent organ doses involved in the procedure [34–37].

5.3.1. Average organ dose

At the low doses encountered in diagnostic imaging, the average absorbed dose in the organ (or tissue), which is defined as the ratio of the energy imparted $\bar{\varepsilon}_T$ to the tissue or organ and the mass m_T of the tissue or organ, is used as the basic physical quantity to correlate dose with radiation detriment:

$$D_T = \frac{\bar{\varepsilon}_T}{m_T} \tag{34}$$

5.3.2. Estimation of equivalent organ dose

The equivalent dose H_T to an organ or tissue T is used to characterize the effects of different radiation types in causing stochastic effects. For a single type of radiation R, it is the product of a radiation weighting factor w_R for radiation R and the organ dose D_T:

$$H_T = w_R D_T \tag{35}$$

For X rays, the radiation weighting factor is one. The equivalent dose is recommended by the ICRP for risk–benefit assessment as seen in their statement that:

> "in the low dose range, below about 100 mSv, it is scientifically plausible to assume that the incidence of cancer or heritable effects will rise in direct proportion to an increase in the equivalent dose in the relevant organs and tissues." [33]

The equivalent organ dose in a reference person can be estimated using conversion coefficients that relate the physical quantities describing the radiation field to the organ dose. Usually, in projection radiography and fluoroscopy, the incident air kerma K_i, the ESAK K_e or the P_{KA} are used in conjunction with conversion coefficients that are typically a function of the X ray source and geometry (beam quality, i.e. tube voltage, filtration and HVL, field size, focal surface distance) and patient anatomical considerations, such as the direction and location of the X ray field with respect to the patient, as well as the size, shape and composition of the patient (or patient model). Normally, such conversion coefficients are determined through Monte Carlo calculation, although in some cases, they could also be derived experimentally with physical phantoms and dosimeters such as TLDs.

It should be recognized that imaging the paediatric patient generally involves very different radiographical technique factors (tube voltage,

tube current, filtration, field size (or scan length in CT)) compared to those corresponding to adult examinations. In combination with the significant size variation of organs and in patient thickness in the direction of the X ray beam with age, dose estimation in paediatrics is a delicate task that requires careful attention at the time of choosing the required conversion coefficients appropriate, both for the imaging task as well as for the specific paediatric age group. The International Commission on Radiation Units and Measurements (ICRU) summarizes this by stating that:

> "when a dose conversion coefficient is needed for a specific situation, the best approach is to select a value from the available data based on similarities in exposure conditions (projection, view, field size, and radiation quality) and patient model." [38]

As the greatest influence on the average dose to a tissue or organ is the extent to which it is in the primary X ray beam, it is important to ensure that the data used match the primary irradiated organs correctly, even if this necessitates using a nominally different examination projection.

In CT examinations, the SSDE, as defined in Section 4.4.1, may be used as a first approximation of the patient organ dose, provided that the organ is relatively large and is completely contained within the scan length [29] (see Section 5.3.6 for examples of tables of conversion coefficients for organ dose and software packages that can be used to calculate organ doses directly for diagnostic radiology).

5.3.3. Patient models

Conversion factors are necessary in order to conveniently determine organ or tissue dose from simple dosimetric quantities, such as incident air kerma K_i (Section 2) as described below:

$$c_{D_T,K_i} = D_T / K_i \tag{36}$$

and for C_W or C_{VOL} for CT applications:

$$c_{D_T,C_{VOL}} = D_T / C_{VOL} \tag{37}$$

These conversion factors can be determined through either direct measurement of D_T with the use of physical anthropomorphic phantoms or computational modelling, normally using Monte Carlo code, utilizing either mathematical or voxel phantoms to represent the human body [38].

Generic or 'standard' models for the human body have been based on publications such as the reference man [39]. These models have more recently been expanded with ICRP publication 89 [40] which includes age and sex specific data. This material is based mainly on European and North American data. While ethnic and geographical issues may affect the mean size of people and, thereby, the mean conversion coefficients, individual variation within any group is large, as is seen in Appendix I. In order to estimate the mean doses in a group, it is best to estimate the doses in the various sized individuals and then calculate the average doses in the group. The use of standard model data along with accurate tissue substitute materials [41] and fabrication methodologies [42, 43] has allowed the production of accurate anthropomorphic phantoms and these have included paediatric phantoms [44]. Increasingly, computational modelling is used to determine conversion coefficients. The use of segmented datasets from cross-sectional imaging to create 'voxel' phantoms has contributed to an ever increasing number of adult patient models [45]. The ICRP recently defined reference models for adult dosimetric calculation [46]. At this stage, the number of paediatric models is more limited [47–49]. An overview of the different models applied to estimate organ and tissue doses in diagnostic radiology are summarized in ICRU publication 74 [38], with paediatric examples given in table 5.2 of that publication.

5.3.4. Use of effective dose

The effective dose E is a measure of the combined detriment from stochastic effects for all organs and tissues for the reference man. It is the sum over all of the organs and tissues of the body of the product of the equivalent dose H_T to the organ or tissue and the tissue weighting factor w_T for that organ or tissue:

$$E = \sum_T w_T H_T \tag{38}$$

This quantity is designed for protection purposes for whole body irradiation of populations and is based on combined risk information for both males and females. The tissue weighting factors w_T of Ref. [33] are shown in Table 13. The tissue weighting factors take into account variations in radiation sensitivity between organs, and represent mean values over both sexes and account for population age distribution. Consequently, the effective dose is not designed to be used to estimate the risk for incidence of cancer and/or heritable effects for a particular individual patient, and should not be applied for this purpose, as is specifically stated in Ref. [33]. Furthermore, the estimation and interpretation of effective dose becomes more problematic when the organs receive only

partial, and/or a very heterogeneous exposure, as is the case when undergoing a diagnostic X ray examination.

TABLE 13. TISSUE WEIGHTING FACTORS *(from Ref. [33])*

Tissue or organ	Tissue weighting factor (w_T)	$\sum w_T$
Bone marrow, colon, lung, stomach, breast, remainder tissues[a]	0.12	0.72
Gonads	0.08	0.08
Urinary bladder, oesophagus, liver, thyroid	0.04	0.16
Bone surface, brain, salivary glands, skin	0.01	0.04

[a] The tissue weighting factor for remainder tissues is applied to the arithmetic mean of the doses to the following 14 organs/tissues: adrenals, extrathoracic region, gall bladder, heart, kidneys, lymphatic nodes, muscle, oral mucosa, pancreas, prostate, small intestine, spleen, thymus and uterus/cervix.

The ICRP [33] recommends that the use of effective dose be restricted to comparison of the risk related dose burdens from different types of (diagnostic) procedure, or in inter-comparison of procedures performed in different hospitals or countries.

Within the context of paediatric imaging, it should be recognized that the relative tissue weighting for organs may not be appropriate for paediatric patients as is clearly seen from Fig. 4. The effective dose does not accurately reflect the differences in the age dependency of the radiation sensitivity of various tissues and organs. The comparison of effective doses estimated for patients undergoing paediatric examinations with corresponding adult patients might, therefore, be misleading for judging the risk of a given paediatric procedure, even if one would use an additional general age related risk factor (see Table 12). Yet another concern relates to the unit in which effective dose is expressed — the sievert — as it is the same unit used for equivalent dose. To avoid misinterpretation of the dose value given, the dose quantity (i.e. equivalent dose or effective dose) should always be clearly stated.

If effective dose is to be utilized, for the reasons mentioned above, the set of tissue weighting factors used by the program should also be checked. Codes, such as PCXMC [50] for projection radiography and fluoroscopy, and ImPACT CT [51] and CT Expo [52] for CT, have all adopted the revised set of tissue weighting factors given in Ref. [33]. PCXMC and CT Expo include both adult and paediatric patient models, while the ImPACT CT dosimetry calculator only estimates dose in adult patients, although some correction factors are provided

for paediatric examinations. A full Monte Carlo simulation of the (typically radiotherapy) dose distribution using the actual patient CT data is available with the software ImpactMC[26].

It may be anticipated that as further data continue to become available for assessing radiation risks, particularly at low doses, there may be further changes in tissue weighting factors in the future. This can lead to significant changes in the effective dose quantity, as has already been demonstrated for the recent changes which have typically led to increases of around 35% in effective dose for X ray examinations of the head and decreases of around 40% for X ray examinations of the pelvis [53]. Equivalent organ dose, on the other hand, by definition does not depend on tissue weighting factors and is, in this sense, a more robust dose metric than effective dose.

5.3.5. Risk assessment

The assessment of the risk associated with stochastic health effects of an X ray procedure should account for the radiation sensitivity of individual organs and tissues, and its variation with age and sex, and the lifespan and cancer statistics of the relevant demographic group[27]. Data on the cancer incidence and mortality for organs and tissues, as a function of both sex and age, have been compiled in Ref. [1][28]. The cancer incidence and mortality data are shown in Tables 14 and 15. It should be noted that these relate to US cancer and life statistics, and figures for other populations may differ[29]. In many circumstances, if the equivalent dose can be determined for a number of 'critical organs' (see Table 13), i.e. radiosensitive organs in or near the primary beam, it may be appropriate to apply age specific risk factors for these particular organs. This would be preferable to using a computational program, designed to calculate effective dose, that does not properly address the clinical application. At the time of selecting tables or choosing a software package to perform organ dose calculations, the different phantom models used to derive these factors should be established, in particular noting whether paediatric models were used. Assessing risk using two different analysis methods can be a good way to validate conclusions. For example, a manual estimate can be made to compare with the results obtained from an available computational program (see Section 5.3.6 on

---

[26] http://www.ct-imaging.de/en/ct-software-e/impactmc-e.html

[27] http://globocan.iarc.fr/

[28] Risk data also vary with population [1].

[29] Reference [33] presents mortality rates and cancer incidence for 'Asian' and 'Euro-American' populations (tables A.4.10–A.4.17). Such data can also be obtained from various national statistics.

dose conversion factors). Cancer risk estimates, based on individual organ doses, that are age and sex specific are presently implemented using software programs such as PCXMC for projection radiography, and could also be implemented in other software codes, including those designed to address CT.

TABLE 14. LIFETIME ATTRIBUTABLE RISK OF CANCER INCIDENCE PER 100 000 PERSONS EXPOSED TO A SINGLE DOSE OF 0.1 Gy *(reprinted from Ref. [1])*

Cancer site	Age at exposure (years)										
	0	5	10	15	20	30	40	50	60	70	80
Males											
Stomach	76	65	55	46	40	28	27	25	20	14	7
Colon	336	285	241	204	173	125	122	113	94	65	30
Liver	61	50	43	36	30	22	21	19	14	8	3
Lung	314	261	216	180	149	105	104	101	89	65	34
Prostate	93	80	67	57	48	35	35	33	26	14	5
Bladder	209	177	150	127	108	79	79	76	66	47	23
Other	1123	672	503	394	312	198	172	140	98	57	23
Thyroid	115	76	50	33	21	9	3	1	0.3	0.1	0.0
All solid	2326	1667	1325	1076	881	602	564	507	407	270	126
Leukaemia	237	149	120	105	96	84	84	84	82	73	48
All cancers	2563	1816	1445	1182	977	686	648	591	489	343	174
Females											
Stomach	101	85	72	61	52	36	35	32	27	19	11
Colon	220	187	158	134	114	82	79	73	62	45	23
Liver	28	23	20	16	14	10	10	9	7	5	2
Lung	733	608	504	417	346	242	240	230	201	147	77
Breast	1171	914	712	553	429	253	141	70	31	12	4
Uterus	50	42	36	30	26	18	16	13	9	5	2
Ovary	104	87	73	60	50	34	31	25	18	11	5
Bladder	212	180	152	129	109	79	78	74	64	47	24

TABLE 14. LIFETIME ATTRIBUTABLE RISK OF CANCER INCIDENCE PER 100 000 PERSONS EXPOSED TO A SINGLE DOSE OF 0.1 Gy *(reprinted from Ref. [1])* (cont.)

Cancer site	Age at exposure (years)										
	0	5	10	15	20	30	40	50	60	70	80
Other	1339	719	523	409	323	207	181	148	109	68	30
Thyroid	634	419	275	178	113	41	14	4	1	0.3	0.0
All solid	4592	3265	2525	1988	1575	1002	824	678	529	358	177
Leukaemia	185	112	86	76	71	63	62	62	57	51	37
All cancers	4777	3377	2611	2064	1646	1065	886	740	586	409	214

Note: These estimates are obtained as combined estimates based on relative and absolute risk transport, and have been adjusted by a dose and dose rate effectiveness factor of 1.5, except for leukaemia, which is based on a linear–quadratic model.

TABLE 15. LIFETIME ATTRIBUTABLE RISK OF CANCER MORTALITY PER 100 000 PERSONS EXPOSED TO A SINGLE DOSE OF 0.1 Gy *(reprinted from Ref. [1])*

Cancer site	Age at exposure (years)										
	0	5	10	15	20	30	40	50	60	70	80
Males											
Stomach	41	34	30	25	21	16	15	13	11	8	4
Colon	163	139	117	99	84	61	60	57	49	36	21
Liver	44	37	31	27	23	16	16	14	12	8	4
Lung	318	264	219	182	151	107	107	104	93	71	42
Prostate	17	15	12	10	9	7	6	7	7	7	5
Bladder	45	38	32	27	23	17	17	17	17	15	10
Other	400	255	200	162	134	94	88	77	58	36	17
All solid	1028	781	641	533	444	317	310	289	246	181	102
Leukaemia	71	71	71	70	67	64	67	71	73	69	51
All cancers	1099	852	712	603	511	381	377	360	319	250	153

TABLE 15. LIFETIME ATTRIBUTABLE RISK OF CANCER MORTALITY PER 100 000 PERSONS EXPOSED TO A SINGLE DOSE OF 0.1 Gy *(reprinted from Ref. [1])* (cont.)

Cancer site	Age at exposure (years)										
	0	5	10	15	20	30	40	50	60	70	80
Females											
Stomach	57	48	41	34	29	21	20	19	16	13	8
Colon	102	86	73	62	53	38	37	35	31	25	15
Liver	24	20	17	14	12	9	8	8	7	5	3
Lung	643	534	442	367	305	213	212	204	183	140	81
Breast	274	214	167	130	101	61	35	19	9	5	2
Uterus	11	10	8	7	6	4	4	3	3	2	1
Ovary	55	47	39	34	28	20	20	18	15	10	5
Bladder	59	51	43	36	31	23	23	22	22	19	13
Other	491	287	220	179	147	103	97	86	69	47	24
All solid	1717	1295	1051	862	711	491	455	415	354	265	152
Leukaemia	53	52	53	52	51	51	52	54	55	52	38
All cancers	1770	1347	1104	914	762	542	507	469	409	317	190

Note: These estimates are obtained as combined estimates based on relative and absolute risk transport, and have been adjusted by a dose and dose rate effectiveness factor of 1.5, except for leukaemia, which is based on a linear–quadratic model.

5.3.6. Dose conversion factors in paediatrics

Sources of data on dose conversion coefficients together with information on the type of phantom models used to obtain each set of data are summarized in ICRU Report 74 [38]. Table 16 gives references concerning coefficients for paediatric patients. Work is continuing on organ dose coefficients for CT as a function of size [60].

TABLE 16. IMPORTANT FEATURES OF SOURCES OF DOSE CONVERSION COEFFICIENTS FOR MEDICAL PAEDIATRIC X RAY IMAGING

Type of examination	No. of views	No. of organs	No. of spectra	Normalization quantity	Phantom	Reference
Radiography	[a]	24	[a]	K_i, P_{KA}	Cristy hermaphrodite[a,b]	[54]
	20	6	3	K_i	0, 1, 5 years, hermaphrodite	[55]
	20	26	72	K_i, P_{KA}	0, 1, 5, 10, 15 years, hermaphrodite	[56, 57]
	5/6	16/11	1[c]	K_i	Voxel baby, voxel child	[49, 58]
Computed tomography	45 slices	35	2	C_W	Voxel baby	[59]
	66 slices	37	2	C_W	Voxel child	[59]

[a] Views, spectra and phantom sizes can be freely selected.
[b] Available as a software program [50].
[c] Per view.

6. FACTORS AFFECTING MANAGEMENT OF RADIATION DOSE IN PAEDIATRIC RADIOLOGY

6.1. INTRODUCTION

The previous sections discuss methods that allow the collection of dosimetric data and their analysis to estimate the radiation dose to the paediatric patient and an analysis of the associated risk. X ray equipment, appropriately configured for adult imaging, does not usually result in properly managed paediatric examinations with appropriate dose levels and good diagnostic image quality [61, 62]. To achieve this optimal situation requires specific attention during the equipment specification [63–65] prior to purchase and configuration [66, 67] during commissioning phases in the equipment life cycle [5, 68]. After appropriate configuration, the medical physicist must verify equipment performance by conducting appropriate performance tests [69–74]. Two examples of appropriate performance tests are the dose per radiographic image acquisition or dose rate during fluoroscopy. This performance testing should initially occur before the X ray equipment is put into routine clinical use, with repeat testing at set intervals.

Once X ray equipment is in clinical use, the role of clinical staff becomes critical to the reduction of patient dose through the selection of the appropriate examination (justification) [12], selection of the equipment used, the use of correct scanning parameters (radiographic technique), comprehensive staff training and careful acquisition of the images (cooperation and positioning of the patient), and avoidance of unnecessary image acquisition during an examination.

Focused care designed to address the unique needs of paediatric imaging optimizes diagnosis and reduces radiation dose to paediatric patients. Ultimately, this means the use of paediatric hospitals, with dedicated paediatric facilities, using dedicated paediatric X ray equipment by dedicated paediatric radiological staff. If full dedication is not possible, the best compromise should be reached. For example, staff specifically trained in paediatric imaging, both radiologists and radiological technologists, should improve paediatric imaging, even if the imaging equipment and facilities are not totally modified for the unique needs of paediatric imaging. The best possible diagnostic performance at a properly managed patient dose is obtained when appropriately trained staff operate properly configured X ray equipment [75]. This section discusses factors that critically affect the level of radiation dose delivered to the paediatric patient during diagnostic examinations that involve the modalities of radiography, fluoroscopy or CT scanning. Any change of the critical factors will not only affect

the radiation dose delivered to the patient, but will also potentially affect the quality of the diagnostic image. One must always analyse potential loss of image quality associated with dose reduction configurations of the imaging equipment. As dose is reduced, a point is reached where the technique will not be used due to unacceptable image quality. It is better to have acceptable image quality at a somewhat reduced dose; an operational mode that will get used. Therefore, this optimization process ideally requires the cooperation of an imaging medical physicist with experience in paediatric diagnostic radiology, an experienced paediatric radiographer and a trained paediatric radiologist. After installation and configuration of the imaging equipment, a careful evaluation of image quality must be completed to ensure appropriate patient care [5]. While some comments concerning image quality changes associated with radiation dose changes are contained in the discussion below, a complete discussion of this important topic is beyond the scope of this publication.

As illustrated in Table 17 [76], two independent, yet interrelated, approaches are required to achieve an appropriate patient dose consistent with good diagnostic outcomes. First, the radiation dose delivered to the paediatric patient per image should be properly managed. It should be noted that the terms 'image' and 'images/study' in Table 17 refer to both the images created during fluoroscopy and in the radiography mode for archiving. While the fluoroscopic images only appear momentarily on the monitor of the imager, the production of each contributes dose to the patient. Secondly, the number of images should be minimized. The total number of images produced during the examination is determined by the total number of fluoroscopic images (pulse rate × fluoroscopy time) and archived images (acquisition rate × run time of acquisition). The dose per image on the left side of Table 17 usually differs by approximately an order of magnitude between the fluoroscopic image and the acquired image. Finally, the total dose to the patient is determined using these two approaches. A combination of these approaches should be considered during the equipment purchase phase by specifying the required hardware from the vendor that best addresses the unique imaging challenges of the paediatric patient.

TABLE 17. MANAGING TOTAL PATIENT RADIATION DOSE: MODALITY

Dose/image	Number of images/study
Specification of X ray equipment	Clinical justification
Configuration of X ray equipment	Non-ionizing modality substitution
Operator control of X ray equipment	Operator control of X ray equipment

Once purchased, the X ray hardware needs to be installed, configured and performance tests carried out (equipment commissioning). The configured features control the X ray image acquisition parameters of the equipment and the subsequent image processing algorithms to be applied to the acquired images. After any modification of the equipment, functional testing of all affected performance aspects of the imager is necessary prior to the first clinical use of the equipment [74, 77, 78]. Both of these processes must address the unique needs of paediatric X ray imaging [79].

After the proper X ray hardware has been installed, configured and performance tests carried out, the radiographer or any other operator must properly understand all of the controls and features of the X ray unit. At this point, in conjunction with the medical physicist, the examination protocols can be further developed to manage the radiation dose to the patient per image acquisition or per unit time for fluoroscopy. This important step cannot be achieved unless the radiographer receives extensive and appropriate training on basic imaging principles and on the unique controls of the purchased equipment [68].

The second approach to dose reduction (right side of Table 17) involves proper patient management to minimize the production of unnecessary images during the imaging examination, e.g. managing the number of images created during either radiography or fluoroscopy. First, the examination should be justified [12], i.e. the referring physician and radiologist should review the clinical need for the study relative to the associated risk of the examination. Non-ionizing alternative imaging modalities should be considered. Finally, the appropriately trained radiographer or radiologist [80] must carefully manage the acquisition process of the images to ensure that only necessary images are created during the examination.

6.2. X RAY EQUIPMENT SPECIFICATION

The first step in the optimal management of paediatric radiation dose is the correct specification of the hardware to be used for paediatric imaging. Consultation between the radiologist (who best understands the clinical needs of the examinations) [80–82], the X ray equipment vendor (who best knows their equipment product line) and the medical physicist specialized in diagnostic radiology is essential to properly select the appropriate X ray hardware. The following sections detail the various aspects of equipment performance that should be considered. Some of these dose reduction features may entail additional cost to the base price of the equipment.

The concept of dedicated equipment for paediatric imaging is important as some of the following recommendations may be difficult to implement if the

equipment is to be used for a mixed adult and paediatric patient population. Any unique equipment hardware or configuration for paediatric imaging should be specified and negotiated with the vendor prior to purchase of the equipment, especially in the case of complex equipment such as CT scanners or interventional equipment. The equipment should be configured during installation and this should be followed by application training. After the radiographer or radiologist obtains initial experience performing cases with the imager for 4–6 weeks, advanced application training is normally more effective [68].

6.2.1. Radiography/fluorography

6.2.1.1. Image receptors

Analogue (screen film) image receptors usually consist of a dual emulsion film sandwiched between two fluorescent screens contained within a light tight cassette. The combination of the emulsion characteristics of the film and the fluorescent properties of the screen determine the sensitivity of the analogue image receptor, which directly affects the paediatric patient dose [5]. Typically, sensitivity classifications for general paediatric imaging are approximately double (more sensitivity results in less radiation dose to the patient) those used for extremity paediatric imaging. Multiple sized image receptors ranging from 18 cm × 24 cm to 35 cm × 43 cm are needed. The sensitivity class of analogue image receptors should be carefully considered when purchased.

Two different types of digital image receptor are common in radiography, computed radiography[30] (CR) and direct radiography. CR plates are contained within a cassette and come in the same dimensions as analogue image receptors. The radiographer handles the plates housed within cassettes similarly to the way analogue image receptors are handled, thus eliminating the need to modify the X ray machine to obtain a digital image. After exposure, the image on the CR plate is digitized with an external processing unit and stored as a digital electronic image. Since single sided CR readers are normally operated with a sensitivity classification of 200 for general radiography [83], the patient's radiation dose may be approximately doubled compared to the dose received from an analogue image receptor with a sensitivity classification of 400. CR readers with newer technology can decrease patient radiation dose relative to analogue image receptors, e.g. CR plates read on both sides, and needle phosphor plates.

The second type of digital image receptor, the flat panel detector (direct radiography), directly converts the energy of the image X ray pattern emitted

[30] Technology using photo-stimulable phosphors to capture an image.

from the patient's body to a digital image that is stored [84, 85]. This image receptor is mounted in the X ray equipment in place of the standard Bucky tray. This detector's dimensions are usually 43 cm × 43 cm for radiography. This direct digital image receptor eliminates the need for the radiographer to handle the image receptor during the exposure process. The digital detector, when properly configured and used, normally provides comparable or better image quality at equal or less patient dose than traditional analogue image receptors [86].

The majority of image equipment manufacturers offer both small and large format image receptors for interventional fluoroscopic equipment. The small format is usually 20 cm × 20 cm while the large format may be 30 cm × 40 cm or 40 cm × 40 cm. The small format image receptor, typically found in the adult catheterization laboratory, is designed to image the adult heart, but may be replaced by a larger image receptor in a paediatric catheterization laboratory to allow the visualization of the heart and the pulmonary vessels of the lung fields in the same FOV in the smaller patient [86].

Image receptors exhibit different detector quantum efficiency (DQE) [5, 87–90], which is a measure of the detector's ability to convert X ray quanta into image quality. Paediatric radiation doses may be reduced by the use of an image receptor with a higher DQE. For example, double sided CR plates provide a higher sensitivity or DQE than equivalent single sided plates. The DQE of flat panel detectors normally exceeds the DQE of analogue image receptors [91]. The DQE of image receptors should be carefully compared when purchasing imaging equipment for paediatric applications [92].

6.2.1.2. Grid

The ability of a grid to attenuate scatter radiation prior to the image receptor is directly related to the lead content of the grid (in grams per square centimetre). This parameter is determined by the height and width of the grid strips and the width of the interspace material of the grid [93]. Scatter levels during paediatric imaging are reduced due to the smaller volume of the patient's body; less lead content is required. A grid with less lead content reduces the radiation dose to the paediatric patient. Either reducing the grid ratio or decreasing the lead strip thickness can achieve this. In addition, the use of carbon fibre cover sheets for the grid also reduces the patient dose by 20–30% [94, 95]. The selection of interspace material with low Z composition (e.g. carbon) will have a similar effect. The focal line of the grid must match the focus image receptor distance of the examination. Parallel as opposed to focused grids with low grid ratios are easier for the radiographer to position when performing mobile X ray examinations.

The number of lines specified for a stationary grid must be increased to reduce artefacts in the image due to interaction of the grid line shadows

superimposed on the displayed image. Since the increase in the number of lines in the grid reduces the grid's lead content, if the grid ratio or lead septa thickness is unchanged, the ability of the high line number grid to remove scatter is reduced. Alternatively, increasing the number of lines for a stationary grid can be avoided if the digital image receptor has the ability to mask the lines with digital image processing. Since smaller paediatric patients can be successfully imaged without a grid, an imager with a removable grid should be specified where possible and documented within written protocols.

6.2.1.3. Tabletop material

The tabletop must be strong enough to support the patient's mass, but ideally should transmit all of the X rays emitted from the patient. The specification of the aluminium equivalent of the tabletop indicates the amount of X ray attenuation that will occur. In radiographic applications, an aluminium frame usually supports a tabletop material of low Z materials. Care is required in selecting table pads. Pads designed to efficiently pass X rays are normally more expensive. If the tabletop and pad are between the patient and image receptor, e.g. most radiographic applications or remote fluoroscopic units with the X ray tube overhead, patient radiation dose increases when tabletop and pad attenuation increases. Tabletops with reduced aluminium equivalence [96] reduce dose to the paediatric patient by approximately 10% [95]. For interventional fluoroscopic equipment, the tabletop, usually consists of carbon fibre, which is strong enough to support the mass of the patient despite the cantilevered geometry of the tabletop relative to the pedestal base. Since the patient is between the tabletop/pad and image receptor for most geometries used in interventional equipment, attenuation in the tabletop/pad does not affect patient dose.

6.2.1.4. Focal spot sizes

X rays are generated [97–99] at the focal spot on the anode of the X ray tube [100, 101] contained within its protective housing [102]. The use of a smaller focal spot results in less geometric unsharpness in the image, but restricts the tube loading. Most X ray tubes contain two focal spots of differing dimensions, e.g. nominally 0.6 and 1.2 mm for general radiography or fluoroscopy. Paediatric imaging does not require as much X ray tube loading as adult imaging which allows the use of smaller focal spots. Some manufactures have dual focal spot combination tubes of 0.3 and 1 mm or 0.3 and 0.6 mm nominal size [103], which may be better choices for a radiographic room or general fluoroscopic room if the imager can be dedicated to paediatric patients.

X ray tubes in interventional fluoroscopic equipment may have a nominal small spot of 0.4–0.5 mm and a large focal spot of 0.8–0.9 mm. Some X ray tubes are available with three focal spots, typically 0.3, 0.6 and 1 mm nominally. This flexibility of three focal spot sizes allows imaging the smallest, medium and largest paediatric patients with a focal spot with appropriate loading. The smallest focal spot, with an adequate kilowatt rating to image up to 3–5 year olds, results in less geometric unsharpness in the image of the patients with the smallest anatomical detail. While a triple focal spot X ray tube does not reduce radiation dose, the image quality on the smallest paediatric patients is improved at the same dose level [103].

6.2.1.5. Added beam filtration

Patient radiation dose can normally be reduced relative to the dose with standard filtration of approximately 2.5–3 mm Al total filtration by adding fractional millimetre filters with atomic numbers significantly greater than that of aluminium, such as copper [103, 104–118]. The ideal filter material may depend on the composition and energy response of the image receptor [119–122]. Since the added filter attenuates a significant portion of the lower energies within the radiation beam, these higher atomic number filters require relatively high kilowatt ratings for the selected X ray tube focal spot and generator for larger children. Thicker filters may be successfully used for smaller patients to more effectively reduce radiation dose if the imager has the capability of changing the selected added filtration. This requirement can be programmed into the protocol settings on some digital equipment [123].

6.2.1.6. Automatic exposure control

AEC[31] devices measure the rate of energy arriving at the image receptor and terminate the radiation exposure when the correct level has been delivered. Typically, the use of AEC devices results in a more consistent delivery of the correct amount of energy to the image receptor since the radiographer is not required to estimate the attenuation of the patient's body. Unfortunately, the geometry and spacing of the individual sensors of the AEC device are usually optimized for adult sized patients. If the manufacturer provides an AEC sensor geometry more suitable for paediatric imaging, this option should be selected.

---

[31] AEC systems may also be known by other names including 'automatic dose control', 'automatic dose rate control' and 'automatic brightness control'. The latter originally described the automatic control of video voltage levels from TV cameras, but is now sometimes applied to the exposure control of fluoroscopic systems.

6.2.1.7. X ray generator

The X ray generator specified for paediatric patients should have a relatively high power rating greater than 75 kW. Higher kilowatt generators usually have faster rise and fall times of the applied high voltage, which reduces the low energy X rays that contribute only to patient dose at the beginning and end of each exposure [100]. The faster switching is better suited to the use of AEC, especially for small patients that require very short exposure times. The higher kilowatt rating is needed for small patients if higher Z beam filters are used to reduce patient dose.

6.2.1.8. Kerma area product meter

KAP meters provide the information necessary to track the air P_{KA} associated with radiographic or fluoroscopic procedures [9, 124]. While most manufacturers include this type of dosimeter in their product line, some manufacturers offer this capability only as an additional cost option. In the case of paediatric imaging, where knowledge of patient radiation dose may be necessary to provide good patient care, the option to include a KAP meter when purchasing equipment should be selected despite the additional cost. The KAP meter should ideally have a digital resolution (0.1 μGy·m^2 or better) for paediatric exposures. Any KAP meter that is present should be calibrated annually as discussed in Section 2.2.2.

6.2.1.9. Number of imaging planes

Typical paediatric interventional fluoroscopy equipment consists of two imaging planes [86]. The toxicity of iodine limits the total burden of this contrast agent that the small paediatric patient can tolerate [103, 125]. This requires the simultaneous imaging in two planes during each injection of contrast to obtain all of the required imaging projections prior to reaching the contrast limit of the patient.

6.2.1.10. 'Last image hold' and 'grab'

This feature continuously displays the last video frame of fluoroscopy after the exposure switch is released. Since this feature allows the operator to study the displayed static image after release of the exposure switch, it is imperative for any fluoroscopic imager used for paediatric imaging. The 'grab' feature allows the fluoroscopic single image frame to be stored.

6.2.1.11. 'Fluoro-loop store/playback'

This feature allows the operator to store the most recent fluoroscopic sequence in the memory of the imager after the fluoroscopic exposure switch has been released. After the store process is complete, the operator may replay the stored fluoroscopic sequence in real time. Since the fluoroscopic sequence is stored in the imager's memory, this sequence may, in some instances, be used in place of a higher dose rate acquisition run for documenting the results of the study. Some manufacturers only offer this feature as an additional cost option. This option should be selected if the imager is going to be used for paediatric imaging.

6.2.1.12. Collimator features

Some collimators provide a graphical indication of the location of the collimator blades, sometimes called virtual collimation, while they are actively being moved on the last image hold fluoroscopic image. This feature eliminates the need to irradiate the patient while adjusting the position of the collimator blades. If the manufacturer offers this feature only as an additional cost option, the option should be selected to reduce radiation dose to the paediatric patient.

Adjustable equalization filters, consisting of movable wedges, compensate for attenuation differences between adjacent tissues, e.g. the mediastinum and lung fields, to improve image quality and reduce the integral dose to the patient. Since the position of these wedges is typically graphically displayed as described in the previous paragraph, the operator can carefully position the wedges without delivering an additional radiation dose to the patient.

6.2.2. Computed tomography

An independent evaluation of the scanners under consideration may be helpful in determining which vendor's equipment is best suited to the institution's imaging requirements.

6.2.2.1. Image detector sensitivity

The image detectors of CT scanners exhibit different DQEs, which is dependent on the solid state material used by the manufacturer. Paediatric radiation doses may be reduced by the use of an image receptor with a higher DQE. The DQE of image receptors should be carefully compared when selecting the manufacturer of a CT scanner.

Key points for writing specifications for paediatric radiography/fluorography equipment

Higher priorities in a resource limited setting

— *Select a sensitive image receptor. If using a screen film system, select the speed class 400/200 for general/extremity work.*
— *Fluoroscopy equipment should have 'last image hold' and 'grab' capability.*
— *Ensure that the grid can be removed when required.*
— *Select grid(s) with appropriate grid characteristics.*
— *Select the image receptor with the highest detector quantum efficiency.*
— *Select a grid with low Z cover and interspace material.*
— *Obtain equipment with a range of additional filtration options, preferably with programmable selection.*
— *Obtain graphically displayed collimators, where possible.*
— *Ensure that a kerma area product meter with a digital resolution of 0.1 μGy·m² or better is included.*
— *Obtain 'fluoro-loop store/playback', if available.*
— *Avoid tabletop pads for radiographical examinations.*

Lower priorities in a resource limited setting

— *Select a low attenuating tabletop.*
— *If using a computed radiography system, select double sided computed radiography plates.*
— *Where possible, obtain equipment with a range of focal spot sizes, down to 0.3 mm.*
— *Select paediatric automatic exposure control, if available.*
— *Obtain equalization filters, where possible.*
— *Select a higher kilowatt generator to obtain faster switching times and allow the use of thicker spectral filters.*
— *For interventional fluoroscopy, two (simultaneous) imaging planes are preferable to one.*

6.2.2.2. Number of detectors in the z direction

The z direction of the CT scanner is parallel to the long axis of the patient when lying supine on the patient support. Single slice CT scanners provide only one detector in the z direction, which allows the acquisition of data for only one image slice of anatomy per revolution of the gantry. Currently, CT scanners are

available with up to hundreds of detector elements in the z direction [126–128]. This allows acquisition of a larger volume of data with each revolution of the scanner and, hence, reduced examination time. The ability to complete paediatric examinations in less time may eliminate the need to sedate or anaesthetize young children. The need for speed in paediatric imaging should be weighed against the increased cost when a new CT scanner is purchased. A feature of some multi-detector CT scanners is adaptive collimation, which reduces the dose at the beginning and end of the helical scan acquisition. As over-ranging can give a large increase in patient dose, including irradiation of organs outside the volume of interest, such collimation should be obtained if at all possible [129].

6.2.2.3. Number of X ray sources

Traditionally, CT scanners have utilized a single source of X rays and one detector array. Currently, a system is available with two X ray sources and two detector systems [130]. The duplicate sources can be used to complete an examination more quickly, to allow improved imaging of rapidly moving organs such as the heart, or to facilitate the use of dual energy acquisitions. Since two imaging planes significantly increase the cost of the scanner, clinical advantages must be weighed against increased cost at the time of purchase.

6.2.2.4. Image analysis packages

Creating diagnostic CT images is primarily a two-step process. First, the X ray pattern in space exiting the patient is captured by the image receptor in the form of a cylindrical volume of raw data. The ability to generate different types of clinical image from this raw dataset is dependent on the types of image analysis software package available. For example, a different software package is usually needed to create transverse, sagittal or coronal images, to create 3-D images, to complete a ‘fly through’ of the colon, to perform CT angiography, to perform cardiac CT, to perform specialized dental examinations and to perform bone densitometry. The site’s unique clinical practice should be carefully evaluated to determine the number of necessary software options [131].

6.2.2.5. Partial scanning

If the scanner has the capability of turning off the X ray beam for a portion of each 360° rotation, this feature can be used to reduce the dose to surface organs, such as the breast, eyes and male gonads.

6.2.2.6. Cone beam computed tomography

CT scanners with extended detectors in the z direction allow coverage of larger patient scan lengths with a single rotation of the scanner. In some paediatric applications, the scan length from a single rotation may be sufficient. In this case, the entire study can be completed in less than 1 s, which minimizes motion artefacts in children that may be prone to movement during the acquisition.

Key points for writing specifications for paediatric computed tomography equipment

Higher priorities in a resource limited setting

— *When selecting a computed tomography scanner, compare the detector quantum efficiency of the detectors.*
— *Obtain suitable paediatric software packages.*
— *Consider the number of detectors in the z axis.*
— *Consider effects of over-ranging and the need for speed when selecting the number of detectors and imaging planes.*
— *Consider partial scanning to reduce the dose to surface organs.*

Lower priorities in a resource limited setting

— *Consider the use of two X ray tubes and detectors giving two planes of acquisition.*
— *Consider the use of a dual energy X ray system.*
— *Consider cone beam computed tomography.*

6.3. CONFIGURATION OF SELECTED EQUIPMENT

To achieve a proper configuration, the radiologist, other clinical staff members and the medical physicist must clearly communicate the clinical needs and paediatric imaging challenges to the vendor's representatives [132]. The vendor's representatives, typically senior application specialists and senior design engineers, must, in turn, communicate with the appropriate facility staff and demonstrate the operational design capabilities of their equipment that can be harnessed to meet clinical objectives. The configuration of anatomical programming features used for acquisition and image processing by the unit must be set up properly to meet the unique clinical needs of the facility prior

to the beginning of functional testing of all aspects of the imaging acquisition and processing prior to the first clinical use of the unit [68]. This might also be followed by a similar review 4–6 weeks after the commencement of routine clinical examination to confirm that the desired operation of the X ray unit is available and understood by the clinical staff.

After the initial commissioning of an X ray unit, periodic testing must be performed by a medical physicist to ensure its continued proper performance [68]. Annual results should be compared to original baseline performance data collected from the X ray unit during commissioning. The ability to change commissioned configurations should be limited to individuals under the supervision of the medical physicist.

The acceptable paediatric patient dose is driven by the imaging task. Since increases in the quantum mottle should be acceptable in some high contrast studies, significant dose reduction in these types of study may be possible. Since increased quantum mottle directly reduces low contrast image quality, tolerable dose reductions for these images will likely be smaller. The facility should make these types of adjustment to protocols in consultation with the medical physicist [103].

6.3.1. Radiography/fluoroscopy

If the imager has an anatomical program feature, the configuration of the acquisition parameters should be set to select the appropriate parameter as a function of patient size within this feature. This means that specific examination set-ups, e.g. posteroanterior (PA) chest, should contain multiple sub-set-ups, one each for a small range of patient sizes (approximately 6–8 ranges). Four to six should be adequate for fluoroscopic studies. The configuration should address each of the parameters described below.

If the imager does not provide anatomical programming or it is not possible to customize it for paediatric patients, the following parameters should be set manually as a function of patient size. Agreed upon protocols should be documented and be readily available.

6.3.1.1. Focal spot size

As discussed in Section 6.2.1.4, less usual focal spot size combinations can provide significant benefits during paediatric imaging. The anatomical programming of the imager should be configured to select the smallest available focal spot that provides adequate tube loading as a function of patient size.

In an interventional fluoroscopy room, the size of focal spots available, the size of the patient and the resolving capability of the image receptor dictate

the appropriate focal spot size for a given examination [103]. For example, in a cardiac catheterization laboratory, it can ideally be assumed that 0.3, 0.6 and 1 mm focal spot X ray tubes are available. Fluoroscopy should be performed on the 0.3 mm focal spot until patients reach the size of small teenagers. Small to large adults should be imaged with the 0.6 mm focal spot. The 0.3 mm focal spot has an adequate kilowatt rating to image up to 3–5 year olds during radiographic acquisitions at up to 30 frames/s and results in less geometric unsharpness on the smallest patients. The 0.6 mm focal spot is appropriate for small children to small teenagers. The 1.0 mm focal spot provides the kilowatt rating needed to penetrate the largest adults.

6.3.1.2. High voltage, tube current and pulse width

Radiographic technique factors, X ray tube voltage (kV), tube current (mA) and duration of the exposure (s) are the fundamental controls the radiographer uses to control radiation dose to the patient and resultant image quality of the examination [93]. The following provides one possible approach. Where possible (typically the smallest patients), the effective energy of a highly filtered X ray beam should just exceed the k-edge response of the image receptor or contrast media [106, 123]. A typical k-edge energy response for iodine contrast media is approximately 35 keV. For the smallest children, this is achieved with added filtrations up to 0.9 mm Cu, with approximately 58 kVp. As the size of the patient increases (pre-teenagers), the added filtration is decreased and the kVp is increased until it reaches 66 kVp and 0.2 mm Cu. For larger body sizes, the kVp is increased to provide adequate penetration with either 0.2 or 0.1 mm Cu filtration, depending on the desired level of dose reduction; maintaining reasonable dose levels results in some loss of subject contrast as the patient approaches the size of an adult.

Radiation doses may be reduced in some cases with the use of digital image receptors by increasing the tube voltage by 10 kV with respect to the optimum base line value [133]. The greater penetration of the higher energy X rays through the patient's body reduces the necessary incident air kerma for a selected detector dose, which reduces radiation dose to the patient. The loss of subject contrast by the increase of tube voltage is recovered in the image by the radiologist or the interpreting physician when viewing the digital radiographs by the selection of a narrower viewing window. A detailed management of radiation dose would go in parallel with an optimization study of image quality. This involves measurement of the signal-to-noise ratio (SNR) and could, for example, be through a metric such as the $(SNR)^2$/dose [134].

The duration of the exposure for small paediatric patients whether during pulsed fluoroscopy or radiographic modes should be

approximately 5–8 ms [86, 103]. Exposure times longer than this range create images with unnecessary motion unsharpness. Exposure times shorter than this range in the radiographic mode are difficult to properly control because of the finite time required for the AEC to terminate the exposure. Since the appropriate tube voltage is restricted by contrast demands in the image and the exposure duration is limited by patient motion, the X ray fluence required due to the size of the paediatric patient should be accommodated by changes in the X ray tube current where possible. This means that the exposure time resulting from a falling load generator (generator designed to maximize the tube current and minimize exposure time for a selected high voltage) during paediatric imaging could be too short to provide consistent results when using the AEC mode.

6.3.1.3. Pulse rate

The pulse rate is the number of radiation pulses that occur per second in either the fluoroscopic mode or serial radiographic (acquisition) mode. The ability to reduce the pulse rate can make a significant contribution to patient dose reduction, with only a small degradation of image quality due to loss of temporal resolution if equipment is set up and used properly. The appropriate pulse rate for each segment of a procedure is a function of the operator's ability to deal with the loss of temporal resolution and the imaging challenge of that segment of the study. In general, cardiac studies in children require higher pulse rates than do those in adults because of the faster heart rate of children [86]. Either 15 or 7.5 pulses per second, instead of 30, may suffice during either fluoroscopy or radiographic acquisitions during interventional cardiac catheterizations. Non-cardiac interventions are normally performed with similar pulse rates during fluoroscopy; 4, 3, 2 or 1 radiographic acquisitions per second are used [103]. For fluoroscopic studies in the gastrointestinal/genitourinary examination room, 8, 4, 2 or 1 fluoroscopic pulses per second are typical [135].

6.3.1.4. Added beam filtration

Provided the image equipment has the capability of selecting different thicknesses of higher atomic number filters, appropriate filter thicknesses, as a function of patient size, should be programmed. The manufacturer's recommended programs for adults tend to use high pulse widths to provide the large number of photons needed to penetrate the filter and large patient during fluoroscopy [103]. The large pulse width is not appropriate for children due to increased motion unsharpness. The thickness of the filter is limited by the kilowatt loading of the focal spot, by the need for short pulse widths and by the thickness of the body part being imaged. For example, neonates and babies can

usually be imaged at lower radiation dose levels with reasonable exposure times by adding copper or equivalent filtration with a reduced tube voltage to maintain reasonable subject contrast. Similar strategies can be used in most paediatric situations. Neonates and babies can usually be imaged at the lowest radiation dose levels with reasonable exposure times by adding up to 0.9 mm of copper or equivalent filtration with a reduced tube voltage to maintain reasonable subject contrast. As the child increases in size, the thickness of the added copper filter should be reduced as discussed in Section 6.3.1.2.

6.3.1.5. Automatic exposure control

Depending on the type of radiographic examination, a unique combination of the three standard sensors on the AEC detectors is activated. For example, an adult PA chest examination would typically utilize the lateral sensors. Since the area of the lung fields of the smaller child is not large enough to shadow the lateral sensors, the PA chest of the smaller child must be acquired using only the central sensor. The paediatric lateral chest projection should also use the central sensor. In some examinations, the limited size of the patient does not allow the use of AEC. The proper use of AEC must be included in each appropriate anatomical program. If the anatomical programming allows the duration of the backup timer to be adjusted, the programmed backup mAs for a given patient size should be approximately double the anticipated mAs required for the examination.

In the case of fluoroscopy, the added filtration should be changed by the AEC curve as a function of patient size to provide the appropriate pulse width as specified in Section 6.3.1.2. Large thicknesses of filtration appropriate for small patients result in excessive pulse widths if the filter thickness is not reduced for larger patients [103, 136]. Most manufacturers provide multiple sets of curves; the most appropriate one for each type of examination should be selected at the configuration of the imager.

6.3.1.6. Incident air kerma at image receptor (radiographic mode)

Analogue image receptors immediately indicate inappropriate image receptor incident air kerma through either a low optical density on the radiograph (indicating under exposure) or a high optical density (indicating high patient exposure). Since digital receptors are designed to provide the appropriate brightness in the image irrespective of any under or overexposure to the patient [90], this important direct feedback to the operator is lost. The quantum mottle in under exposed images is excessive, and most radiologists will identify and object to these images. However, most radiologists will not complain about overexposed digital radiographs, since the brightness is correct and the quantum mottle will be less than normal. If

radiographers select their own radiographic techniques, they may learn, when using digital image receptors, that the number of complaints they receive from radiologists can be minimized if the radiation dose to the patient is increased. This is known as 'dose creep' [89] and can be avoided by loading standardized radiographic technique factors into the anatomical programs of the imager's generator or, where this is not possible, tabulating factors as a function of size, and insisting that all staff members use these technique factors. The sensitivity of the AEC sensors must be carefully adjusted to provide the appropriate entrance air kerma at the image receptor to provide good image quality by the chosen type of image receptor.

6.3.1.7. Image receptor incident kerma rate (fluoroscopic mode)

An optimum entrance air kerma rate to the patient is achieved by maintaining the proper image receptor incident kerma rate for each created image during a variety of operational modes of either fluoroscopy or image recording. For a given examination, this is a function of the radiographic technique factors, the DQE of the image receptor, the operator's tolerance of quantum mottle in the image and the specific imaging task [137–139]. All of these factors must be considered when initially calibrating the imager.

For image intensifiers, the image receptor incident kerma rate changes as a function of the FOV selected by the operator. Here, it is typically proportional to $1/FOV^2$, 1/FOV or a constant depending on the presence of a configurable aperture. These designs, respectively, increase the image receptor incident kerma rate fourfold, twofold and not at all as the FOV is reduced to half of its original size. Proportionality to 1/FOV is a reasonable choice for paediatric imaging with image intensifiers [103]. If the image receptor is a flat panel that does not change binning as the FOV changes, constant image receptor incident kerma rate is a choice that prevents increases in patient dose as the FOV gets smaller and should provide adequate image quality [103]. Provided the recommendations of this paragraph are followed, an image intensifier based fluoroscope will increase image receptor incident kerma rate more than a flat panel detector fluoroscope as the operator reduces the FOV.

The incident kerma per image during fluoroscopy should ideally be configured to increase when the operator reduces the pulse rate[32] from 30 to 7.5 pulses per second during pulsed fluoroscopy to maintain a constant perceived noise level in the image [140]. For frame rates exceeding 6 frames/s, the incident air kerma per image as a function of frame rate is proportional to the square root

[32] The typical reference pulse rate for equipment in the USA is 30 pulses per second. In other regions, the pulse rate may be set at other frequencies (e.g. 25 pulses per second).

Key points for the configuration of paediatric radiography/fluoroscopy equipment

— *Set up size specific protocols for each examination type — ideally within an anatomical program feature, or else using a hard copy display.*
— *Set tube voltage/filtration to provide an adequate contrast to noise ratio at reasonable patient doses.*
— *Set the generator to ensure the pulse or exposure time is 5–8 ms for small patients.*
— *Ensure that reduced pulse rates are implemented.*
— *Optimize filtration to allow short exposure times at low dose. Check the effect of automatic exposure control on filter selection.*
— *Ensure that the appropriate focal spot is configured for different examinations and patient sizes.*
— *Ensure that the image receptor incident kerma rate is set to obtain the needed image quality without unneeded patient dose.*
— *Ensure that the correct field of view is set for appropriate procedures.*
— *Configure the automatic exposure control for both radiography and fluoroscopy for all appropriate examinations.*
— *Ensure appropriate image processing parameters are used in the needed procedures*.
— *Post charts or have a documented manual nearby to assist radiographers in understanding the automatic programme set-up, including options for low dose and high contrast automatic exposure control settings for radiography and fluoroscopy.*
— *For complex procedures, ensure that an examination setting and teaching file is available.*

of (30 pulses per second/pulse rate). If the pulse rate is less than 6 frames/s, the incident kerma per image is constant [103].

Finally, when copper filters or filters with atomic numbers greater than copper are added to the X ray beam compared to the standard added filtration of aluminium, the effective energy of the X ray beam exiting the patient is increased. Thus, fewer information carriers (X rays) are required to deliver the same energy to the entrance plane of the image receptor. The reduction in X rays increases quantum mottle in the image unless image receptor incident kerma rate is increased. It has been recommended [103, 141] that image receptor incident

kerma rate be increased by a factor of 1.4 or 2 if the added filtration is <0.2 mm copper or >0.2 mm, respectively.

6.3.1.8. Image post-processing parameters

The previously discussed considerations in Section 6.2.1 improve the acquisition process of the images with a reasonable radiation dose to the patient [85]. In addition, image processing parameters must be carefully optimized for each type of examination as a function of patient size to produce a reasonable image. Image processing is normally achieved by defining the appropriate lookup table in combination with different image filters [84]. For example, the edges in the image may be sharpened to improve high contrast resolution at the expense of increased perceived noise when the imaging task involves high contrast objects. If the imaging task involves the detection of low contrast objects, perceived noise needs to be reduced by smoothing the image at the expense of the sharpness of edges within the image. Images that are appropriately processed (enhanced) may allow the imaging task to be achieved with a reduced dose to the image receptor and subsequent reduced radiation dose to the patient.

6.3.2. Computed tomography

The configuration of the available scan parameters ultimately affects the radiation dose per image [142] to the patient and the volume of patient anatomy that is irradiated. Combinations of scan parameters for each type of study should be considered, selected and inserted into the scanner's anatomical programs. In children, the first step in managing patient dose involves controlling the patient dose as a function of the size of the patient.

6.3.2.1. Patient dose versus patient size

The small size of the neonate or infant relative to a large adult requires a large dynamic range of radiological technique factors. A neonate has a PA thickness of about 6 cm, while a large adult can have a PA thickness of more than 30 cm [143], as illustrated in Fig. 5 [103]. If the HVL of tissue is assumed to be approximately 4 cm at 120 kV for a CT scanner with typical bowtie filtration, the range of patient sizes approximates six or more HVLs. This requires a dynamic range of tube current values of approximately 50–100 mA if the tube voltage, rotation time and pitch of the scan are unchanged to deliver approximately the same photon fluence to the detector of the CT scanner.

Two steps are needed to develop size appropriate CT scan parameters for children. In the first step, a medical physicist specialized in diagnostic radiology

should measure the radiation output from the facility's CT scanner in accordance with the methods outlined in Section 2 and estimate the radiation dose for an adult sized abdomen and head CTDI phantom, using typical scan parameters for the average adult patient. It should be ensured that protocols for adults have been set up properly. Under no circumstances should estimates of patient dose be based on comparison of scan parameters between two different scanner manufacturers or models due to differences in CT scanner design.

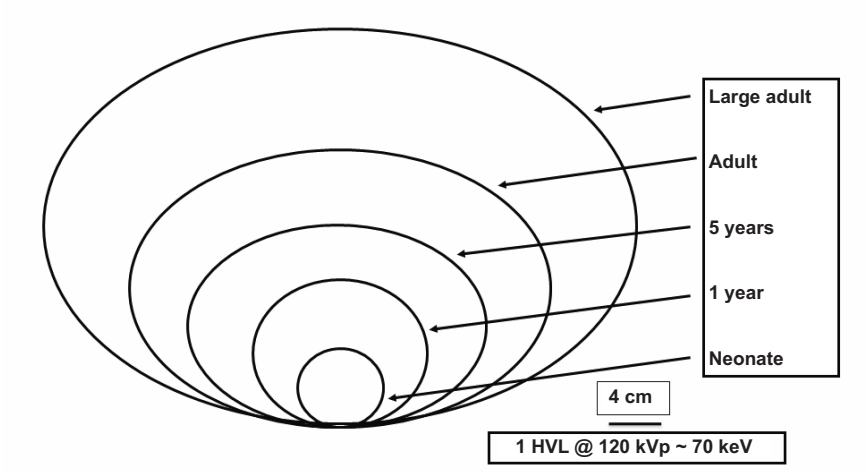

FIG. 5. Effect of patient size on displayed $CTDI_{VOL}$ and dose length product. HVL: half-value layer.

The second step is the development of appropriate CT scan parameters for children based on the facility's adult standards established in the previous paragraph. The simplest reduction of radiation/image rate from the scanner for children results from reducing the tube current time product of the scanner. Universal manual technique protocols (protocols that can be applied to any scanner of any manufacturer, model or age) that recommend reduction of mAs as a function of patient size are available[33]. These instructions assume that all other technique factors remain fixed. If this simple protocol is followed, the patient dose will be approximately independent of patient size and approximately equal to the radiation dose delivered by the facility to its adult sized patients. If the AEC features of the CT scanner are being used, the AEC system may automatically reduce the exposure parameters for children provided the adult baseline is set up

[33] www.imagegently.org

properly; the correct operation of the AEC and resultant clinical setting should be verified following steps 1 and 2 above.

Several authors have advocated reducing tube voltage in order to reduce paediatric radiation doses [144–149]. One strategy is to reduce the tube voltage to improve contrast in the image and adjusting the mAs to maintain the original dose, which should result in improved image quality at the same patient dose. Another strategy is reducing the dose when lowering the tube voltage. In this case, more quantum mottle should be tolerable in the image (lower patient dose) because the contrast in the image is improved by the reduced tube voltage. Hence, if the contrast and quantum mottle increase by the same ratio, the contrast to noise ratio should remain unchanged. In this case, image quality should remain unchanged while patient dose is decreased. The facility should work closely with a medical physicist to ensure appropriate maintenance of image quality when patient dose reductions are implemented.

6.3.2.2. Scan projection radiography

Scan projection radiography (SPR), also known as scanograms or scout views, should be acquired in PA as opposed to anteroposterior (AP) projection. This may require reprogramming of the SPR view default. This reduces organ doses to radiosensitive organs of the patient such as male gonads, breast, thyroid and the lens of the eye. Proper adjustment of the high voltage and tube current used for the projection view also affects radiation dose to the patient [150].

6.3.2.3. Manual versus automatic exposure control

More recent CT scanners provide AEC features that are designed to change the tube current (mA) in response to the length of the pathway of the X rays through the patient's body. The tube current changes as the beam rotates around the patient and as the beam translates along the z direction of the patient's body. AEC strives to create images with the same quantum mottle regardless of the path length of the radiation through the patient's body [151]. Some scanners allow straight forward application of AEC to adult or paediatric patients. Other scanners' AEC may not be as intuitive and may require additional choices by the operator as a function of patient size. This automatic mode can be selected or deselected by the operator. When the automatic mode is 'off', the tube current operates at a constant value regardless of the rotational projection of the beam or the location of the beam along the z axis of the patient. The AEC mode of the CT scanner should not be used for paediatric imaging if a medical physicist has not verified with measurements that its performance is appropriate for paediatric imaging. In some instances, use of the AEC mode

may increase the patient dose relative to the manual mode. If the CT scanner's configuration of the AEC mode is not properly adjusted for the smaller body parts of children, the radiation output of the scanner in the AEC mode may exceed the radiation output of the scanner when the operator selects appropriate paediatric techniques manually.

6.3.2.4. Focal spot size

CT scanners are typically equipped with two focal spot sizes. The smaller focal spot provides better high contrast resolution. The larger focal spot provides the increased tube currents necessary to acquire scan data in the shortest period of time. While almost all scanning of large patients is performed with the large focal spot to reduce scan time, a significant amount of scanning of smaller patients can be performed with the smaller focal spot. However, the selection of the smaller focal spot may need to be programmed into protocols that will be used for smaller patients within the anatomical programs of the scanner.

6.3.2.5. High voltage, tube current and rotation time

The product of the tube current (rate of X ray production) and rotational scan time (duration of X rays per revolution of the gantry), commonly known as the mAs, controls the number of X rays produced during the scan. For a fixed tube voltage, patient radiation dose is proportional to mAs and quantum mottle is proportional to $1/mAs^{0.5}$. If the manual tube current mode is used, the mAs should be adjusted in response to the patient's physical dimensions (see Section 6.3.2.1). The required mAs is also dependent on the specific imaging task (see Section 6.3.2.1). When performing a high resolution chest CT examination, a lower mAs can be used to assess airway patency and parenchymal lung disease, since high contrast images are primarily affected by sharpness. Similarly, the use of special low dose protocols to view the ventricular size and location of the tip of the catheter within the head has been reported [152]. On the other hand, a higher mAs (higher dose) is required to assess the presence of metastases in the liver as the low contrast image is primarily affected by quantum mottle. If tube current modulation is used, a setting is usually required to adjust the quantum mottle in the image.

Increasing the tube voltage increases the energy carried by each photon and results in a more penetrating X ray beam. A lower tube voltage decreases patient dose and increases quantum mottle in the image, while an increase in the tube voltage has the opposite effect if the mAs is unchanged. Typically, the mAs is changed in the opposite direction of the change in high voltage to reduce the degree of change of the radiation dose and of quantum mottle in the image [153].

The choice of tube voltage should be based on the need for subject contrast (see Section 6.3.2.1) in the image as well as on subject size. The bony details of the patient's anatomy or soft tissue in studies using an intravenous or intraluminal contrast agent are increased by a reduction in tube voltage and an increase in the mAs to maintain acceptable quantum mottle in the image. 100 kV is reasonable for patients with a lateral dimension up to 41 cm, while 80 kV is recommended for patients with a lateral dimension less than 36 cm [149]. To evaluate soft tissues without intravenous or oral contrast, 120 kV is reasonable for the majority of soft tissue imaging in children [144].

6.3.2.6. Field of view/filtration

When image parameters are programmed into the anatomical programming sets of the scanner, the smallest FOV available on the scanner that completely encompasses the patient anatomy should be selected. Artefacts in the image will be created if the FOV does not completely encompass the patient anatomy. Using the smallest FOV reduces the size of the end dimension of the voxel, which improves the high contrast resolution in the image. This allows better visualization of the small anatomical organs of the paediatric patient. Since many models of scanner select a bowtie filter tailored to the size of a patient slightly smaller than the FOV, image quality should be further improved by reducing beam-hardening artefacts by matching the size of the FOV to the size of the patient.

6.3.2.7. Pitch

Pitch is the ratio of the distance the CT table advances through the scanner during a 360° rotation of the gantry relative to the width of the X ray fan beam in the z direction. Typical (non-cardiac) pitch values range from 0.5 to 1.5. Increased pitch reduces radiation dose if other parameters are not changed, since each point of the anatomy is irradiated for a shorter time; however, the majority of more modern scanners will automatically adjust the tube current if the pitch is changed to give the same effective mAs. Effective mAs incorporates the effect of pitch. Radiation dose is proportional to 1/pitch if the same mAs/rotation is used, and this is indicated by a reduction in the effective mAs if this is displayed by the scanner. Larger pitch reduces the acquisition time of the required scan volume. This reduces motion artefacts and problems with breath holding. Increased pitch increases quantum mottle in the images if other parameters are not changed. The choice of pitch must be balanced with the choice of mAs to result in proper patient dose and image quality [154]. Larger pitch values effectively increase over-ranging at the beginning and end of the scan length. In general, paediatric body imaging uses a pitch of ~1.4 and a short rotation time (≤0.5 s) to minimize total scan time.

Key points for the configuration of computed tomography equipment for paediatric use

— *Determine parameters and create a look-up table to allow computed tomography protocols to be altered for patient size.*
— *Ensure the appropriate use of scan mode (axial/helical) for each procedure.*
— *Selection of the optimal tube voltage for each examination is critical.*
— *Ensure that the smallest field of view is selected for particular patient sizes.*
— *Determine whether the manual or automatic exposure control mode should be used for each examination. If automatic exposure control is used, the medical physicist should verify performance.*
— *Optimize the pitch setting for examinations.*
— *Ensure that the correct acquisition detector width in the z direction is used to allow the necessary reconstruction planes to be created after the acquisition.*
— *Ensure that the scan projection radiography defaults to posteroanterior projection.*
— *The selection of the reconstruction kernel has a profound effect on image quality and dose requirements. Ensure that suitable algorithms are selected for each procedure as well as appropriate window widths and levels.*
— *Establish the correct selection of focal spot size.*

6.3.2.8. Reconstructed slice width

During scanning of paediatric patients, scans are normally acquired with the smallest available detector element size in the z direction. While selecting the smallest detector element size may reduce the maximum width of the fan beam and the length of the cylindrical volume of data that can be acquired during a single breath hold, this is typically not a significant trade-off during paediatric imaging as it is during adult imaging. Provided this minimum dimension is ~0.5 mm, the voxel of patient tissue is a cube. Cubic voxels are necessary to reformat images in the sagittal or coronal planes or in a 3-D model without loss of resolution relative to the original transverse plane. After reformatting, multiple ~0.5 mm slices should be combined to increase the length of the voxel (volume of the voxel) and reduce the quantum mottle in the image without increasing the radiation dose to the patient. Loss of image quality due to partial volume

averaging (thick slices) must be balanced against an increase in quantum mottle (thin slices) when selecting the slice thickness at which reformatted images are displayed.

6.3.2.9. Image processing parameters

The previously discussed considerations in Section 6.3.2 improve the acquisition process of the images with a reasonable radiation dose to the patient. See Section 6.3.1.8 for a discussion of the importance of image processing parameters.

6.3.2.10. Application of shielding

The application of shielding in paediatric CT can be considered. It has been demonstrated that a significant dose reduction of the shielded trunk for neonates and infants can be achieved during head CT examinations.

6.4. OPERATOR CONTROL OF DOSE/IMAGE AND IMAGE QUALITY

After specification and selection of the X ray imaging equipment and the appropriate configuring or commissioning of the equipment, a multidisciplinary team consisting of the radiographer, radiologist and medical physicist should properly manage the radiation dose of each created image to reduce the overall radiation dose to the patient during the examination. The following points below should be addressed.

6.4.1. Radiography/fluoroscopy

6.4.1.1. Patient positioning

There are important differences between paediatric and adult positioning during imaging procedures. Infants and toddlers typically have radiographic chest examinations performed supine instead of upright at 100 cm focus to image distance (FID), not because this is the preferred geometry, but because of positioning difficulties of the patient. Patient positioning devices that allow the small child's thorax to be imaged upright improve image quality. FID values that are smaller than normal increase the patient dose per image. FID values that are larger than normal may increase exposure time, which would compromise image quality due to unsharpness.

If the fluoroscopic table allows variable FSD, the longest choice reduces patient dose rate during fluoroscopic procedures [135]. During interventional fluoroscopic procedures, the anatomy of interest should be placed at the isocentre to avoid the shift of the anatomy of interest with changes of projection during the procedure.

6.4.1.2. Use of grid

Section 6.2.1.2 discussed grid specifications for paediatric imaging that reduce the lead content of the grid for imaging large toddlers to small teenaged patients [155, 156]. Completely removing the grid while imaging newborns or toddlers and when imaging the chest of children <10 years of age with the AEC device further reduces paediatric radiation dose with little loss of image quality since the quantity of scatter generated is small [157]. If a manual technique mode is used, the mAs used when removing the grid for small patients must be reduced to ensure that the image receptor is not overexposed and the desired dose reduction to the patient is achieved.

6.4.1.3. Manual versus automatic exposure control

Depending on the examination and the size of the patient, the radiographer may elect to acquire the image using the manual mode of the generator, which requires a selection of high voltage, tube current and exposure time. If the AEC mode is used, the radiographer must make sure that the selected sensor's area will be completely covered by the anticipated patient anatomy during the exposure.

6.4.1.4. Collimation

The area of the radiation beam for a radiographic or fluoroscopic examination should be no larger than the area of the anatomy of interest. Since automatic collimation on radiographic systems reduces the size of the radiographic field to the size of the image receptor, the radiographer may be able to manually reduce the area of the X ray beam further without excluding organs of interest from the image. Likewise, in fluoroscopy, since the automatic collimator adjusts the X ray field size to the size of the FOV of the image receptor, smaller manual collimated X ray field sizes may be appropriate. Tight collimation improves image quality by reducing scatter radiation that reaches the image receptor. While collimation does not reduce the entrance air kerma to the patient, it reduces the volume of tissue irradiated and the overall risk.

6.4.1.5. Anatomical program setting

When conducting a radiographic or fluoroscopic examination, the radiographer must select the anatomical program setting that best corresponds to the size of the patient and the type of examination to properly select the multitude of parameters that affect the acquisition of the image. The most critical items are the AEC curve, filtration, etc.

6.4.1.6. Operator choices

The table side control of the fluoroscope which is available to the operator allows the operator to control patient entrance dose [137, 139, 158] using:

— The low, medium or high entrance dose rate to both the patient and the image receptor: Typically, the low dose is half of the medium dose and the high dose is double the medium dose.
— The 'frame grab' feature, if provided (described in Section 6.2.1.10).
— The 'fluoro-loop store/playback' feature, if provided (described in Section 6.2.1.11).
— Unless the image receptor K_i/image is constant, anytime the operator selects a larger FOV, the skin dose per image decreases.

6.4.1.7. Patient shielding

Critical organs of the patient, e.g. gonads, thyroid, lens of the eye and breast, should be shielded in paediatric patients whenever the placement of the shield does not obscure important information in the clinical image. Standard sized shields can be purchased. Old apron shield stock in good condition can be cut to the appropriate size to make custom sized shields. While shielded organs that are not directly irradiated receive little benefit from external shielding, in most cases, this shielding provides 'peace of mind' for the patient's parent.

6.4.2. Computed tomography

The dose delivered to a particular organ of the paediatric patient is primarily determined by the choices made during the selection of the parameters discussed in Section 6.3.2 and the settings of these parameters loaded into the anatomical programming settings of the scanner. The operator should be aware that most of these scan parameters can be altered just prior to the acquisition of the scan if the radiologist and/or radiographer has identified something unique about an individual patient that requires scan parameter changes.

Key points for operator control of paediatric radiography/fluoroscopy equipment

— *Ensure the appropriate set-up of focus to image distance for all procedures.*
— *Ensure that grids are only used when necessary and that they have the appropriate focal length for the focus to image distance if used.*
— *Ensure that radiographic automatic exposure control is properly functioning, particularly in relation to the automatic exposure control detectors in relation to the patient size under examination.*
— *Ensure that appropriate collimation is carried out.*
— *Ensure that anatomical programming is understood and properly selected by the radiographers.*
— *Ensure that the fluoroscopist understands the choices available for fluoroscopic automatic exposure control, 'last image hold' and 'fluoro-loop store/playback'.*
— *Ensure that appropriate patient shielding is available.*

6.4.2.1. Centre the patient in the gantry

Since the entrance dose to the skin of the patient is, in part, a function of the distance of the skin from the focal spot of the CT scanner, positioning the z axis of the patient's body in the middle of the CT gantry reduces the radiation dose to the patient [159].

6.4.2.2. Measure size of patient

The appropriate scan parameters for a given paediatric patient are determined, to a large degree, by the design of the CT scanner and the physical size of the patient as discussed in Section 6.3.2. The simplest approach that allows accurate estimation of patient size is the measurement of the lateral dimension of the patient lying supine on the CT gantry couch. This is easily accomplished with a set of simple callipers normally found in radiographic departments at pre-described anatomical landmarks [143] or by measuring the size of the patient electronically on the projection scan.

Key points for operator control of paediatric computed tomography equipment

— *Ensure that radiographers understand the function of the controls of the scanner.*
— *Ensure that all patients are centred on the scanner isocentre.*
— *Ensure that radiographic staff understand the method of determining the patient size from the scan projection radiography and realize the importance of this measurement.*
— *Ensure that the radiographer selects the appropriate protocol for the patient examination.*
— *Ensure that the radiographer calculates the size specific dose estimate from the scanner indicated $CTDI_{VOL}$ before proceeding with the scan.*
— *Ensure that the radiographer understands how to reduce the patient dose indicator (e.g. $CTDI_{VOL}$) before scanning.*

6.4.2.3. Anatomical program setting selection

Based on the measurement of lateral patient size (see Section 6.4.2.2) and the clinical imaging question(s) to be answered, the operator should select the most appropriate anatomical program setting provided by the CT scanner. Prior to initiating the patient scanning, the operator should verify that all of the scan parameters set by the anatomical program selection are appropriate for the imaging task and size of the patient. This should include a review of the $CTDI_{VOL}$ indicated on the control console of the scanner which is used to calculate the SSDE, described in Section 4.4.1, to estimate patient dose before irradiation of the patient. The operator is the last 'gate-keeper' with this opportunity.

6.5. MANAGING THE NUMBER OF IMAGES PER STUDY

6.5.1. Introduction

6.5.1.1. Clinical examination selection

Initially, the clinical need for the study should be considered in relationship to the associated risk of the examination [33, 160]. The results of the study should realistically answer the original clinical question [75]. The referring physician and radiologist or appropriate member of the clinical staff should discuss the availability of other alternative imaging modalities that do not use

ionizing radiation. If an alternative imaging modality can be substituted for an X ray examination, e.g. ultrasound or magnetic resonance imaging instead of CT or projection radiography, with appropriate diagnostic information, this is the most effective dose reduction step of all [75]. Consideration should also be given as to whether a lower dose ionizing procedure can be used, e.g. projection radiography instead of CT or a frame grabbed image instead of a radiographic acquisition, since dose from images acquired in the radiographic mode compared to the fluoroscopic mode is an order of magnitude greater [161].

6.5.1.2. Non-cooperative children

The age or medical condition of the paediatric patient may cause the patient to be non-cooperative. The following measures may help to reduce motion artefacts [162]:

— Input the patient information into the imager and completely prepare the scan room before putting the paediatric patient on the table.
— Swaddle the infant or toddler with a blanket.
— Use distraction techniques or devices to improve cooperation. Projectors with child-friendly images, toys with flashing lights or music, child-friendly images on the ceiling and/or walls, a parent reading a favourite story or talking to them through the console comfort the child.

6.5.2. Radiography

The physician requesting the examination in consultation with the radiologist or appropriate member of the clinical staff (in accordance with the Basic Safety Standards [4]) must either (i) give the radiographer clear instruction concerning the clinical question to be answered or (ii) identify the specific diagnostic examination to be performed. This helps to ensure that the correct anatomical views, and only those views, are included in the examination.

6.5.3. Fluoroscopy

6.5.3.1. Fluoroscopic mode

The operator should take the following steps during fluoroscopy to reduce the number of fluoroscopic images during a clinical fluoroscopic study:

— Depress the fluoroscopic foot pedal intermittently rather than continuously;
— Give their undivided attention to the fluoroscopic monitor when fluoroscopic images are being created;
— Reduce the number of fluoroscopic pulses generated per second by the imager during segments of the examination where less temporal resolution can be tolerated;
— Use the 'live' zoom option, if available, rather than magnifying the image.

6.5.3.2. Radiographic acquisitions

Owing to the larger patient radiation dose associated with each image acquired in radiographic mode, all possible steps that reduce the total number of these images should be taken:

— Exploit the 'last image hold' feature (see Section 6.2.1.10), provided the reduced image quality is adequate.
— Use the 'fluoro-loop store/playback' feature (see Section 6.2.1.11) to review the previous fluoroscopic sequence, especially in teaching applications or to avoid additional radiographic acquisitions, provided the reduced image quality is adequate.
— When radiographic acquisitions are required, reducing the duration of the sequence or the frame rate of the acquisition significantly reduces the total number of acquired images. The frame rate should not exceed that needed to meet the temporal resolution requirements of the examination.

The steps outlined in Section 6.5.3 are important for all paediatric fluoroscopic examinations, but are critical for interventional procedures with potentially high doses [163].

6.5.4. Computed tomography

The operator should take all necessary steps to minimize the volume of irradiated patient tissue and the number of times that tissue is irradiated.

6.5.4.1. Axial versus helical

Body imaging is normally performed in the helical mode, in which the X ray beam is continuously 'on' during the scan from start to finish with the patient anatomy continuously advanced through the gantry. This results in the irradiation of a cylindrical volume of patient anatomy with a specific scan length in the shortest possible time. Some state of the art CT scanners contain

Key points for the management of the number of images per radiography/fluoroscopy examination

— *Justification of the procedure should be verified (possibly by the radiographer/technologist).*
— *During fluoroscopy, intermittent use of X rays should be observed.*
— *During fluoroscopy, reduce the frame rate for less difficult portions of the examination.*
— *All efforts should be made to reduce the use of acquisition runs in favour of fluoroscopy through the use of 'last image hold' or 'fluoro-loop store/playback' features.*
— *When acquisition runs are required, reduce the frame rate or duration of the run to reduce the number of acquisition images acquired.*

programmed collimator blades that reduce irradiation of tissues at each end of the cylinder that are not imaged. One long helical scan, as opposed to multiple shorter scans, eliminates the scan overlap and regions of elevated patient dose.

Head imaging has typically been performed in the axial mode. Some manufacturers allow the radiographer to control the start of irradiation for each slice. When this feature is available, careful observation of the patient by the radiographer allows initiation of each image when the patient is less likely to move [162]. Axial scanning with the gantry tilted or proper positioning of the head during head scans may, in some cases, reduce radiation dose to radiosensitive organs, e.g. the lens of the eye.

In paediatric imaging, the advantages and disadvantages of axial and helical imaging must be carefully considered by the radiographer, radiologist and medical physicist. Helically acquired heads or axially acquired bodies may be the correct choice.

6.5.4.2. Scan length

The radiation risk to the paediatric patient is a function of both the radiation dose the patient's tissues receive and the volume of the patient's tissues that are irradiated. It is imperative for the operator of the CT scanner to limit the length of the projection view and the scan length of the scan volume in addition to limiting the radiation dose to the patient's organs that are directly irradiated. The length of the scout and the scan should be limited to the clinical area of concern [164, 165]. Whenever possible, overlapping scan lengths should be avoided.

6.5.4.3. Number of series

The vast majority of paediatric examinations require only one scan [166]. Performing both a non-contrast and a contrast enhanced abdominal CT scan needlessly results in twice the radiation dose for the child [167]. Pre- and post-contrast scans or delayed imaging rarely provide additional information and should not be performed unless specifically indicated through consultation between the paediatric radiologist and the referring physician.

Key points for the management of the number of images per computed tomography examination

— *The length of the scan projection radiography and the scan acquisitions should be limited to the clinical area of concern.*
— *The number of series should be carefully considered and kept to a minimum.*
— *Strategies to reduce time in the procedure room for the non-cooperative child should be employed.*
— *The use of dose length product is complex in paediatrics, as discussed in Section 4.4.2. It is advantageous to minimize the dose length product.*

6.6. SUMMARY

Reducing the patient dose per image and reducing the number of images while maintaining good image quality effectively reduces the radiation dose to the paediatric patient. An appropriate patient dose per image results from appropriate hardware features in the imaging system, proper configuration of the appropriately selected hardware required to address paediatric imaging challenges, and knowledgeable operation of the imaging system by the operator. An appropriate number of images per paediatric examination occurs when the examination has been properly justified (including ruling out non-ionizing modality substitution) and the operator appropriately manages the number of images generated during the examination.

Appendix I

CHARACTERIZATION OF PATIENT SIZE

I.1. CONCEPT OF EQUIVALENT PATIENT DIAMETER

The most commonly used metric of paediatric size is age, which is the simplest to ascertain but the least specific. The range of size as a function of age is large (Fig. 6), due to variable rates of child growth, obesity or ethnic group.

Patient thickness in the direction of irradiation gives the best indicator of dose related size, as it is well known that dosimetric quantities such as incident air kerma for projection radiography are related exponentially to the patient thickness along the axis of the central X ray beam. However, this can be time-consuming to determine for individual patients. In addition, for fluoroscopy and CT examinations, the beam orientation is likely to vary, resulting in multiple thicknesses for one patient. Patient thickness can be inferred from measurement of patient height and weight using either an analytical formula (Eq. (39)) or from tables (see Appendix II). ECD [169] is a quantity derived from height and weight that gives an 'effective thickness' for an individual, assuming they were equivalent to a cylinder of water. This takes some account of the fact that a tall, thin child may have a very different body thickness and composition to a short, stocky child of similar weight. As it also assumes a circular cross-section, equivalent diameter is a useful quantity when the X ray projection and, thus, apparent body thickness, is variable. For these reasons, relevant patient thickness or height and weight should be recorded.

The equation defining ECD (in centimetres) is:

$$\mathrm{ECD} = 2\sqrt{W / \pi \mathrm{H}} \tag{39}$$

where

W is the weight in grams;

and H is the height in centimetres.

As can be seen from Table 18, the ECD tends to give an average of the AP and lateral dimensions of the body; analytical relationships between ECD and patient thickness are given by the NRPB [26].

I.2.1. Comparisons of paediatric size data

Recent national data on the height and weight of children indicate that there are not very significant differences up to age 15 for the countries compared [168]. This is seen in Fig. 6, which compares height and weight data for boys from Japan, Singapore, the United Kingdom and the USA. In contrast, Fig. 7, with US data of height and weight for boys [174], shows the wide individual variation seen in the population.

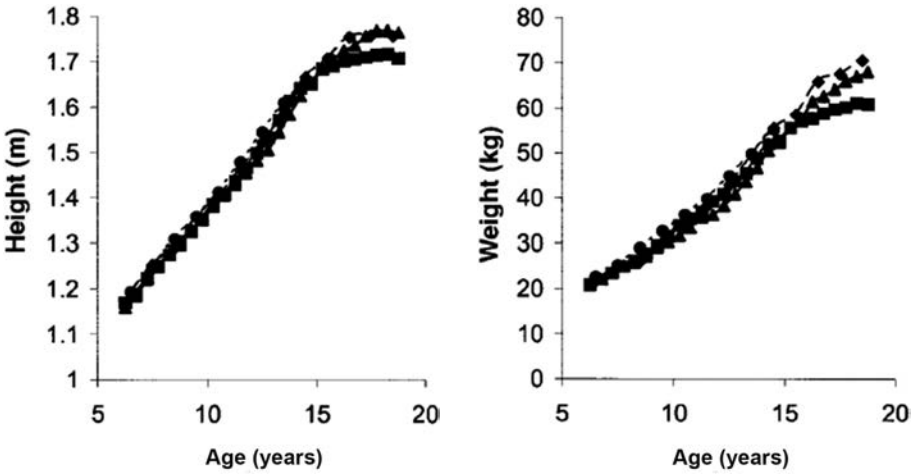

FIG. 6. Mean height and weight for each class for boys from Japan (●), Singapore (■), the United Kingdom (▲) and the United States of America (♦) [168].

The majority of work published on paediatric dosimetry has adopted reference age groups as listed in Table 19 on p. 97. These reference ages are also commonly used for both computerized and anthropomorphic paediatric phantoms (see also Section 5.3.3). The corresponding height and weight of such phantoms are also detailed in this table, although these relate specifically to European data. Table 18 gives corresponding size data for children from various countries.

Table 18 contains a collection of data for body diameters of children as determined by different studies. Figures 8 and 9 illustrate these data for abdomen and chest AP diameters. The data are from Refs [23, 143, 170–173]. The data from Refs [143, 170] were derived by direct measurement. Analytical functions giving the relationship between ECD and body thicknesses [26], calculated from Ref. [170], were used to calculate abdomen and thorax diameter from height and weight data from the other studies.

TABLE 18. MEAN BODY THICKNESS AS A FUNCTION OF AGE AND EXAMINATION

Age (years)	Height (cm)	Weight (kg)	Equivalent cylindrical diameter (cm)	Chest PA (cm)	Chest lateral (cm)	Abdomen PA (cm)	Abdomen lateral (cm)	Scull PA (cm)	Scull lateral (cm)	Pelvis PA (cm)	Pelvis lateral (cm)	Source
0	52.2	3.5	9.2	9.3	10.6	8.8	10.0	11.9	9.3	7.0	9.2	[170]
1	75.2	9.9	12.9	12.0	15.7	12.6	14.7	16.2	12.4	10.6	15.2	
5	116.5	20.5	15.0	13.4	18.8	13.6	17.4	17.8	13.8	13.7	20.2	
7	127.3	25.9	16.1	13.8	19.7	14.4	18.5	17.9	14.0	14.9	21.6	
10	144.7	36.1	17.8	15.3	22.1	15.9	21.1	18.4	14.1	16.4	24.4	
15	167.6	57.8	21.0	17.4	25.9	18.0	24.5	18.9	14.6	19.6	30.4	
0	55.8	4.5	10.1	9.9	11.8	9.5	10.9	13.5	10.2	7.2	10.66	[171]
1	76.6	9.9	12.8	11.6	15.4	11.7	14.3	16.5	12.1	9.7	15.11	
5	111.8	19.7	15.0	13.1	18.2	13.4	17.1	18.1	13.1	12.0	19.04	
7	123.9	24.7	15.9	13.7	19.4	14.2	18.3	18.6	13.3	13.0	20.86	
10	140.2	33.4	17.4	14.8	21.3	15.3	20.2	19.2	13.6	14.6	23.73	
15	165.9	55.1	20.6	17.1	25.3	17.6	23.6	20.2	14.0	17.4	29.84	
2	86.4	12.3	13.4	12.0	16.2	12.2	15.1	17.0	12.5	10.3	16.20	[172]
5	109.2	18.4	14.6	12.8	17.7	13.2	16.7	17.9	13.0	11.6	18.42	
11	143.5	35.2	17.7	15.0	21.6	15.5	20.5	19.3	13.7	14.8	24.23	
16	168.0	57.8	20.9	17.4	25.7	17.9	23.9	20.3	14.0	17.6	30.53	
18	170.0	61.7	21.5	17.8	26.5	18.3	24.4	20.4	14.1	18.0	31.61	
2	86.1	12.3	13.5	12.0	16.2	12.3	15.2	17.1	12.5	10.4	16.29	[173]
3	95.2	14.6	14.0	12.4	16.9	12.7	15.8	17.4	12.7	10.9	17.18	
4	101.7	16.5	14.4	12.6	17.4	13.0	16.3	17.7	12.9	11.3	17.91	

TABLE 18. MEAN BODY THICKNESS AS A FUNCTION OF AGE AND EXAMINATION (cont.)

Age (years)	Height (cm)	Weight (kg)	Equivalent cylindrical diameter (cm)	Chest PA (cm)	Chest lateral (cm)	Abdomen PA (cm)	Abdomen lateral (cm)	Scull PA (cm)	Scull lateral (cm)	Pelvis PA (cm)	Pelvis lateral (cm)	Source
1	74.9	10.4	13.3	11.9	16.0	12.1	14.9	16.9	12.4	10.2	15.95	[23]
5	113.2	17.8	14.1	12.5	17.1	12.8	16.0	17.6	12.8	11.1	17.50	
10	143.5	34.8	17.6	14.9	21.5	15.4	20.4	19.3	13.7	14.7	24.03	
15	171.6	68.1	22.5	18.6	27.7	19.0	25.1	20.7	14.2	18.4	33.44	
1				12.3	17.1	11.2	15.9	16.3	13.1	10.5	15.7	[143]
2				12.9	18.1	11.8	16.8	17.2	13.8	11.1	16.8	
5				14.7	20.8	13.5	19.6	18.5	14.7	12.9	20.3	
7				15.9	22.7	14.7	21.5	18.9	15.0	14.1	22.6	
10				17.8	25.4	16.4	24.3	19.5	15.4	15.9	26.1	
15				20.8	30.0	19.2	28.9	20.1	15.8	18.9	31.8	

Note: PA: posteroanterior.

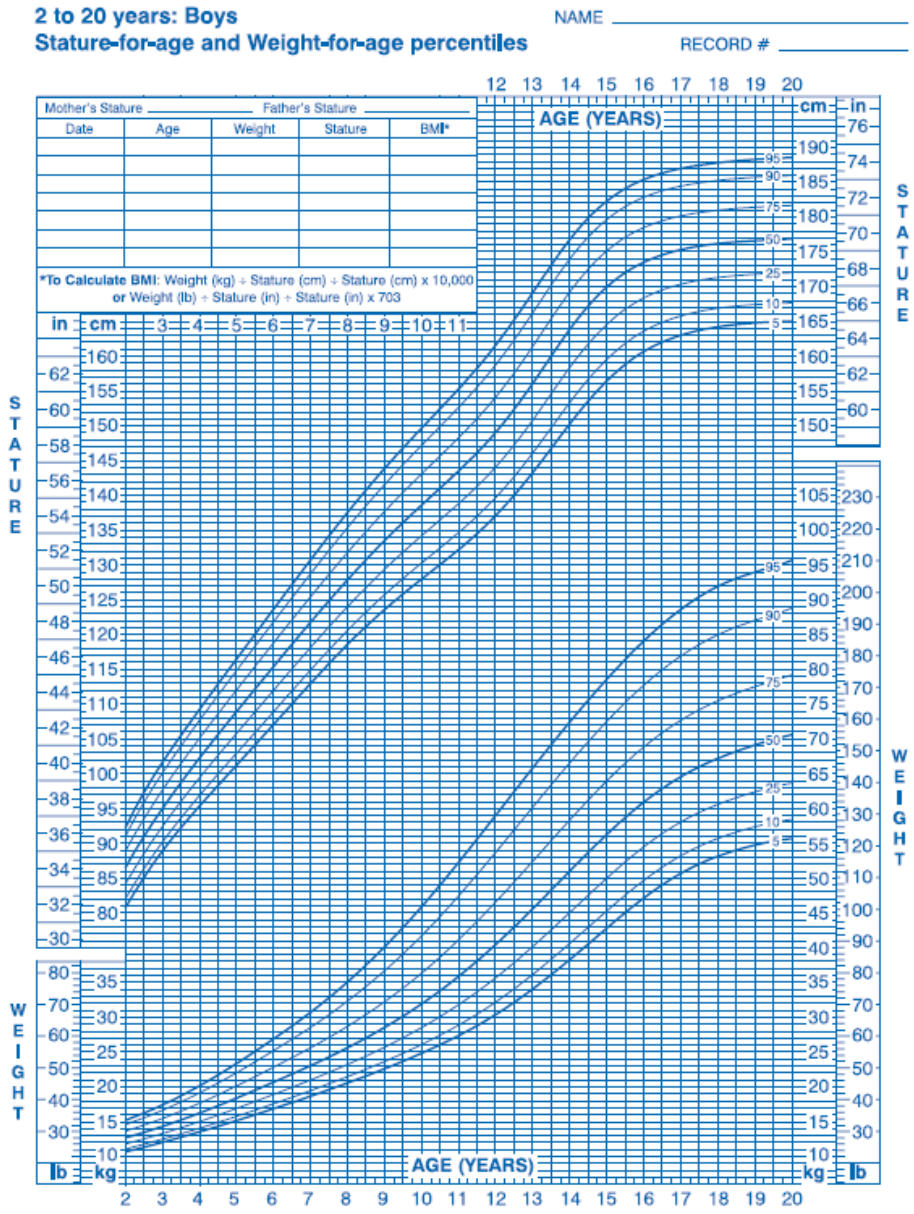

FIG. 7. Stature-for-age and weight-for-age percentile for boys; 2–20 years old [174].

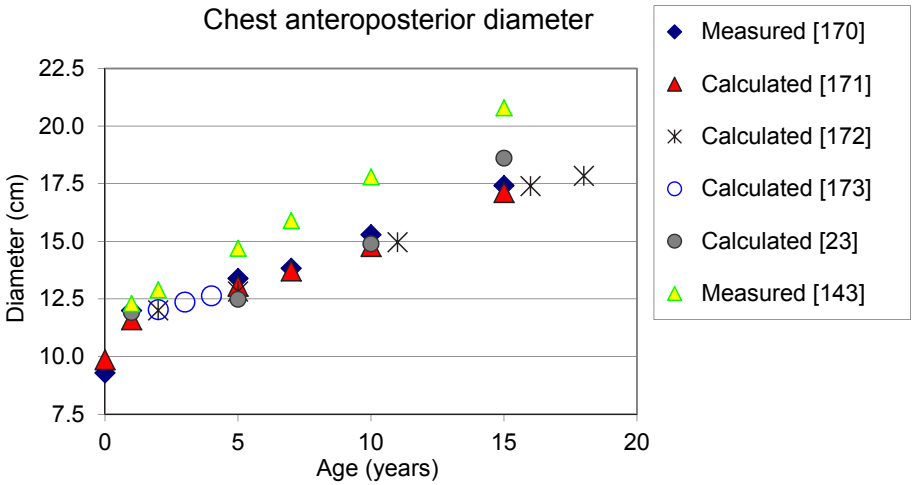

FIG. 8. Chest anteroposterior diameters as a function of age from different studies.

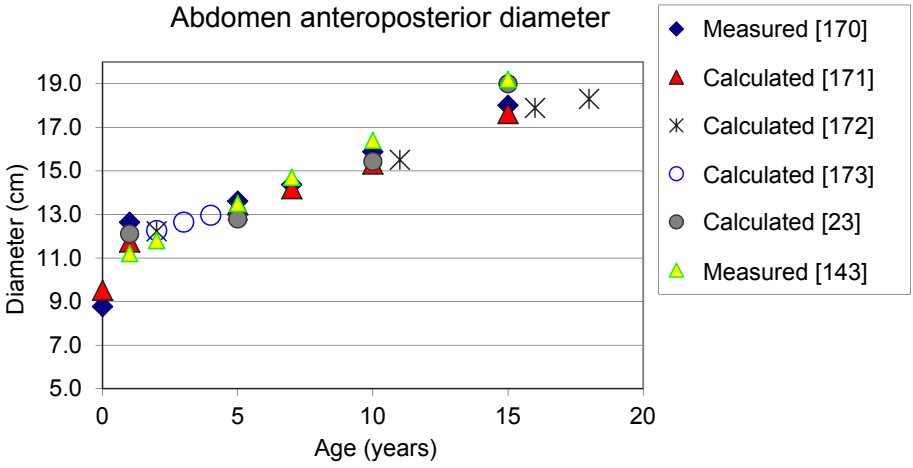

FIG. 9. Abdomen anteroposterior diameters as a function of age from different studies.

These figures demonstrate that abdomen AP diameter is quite consistent, whereas chest AP diameters from Ref. [143] show generally higher values. These data justify using fixed standard thicknesses for evaluation. Nevertheless, once again, it should be noted that the variation in thickness between children at the same age is larger than the difference between several standard age classes.

I.2.2. Data for standard phantoms

A number of standard software phantoms have been developed for use in paediatric dosimetry. These are listed in Table 19, which gives the height, weight and ECD associated with each of these phantoms, along with the assigned age equivalence for reference. It is recommended that doses derived for one of these phantoms, particularly DRLs, be associated with the corresponding equivalent diameter rather than the stipulated age as this will enable comparisons to be made with local data to a much higher degree of accuracy.

TABLE 19. STANDARD PATIENT SIZE DATA

Anthropomorphic phantom (atom) [175]				
Age	Height (cm)	Weight (kg)	Equivalent cylindrical diameter (cm)	Trunk thickness (cm) anteroposterior × lateral
0 years	51	3.5	9.3	9 × 10.5
1 year	75	10	13.0	12 × 14
5 years	110	19	14.8	14 × 17
10 years	140	32	17.1	17 × 20
Soft phantom (PCXMC)				
0 years	50.9	3.4	9.2	9.8 × 10.94[a] (12.7[b])
1 year	74.4	9.2	12.5	13.0 × 15.12[a] (17.6[b])
5 years	109.1	19.0	14.9	15.0 × 19.64[a] (22.9[b])
10 years	139.8	32.4	17.2	16.8 × 23.84[a] (27.8[b])
15 years	168.1	56.3	20.7	19.6 × 29.66[a] (34.5[b])
Voxel phantom (baby) [49, 176]				
8 weeks	57	4.2	9.7	
Voxel phantom (child) [49, 176]				
7 years	115	21.7	15.5	

[a] Trunk width excluding arms.

[b] Trunk width including arms.

Appendix II

POLYMETHYL METHACRYLATE TO TISSUE EQUIVALENCE

Although it is quite common to use PMMA as a phantom material, elemental compositions differ significantly from water or tissue. As a consequence, an energy dependence of attenuation of PMMA relative to tissue is anticipated. PMMA, when used as a tissue substitute (phantom) material to drive the AEC of an X ray device, will simulate slightly different 'patient' or average soft tissue [41, 177] thicknesses as X ray spectra change. In paediatric radiology, lower tube voltage and, often, higher filtrations are used as compared to adult radiography. Thus, a closer look at these energy dependencies should be taken.

Calculations using interaction data [178] and calculated X ray spectra [179] show that the phantom thicknesses of 5, 10, 15 and 20 cm of PMMA correspond to varying tissue thicknesses for different tube voltages and filtrations. Figure 10 illustrates the dependence on filtration and tube voltage for 15 cm of PMMA. This variation is usually within ±1 cm. In softer radiation fields, PMMA simulates less tissue than in harder X ray beams. Thus, incident air kerma values generated under AEC in soft beams using PMMA to simulate the patient may underestimate patient doses to a higher extent than with harder beams (because the PMMA slab will simulate a smaller tissue thickness). This might be an issue if PMMA phantoms are used to optimize beam qualities for paediatric imaging.

As stated in TRS 457 [3], this issue strengthens the argumentation that phantom dose data are best compared to other phantom data employing the same phantom. If compared to patient dose data, considerable uncertainties may be involved.

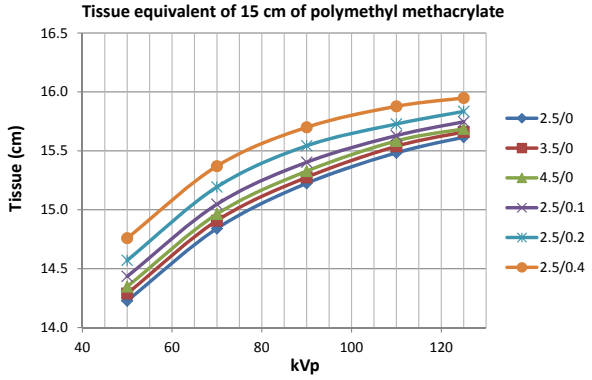

FIG. 10. Variation of International Commission on Radiation Units and Measurements tissue thickness equivalent to 15 cm of polymethyl methacrylate (calculated). The total filtration of the beams is given on the right of the graph as 'x mm aluminium/y mm of copper'.

Appendix III

BACKSCATTER FACTORS FOR PAEDIATRIC USE

III.1. INTRODUCTION

BSFs are the largest of all of the different dosimetric quantities and correction factors playing a role in the dosimetry of diagnostic radiology X ray beams based on ionometric measurements. Depending on the beam quality and field size, their values amount to corrections ranging from about 20% to more than 60% of the air kerma in free air, determined with a detector calibrated at a standards laboratory.

The international code of practice for dosimetry in diagnostic radiology, TRS 457 [3], as well as ICRU Report 74 on patient dosimetry for X rays used in medical imaging [38], have provided values of BSFs for 21 diagnostic beam qualities with tube voltages between 50 and 150 kV, and for three combinations of filtrations (2.5 mm Al; 3 mm Al; 3 mm Al + 0.1 mm Cu). For each tube voltage and filtration, and the beam HVL, specified in millimetres of aluminium, BSFs are given for three field sizes, and 15 cm thick water, "ICRU tissue" and PMMA phantoms; the data in both international recommendations were taken from Ref. [180]. More recent data on BSFs for similar diagnostic beam qualities, or empirical relations to derive them, have been published in Refs [181–184]. In spite of the large amount of data available, the beam qualities included in the references mentioned do not cover the entire range of clinical X ray spectra used in modern diagnostic radiology. To address this problem, a comprehensive study was undertaken [185] where BSFs for beam qualities currently available in radiology equipment were calculated using a combination of Monte Carlo and analytical methods for the standard phantom thickness of 15 cm.

Based on the methodology and procedures developed in Ref. [185], new BSF calculations for the determination of the surface dose in diagnostic radiology, particularly in the fields of infant, paediatric and interventional radiology, have been performed. The new set of data takes into account the X ray beam qualities described in the report on the implementation of TRS 457 [15] as well as appropriate phantom thicknesses for infant and paediatric radiology.

III.2. BACKGROUND

The determination of the absorbed dose at the surface of a patient or phantom can be based on the use of a reference ionization chamber, or a KAP meter, provided with a calibration coefficient in terms of air kerma free-in-air for a quality Q, $N_{K,Q}$, at a calibration standards dosimetry laboratory. The first step consists of determining the incident air kerma free-in-air, for the primary incident spectrum of quality Q, $(K_{\text{air},Q})_{\text{air}}$, at the measuring position; this is achieved by multiplying the ionization chamber reading free-in-air in the Q beam, $M_{\text{air},Q}$, corrected for influence quantities (pressure, temperature, recombination, field size, etc.) by the corresponding calibration coefficient $N_{K,Q}$. The second step involves the transfer of the air kerma free-in-air to the air kerma at the phantom entrance surface; this requires multiplying the $(K_{\text{air},Q})_{\text{air}}$ above by the BSF at the appropriate beam quality $B(Q)$, which is field size dependent as the number of backscattered photons varies with field size. Recalling that the BSF is defined as a ratio of air kermas [3], entrance surface (water) to free-in-air, this is emphasized using the subscript 'air':

$$B_{\text{air}}(Q) = \frac{\left(K_{\text{air},Q}\right)_{\text{w}}}{\left(K_{\text{air},Q}\right)_{\text{air}}} \tag{40}$$

The step yields the ESAK at the measuring position, i.e. the quantity determined is still air kerma, but at the surface of a water phantom, $(K_{\text{air},Q})_w$. The final step requires the transfer of the ESAK to water kerma (or in any other medium) at the same position in the water phantom, $(K_{w,Q})_w$, achieved by multiplying by the mass energy-absorption coefficient ratio, water to air $(\mu_{\text{en}}(Q)/\rho)_{w,\text{air}}$, calculated for the photon spectrum at the phantom entrance surface, which consists of the incident plus backscattered spectra. The water kerma at the phantom surface determined in this manner is equal to the absorbed dose to water in the same position, which can be written as:

$$D_{\text{w},Q} = \left(K_{\text{w},Q}\right)_{\text{w}} = M_{\text{air},Q} N_{K,Q} B_{\text{air}}(Q) \left[\mu_{\text{en}}(Q)/\rho\right]_{\text{w,air}}^{\text{prim+backs}} \tag{41}$$

where both the BSF $B_{\text{air}}(Q)$ and $[\mu_{\text{en}}(Q)/\rho]_{\text{w,air}}^{\text{prim+backs}}$ depend on field size and beam quality.

A summary of the formalism, which is consistent with those in TRS 457 [3] and ICRU Report 74 [38], is illustrated in Fig. 11.

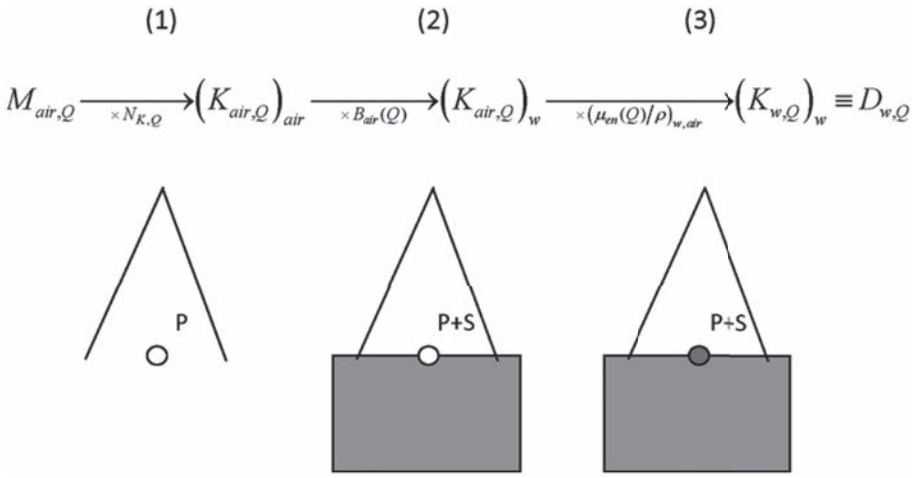

FIG. 11. Schematic steps of the formalism for the determination of the entrance surface water kerma (equal to the absorbed dose) in diagnostic radiology beams from the reading free-in-air of an ionization chamber, using its calibration coefficient (1), the backscatter factor (2) and the mass energy-absorption coefficient ratio (3). P corresponds to incident primary photons and S to backscattered radiation. (From Ref. [185].)

Equation (40) represents the definition of the BSF $B_{\text{air}}(Q)$ in radiodiagnostic dosimetry. It is often assumed that the BSF can be determined experimentally, approximating its definition by a ratio of ionization chamber readings with and without a phantom. Emphasis is given, however, to the fact that an experimental determination of $(K_{\text{air},Q})_{\text{w}}$ would strictly require an $N_{K,Q}$ calibration coefficient for a beam quality which includes both the incident and the backscattered photon spectrum, which is not consistent with the calibrations in terms of air kerma free-in-air provided by standard laboratories. An accurate $B_{\text{air}}(Q)$ can only be determined using Monte Carlo simulations.

III.3. CALCULATIONS FOR CLINICAL X RAY SPECTRA

A comprehensive database for mono-energetic photons between 4 and 150 keV, and different field sizes was created for water phantoms of various thicknesses [185]. Backscattered spectra were calculated with the PENELOPE Monte Carlo system [186], scoring a track-length fluence differential in energy with negligible statistical uncertainty (e.g. <0.05%). The fluence could also be scored in a less accurate manner by counting the photons crossing a surface and correcting for their angle of incidence on the surface, as was done in the calculations of Ref. [180].

Using the Monte Carlo computed primary plus backscatter spectra S, BSFs were calculated numerically for each incident energy using:

$$B_{\mathrm{air}}(S)=\frac{(K_{\mathrm{air},S})^{\mathrm{prim+backs}}_{\mathrm{w\text{-}surface}}}{(K_{\mathrm{air},S})^{\mathrm{prim}}_{\mathrm{air}}}=\frac{\int_0^{E_{\max}}E\left[\Phi_E\right]^{\mathrm{prim+backs}}_{\mathrm{w\text{-}surface}}\left[\mu_{\mathrm{en}}(E)/\rho\right]_{\mathrm{air}}\,\mathrm{d}E}{\int_0^{E_{\max}}E\left[\Phi_E\right]^{\mathrm{prim}}_{\mathrm{air}}\qquad\left[\mu_{\mathrm{en}}(E)/\rho\right]_{\mathrm{air}}\,\mathrm{d}E} \tag{42}$$

where

Φ_E is the calculated photon fluence differential in energy;

and $\mu_{\mathrm{en}}(E)/\rho$ is the mass energy-absorption coefficient, with values taken from the web based NIST database [187].

For the energy range used in the present calculations, log-log interpolations were used to obtain the required values at intermediate energies. A dense database of $B_{\mathrm{air}}(\mathrm{S})$ was then built for the spectra generated by mono-energetic photons with energies between 4 and 150 keV. Thereafter, incident photon spectra $\left[\Phi_E\right]^{\mathrm{prim}}_{\mathrm{air}}$ for diagnostic radiology beam qualities Q were convolved with the BSFs of the mono-energetic database. The procedure is similar to that used in Ref. [188] for averaging stopping-power ratios for megavoltage radiotherapy photon beams from mono-energetic data, and was also used in the calculations of Ref. [180], as well as in those of Ref. [189] for kilovoltage radiotherapy beams.

The BSFs for diagnostic radiology photon spectra of quality Q were obtained by weighting the respective mono-energetic data with the air kerma free-in-air according to:

$$B_{\mathrm{air}}(Q)=\frac{\int_0^{E_{\max}}K_{\mathrm{air}}(E)\,B_{\mathrm{air}}(E)\,\mathrm{d}E}{\int_0^{E_{\max}}K_{\mathrm{air}}(E)\,\mathrm{d}E}=\frac{\int_0^{E_{\max}}E\left[\Phi_E\right]^{\mathrm{prim}}_{\mathrm{air}}\left[\mu_{\mathrm{en}}(E)/\rho\right]_{\mathrm{air}}B_{\mathrm{air}}(E)\,\mathrm{d}E}{\int_0^{E_{\max}}E\left[\Phi_E\right]^{\mathrm{prim}}_{\mathrm{air}}\left[\mu_{\mathrm{en}}(E)/\rho\right]_{\mathrm{air}}\,\mathrm{d}E} \tag{43}$$

where

the fluence $\left[\Phi_E\right]^{\mathrm{prim}}_{\mathrm{air}}$ is the incident primary clinical photon spectrum free-in-air generated as described below;
$B_{\mathrm{air}}(E)$ and $\left[\mu_{\mathrm{en}}(E)/\rho\right]^{\mathrm{prim+backs}}_{\mathrm{w,air}}$ are the BSFs and mass energy absorption ratios calculated for the spectra generated by mono-energetic photons[34];

and the μ_{en}/ρ values were again taken from the NIST database.

[34] It is noted that E represents the incident energy of mono-energetic photons generating the backscatter spectra, calculated with Monte Carlo simulations. The combined primary plus backscatter spectrum has been denoted by S.

An expression corresponding to Eq. (43) was used earlier by Ref. [189] for the calculation of $B_{air}(Q)$ entering into the radiotherapy formalism and then by Ref. [180] for $B_{air}(Q)$, as in the present work. Incident clinical photon spectra were generated with the Monte Carlo based software SpekCalc [190], for tungsten anodes and various combinations of tube voltage and filtration. The adequacy of this software has been verified [185] by its capability to reproduce, within tenths of a per cent, the beam quality parameters HVL_1 and HVL_2, when available, of the IEC [7] and other X ray beams used at primary dosimetry standards laboratories in the diagnostic radiology energy range.

Ideally, BSFs (and mass energy-absorption coefficient ratios) for clinical X ray spectra should be determined from detailed Monte Carlo simulations for the relevant clinical spectrum; this requires an independent, lengthy calculation for each case. As described above, data for mono-energetic photons have been used to compute averaged spectral values according to Eq. (42). It is, however, important to evaluate the consistency of the averaging procedure compared with values directly calculated with full Monte Carlo simulations of clinical spectra. For this purpose, different incident spectra corresponding to typical clinical beams were generated with SpekCalc, and used as the input to Monte Carlo simulations identical to those performed for the mono-energetic photon beams. BSFs were subsequently determined from the Monte Carlo-calculated total spectra and compared to those obtained with the averaging convolution procedure. It was found that the two types of calculation agree within about 0.4%. The difference between the $B_{air}(Q)$ values calculated with the two methods can be used to estimate an uncertainty due to the averaging procedure. Assuming a rectangular distribution for the ratios and using the recommendations of the Guide for Expressing the Uncertainty of Measurements [191], a type-B estimate of 0.3% was obtained for this component.

III.4. RESULTS

BSFs for a broad set of clinical beam quality spectra in the fields of infant and paediatric radiology have been calculated, and a selected compilation is given in Tables 20–22 on pp. 106–111; in the case of infant radiology, data are given for various phantom thicknesses (Table 20). A comprehensive dataset for interventional radiology is provided with the purpose of extending the available range of beam qualities (Table 22); log-log interpolation is recommended.

The uncertainty of the $B_{air}(Q)$ values was obtained combining in quadrature the uncertainties of the respective mono-energetic values and those resulting from the averaging procedure, considering that it is the ratio of such components that needs to be taken into account. A recent estimate of the uncertainty of μ_{en}/ρ ratios

for typical X ray spectra between 50 and 100 kV is 0.2% [192]. The uncertainty associated with the use of the software SpekCalc [190] to derive averaged values for slightly different spectra does not exceed 0.3%. The combined standard uncertainty of $B_{air}(Q)$, thus, became 0.5% (it is noted that a similar uncertainty was obtained for the $(\mu_{en}/\rho)_{w,air}$ values in Eq. (41), i.e. 0.4%).

Figure 12 shows a comparison of $B_{air}(Q)$ for 10 cm × 10 cm clinical beams with the data in TRS 457 [3] and ICRU Report 74 [38], as a function of tube voltage and HVL. It is apparent that the BSFs of many of the clinical beams are extremely close to each other, as are their qualities, but most importantly, the clinical qualities for which $B_{air}(Q)$ data are not given in Refs [3, 38] can be clearly observed. For matching tube voltage, filtrations and HVL, the two datasets differ on average by 0.6%, the maximum difference being 1.1%.

Data for tube voltage, HVL and field size combinations not included in the tables, as well as for other phantom thicknesses can be derived approximately by graphical interpolation from Figs 13 and 14. Figure 13 shows BSFs for a large range of beam qualities generated by kilovoltage potentials between 50 and 150 kV, and filtration combinations of 2.5–4.1 mm of aluminium with 0–0.9 mm of copper for different field sizes [185]. It can be seen that BSFs show a variation with the kilovoltage potential of around 6% for the smallest field size, but this increases rapidly to 10% for square fields with sides of 10 cm. The BSF is, thus, greatly dependent on HVL and field size, with values ranging between approximately 1.20 and 1.70 for energies in the mentioned range. On average, there is an overall 40% dependence on field size, whereas the dependence on tube voltage for a given HVL is of the order of 6–10%. Figure 13 confirms the inadequacy of using HVL as the sole beam quality specifier if results with an accuracy greater than 6–10% are sought. For this, using tube voltage as an additional parameter for the beam quality specification for a given field size is necessary.

The general dependence of the BSFs on field size and phantom thickness is shown in Fig. 14 for a range of X ray beam qualities and three field sizes (5, 20 and 35 cm square fields), where $B_{air}(Q)$ values for each field are normalized to those of a 15 cm thick phantom. The figure gives the factor by which the value of $B_{air}(Q)$ for a 15 cm thick phantom should be multiplied to obtain the value for other thicknesses; the small range of values for this factor precludes significant errors arising from log-log interpolation. It can be seen that for small field sizes the variation is never larger than 2% but, depending on the beam quality, it reaches up to 12% variation for the maximum field size analysed (35 cm square field). A saturation value within about 1% of the reference phantom thickness is achieved only for phantoms thicker than about 12 cm, although this dependence varies with beam quality and field size.

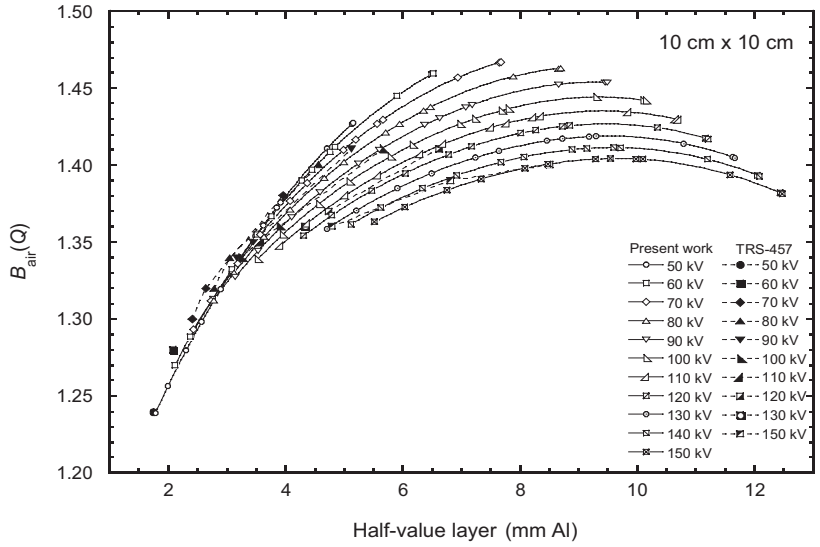

FIG. 12. Comparison of the backscatter factors in water for 10 cm × 10 cm field sizes and different beam qualities for a 15 cm thick phantom, given in Refs [3, 38] (filled symbols, dashed lines), and the new values (open symbols, solid lines). For matching tube voltage and filtrations, the two datasets differ on average by 0.6%.

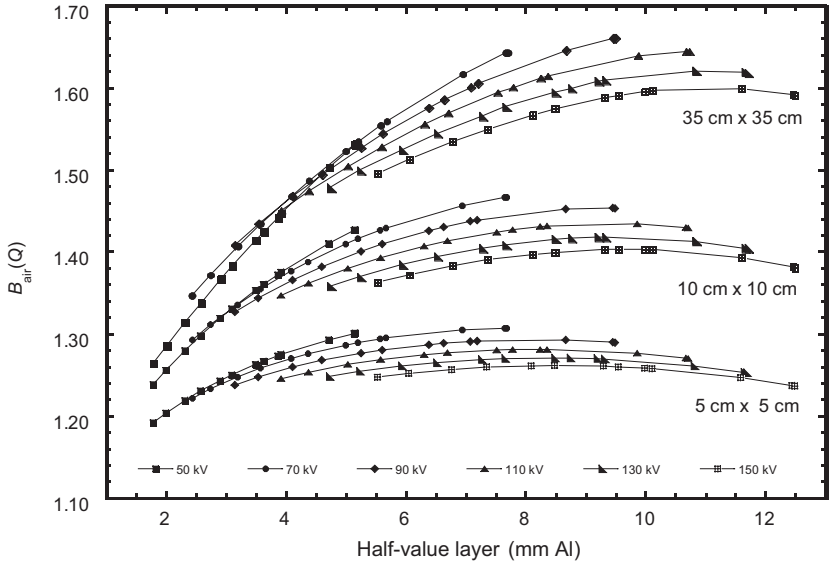

FIG. 13. Backscatter factors at the entrance surface of a 15 cm thick water phantom for clinical beam qualities used in diagnostic and interventional radiology for various field sizes.

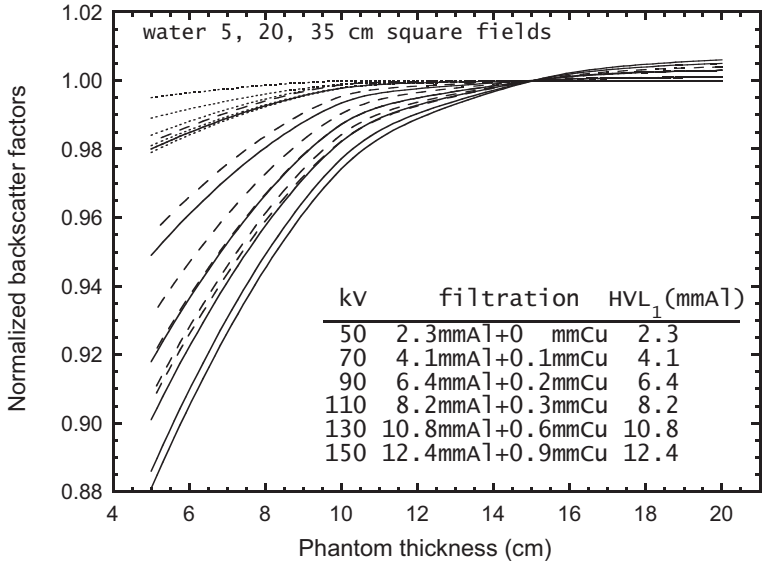

FIG 14. Dependence of the backscatter factors with field size and phantom thickness for a broad range of X ray beam qualities. The $B_{air}(Q)$ values for each square field size are normalized to those of a 15 cm thick phantom. The order of the various lines shown for each field size (from top to bottom: 5 cm, dotted; 20 cm, dashed; 35 cm, solid) correspond to the qualities indicated in the legend.

III.5. TABLES

TABLE 20. BACKSCATTER FACTORS $B_{air}(Q)$ AT THE ENTRANCE SURFACE OF 5–15 cm THICK WATER PHANTOMS FOR SQUARE CLINICAL BEAMS USED IN INFANT DIAGNOSTIC RADIOLOGY[a]

			Water phantom thickness (cm)				
			5	10	15	10	15
			Field size (cm × cm)				
Tube voltage	Filtration (mm)	Half-value layer (mm Al)	5 × 5	5 × 5	5 × 5	10 × 10	10 × 10
50	3 Al	1.96	1.200	1.204	1.204	1.255	1.255
50	3 Al + 0.1 Cu	2.87	1.232	1.240	1.241	1.315	1.317
50	3 Al + 0.2 Cu	3.47	1.250	1.261	1.261	1.350	1.352
60	3 Al	2.33	1.214	1.220	1.221	1.286	1.286

TABLE 20. BACKSCATTER FACTORS $B_{air}(Q)$ AT THE ENTRANCE SURFACE OF 5–15 cm THICK WATER PHANTOMS FOR SQUARE CLINICAL BEAMS USED IN INFANT DIAGNOSTIC RADIOLOGY[a] (cont.)

			Water phantom thickness (cm)				
			5	10	15	10	15
			Field size (cm × cm)				
Tube voltage	Filtration (mm)	Half-value layer (mm Al)	5 × 5	5 × 5	5 × 5	10 × 10	10 × 10
60	3 Al + 0.1 Cu	3.48	1.247	1.257	1.258	1.349	1.351
60	3 Al + 0.2 Cu	4.26	1.264	1.277	1.278	1.385	1.388
70	3 Al	2.69	1.224	1.232	1.232	1.308	1.309
70	3 Al + 0.1 Cu	4.04	1.254	1.267	1.268	1.371	1.373
70	3 Al + 0.2 Cu	4.97	1.269	1.285	1.286	1.404	1.408

[a] The estimated combined standard uncertainty is 0.5%.

TABLE 21. BACKSCATTER FACTORS $B_{air}(Q)$ AT THE ENTRANCE SURFACE OF A 15 cm THICK WATER PHANTOM FOR SQUARE CLINICAL BEAMS USED IN PAEDIATRIC DIAGNOSTIC RADIOLOGY[a]

			Water phantom thickness (cm)			
			15	15	15	15
			Field size (cm × cm)			
Tube voltage	Filtration (mm)	Half-value layer (mm Al)	10 × 10	15 × 15	20 × 20	25 × 25
60	3 Al	2.33	1.286	1.307	1.322	1.327
60	3 Al + 0.1 Cu	3.48	1.351	1.384	1.408	1.417
60	3 Al + 0.2 Cu	4.26	1.388	1.429	1.459	1.470
60	3 Al + 0.3 Cu	4.83	1.411	1.458	1.492	1.506
70	3 Al	2.69	1.309	1.337	1.357	1.365
70	3 Al + 0.1 Cu	4.04	1.373	1.414	1.444	1.456
70	3 Al + 0.2 Cu	4.97	1.408	1.458	1.495	1.510
70	3 Al + 0.3 Cu	5.65	1.429	1.486	1.527	1.545

TABLE 21. BACKSCATTER FACTORS $B_{air}(Q)$ AT THE ENTRANCE SURFACE OF A 15 cm THICK WATER PHANTOM FOR SQUARE CLINICAL BEAMS USED IN PAEDIATRIC DIAGNOSTIC RADIOLOGY[a] (cont.)

			Water phantom thickness (cm)			
			15	15	15	15
			Field size (cm × cm)			
Tube voltage	Filtration (mm)	Half-value layer (mm Al)	10 × 10	15 × 15	20 × 20	25 × 25
80	3 Al	3.07	1.328	1.361	1.385	1.396
80	3 Al + 0.1 Cu	4.63	1.390	1.438	1.473	1.489
80	3 Al + 0.2 Cu	5.68	1.421	1.478	1.520	1.540
80	3 Al + 0.3 Cu	6.45	1.438	1.502	1.549	1.571
90	3 Al	3.47	1.342	1.381	1.409	1.422
90	3 Al + 0.1 Cu	5.20	1.400	1.454	1.493	1.512
90	3 Al + 0.2 Cu	6.35	1.427	1.490	1.536	1.558
90	3 Al + 0.3 Cu	7.17	1.440	1.509	1.560	1.585
100	3 Al	3.88	1.353	1.396	1.428	1.442
100	3 Al + 0.1 Cu	5.75	1.405	1.464	1.507	1.528
100	3 Al + 0.2 Cu	6.95	1.427	1.494	1.544	1.569
100	3 Al + 0.3 Cu	7.79	1.437	1.510	1.563	1.591
110	3 Al	4.30	1.360	1.408	1.442	1.459
110	3 Al + 0.1 Cu	6.26	1.407	1.469	1.515	1.537
110	3 Al + 0.2 Cu	7.49	1.425	1.495	1.546	1.573
110	3 Al + 0.3 Cu	8.33	1.432	1.506	1.562	1.590
120	3 Al	4.71	1.365	1.415	1.452	1.471
120	3 Al + 0.1 Cu	6.74	1.407	1.471	1.518	1.543
120	3 Al + 0.2 Cu	7.98	1.421	1.492	1.545	1.573
120	3 Al + 0.3 Cu	8.83	1.425	1.501	1.557	1.587

[a] The estimated combined standard uncertainty is 0.5%.

TABLE 22. BACKSCATTER FACTORS $B_{air}(Q)$ AT THE ENTRANCE SURFACE OF A 15 cm THICK WATER PHANTOM FOR SQUARE CLINICAL BEAMS USED IN INTERVENTIONAL RADIOLOGY[a]

			Water phantom thickness (cm)			
			15	15	15	15
			Field size (cm × cm)			
Tube voltage	Filtration (mm)	Half-value layer (mm Al)	10 × 10	15 × 15	20 × 20	25 × 25
60	2.5 Al	2.11	1.272	1.291	1.304	1.309
60	3 Al	2.33	1.286	1.307	1.322	1.327
60	3 Al + 0.1 Cu	3.48	1.351	1.384	1.408	1.417
60	3 Al + 0.2 Cu	4.26	1.388	1.429	1.459	1.470
60	3 Al + 0.3 Cu	4.83	1.411	1.458	1.492	1.506
60	3 Al + 0.6 Cu	5.89	1.445	1.503	1.545	1.563
60	3 Al + 0.9 Cu	6.51	1.460	1.524	1.572	1.592
70	3 Al	2.69	1.309	1.337	1.357	1.365
70	3 Al + 0.1 Cu	4.04	1.373	1.414	1.444	1.456
70	3 Al + 0.2 Cu	4.97	1.408	1.458	1.495	1.510
70	3 Al + 0.3 Cu	5.65	1.429	1.486	1.527	1.545
70	3 Al + 0.6 Cu	6.93	1.457	1.525	1.576	1.599
70	3 Al + 0.9 Cu	7.67	1.467	1.542	1.597	1.623
80	3 Al	3.07	1.328	1.361	1.385	1.396
80	3 Al + 0.1 Cu	4.63	1.390	1.438	1.473	1.489
80	3 Al + 0.2 Cu	5.68	1.421	1.478	1.520	1.540
80	3 Al + 0.3 Cu	6.45	1.438	1.502	1.549	1.571
80	3 Al + 0.6 Cu	7.87	1.458	1.533	1.589	1.617
80	3 Al + 0.9 Cu	8.68	1.462	1.544	1.604	1.635
90	3 Al	3.47	1.342	1.381	1.409	1.422
90	3 Al + 0.1 Cu	5.20	1.400	1.454	1.493	1.512
90	3 Al + 0.2 Cu	6.35	1.427	1.490	1.536	1.558
90	3 Al + 0.3 Cu	7.17	1.440	1.509	1.560	1.585

TABLE 22. BACKSCATTER FACTORS $B_{air}(Q)$ AT THE ENTRANCE SURFACE OF A 15 cm THICK WATER PHANTOM FOR SQUARE CLINICAL BEAMS USED IN INTERVENTIONAL RADIOLOGY[a] (cont.)

			Water phantom thickness (cm)			
			15	15	15	15
			Field size (cm × cm)			
Tube voltage	Filtration (mm)	Half-value layer (mm Al)	10 × 10	15 × 15	20 × 20	25 × 25
90	3 Al + 0.6 Cu	8.65	1.452	1.532	1.591	1.621
90	3 Al + 0.9 Cu	9.48	1.452	1.537	1.600	1.633
100	3 Al	3.88	1.353	1.396	1.428	1.442
100	3 Al + 0.1 Cu	5.75	1.405	1.464	1.507	1.528
100	3 Al + 0.2 Cu	6.95	1.427	1.494	1.544	1.569
100	3 Al + 0.3 Cu	7.79	1.437	1.510	1.563	1.591
100	3 Al + 0.6 Cu	9.29	1.443	1.525	1.585	1.617
100	3 Al + 0.9 Cu	10.10	1.441	1.527	1.590	1.625
110	3 Al	4.30	1.360	1.408	1.442	1.459
110	3 Al + 0.1 Cu	6.26	1.407	1.469	1.515	1.537
110	3 Al + 0.2 Cu	7.49	1.425	1.495	1.546	1.573
110	3 Al + 0.3 Cu	8.33	1.432	1.506	1.562	1.590
110	3 Al + 0.6 Cu	9.84	1.434	1.516	1.577	1.610
110	3 Al + 0.9 Cu	10.70	1.429	1.515	1.578	1.614
120	3 Al	4.71	1.365	1.415	1.452	1.471
120	3 Al + 0.1 Cu	6.74	1.407	1.471	1.518	1.543
120	3 Al + 0.2 Cu	7.98	1.421	1.492	1.545	1.573
120	3 Al + 0.3 Cu	8.83	1.425	1.501	1.557	1.587
120	3 Al + 0.6 Cu	10.30	1.424	1.506	1.567	1.600
120	3 Al + 0.9 Cu	11.20	1.418	1.502	1.565	1.601
150	3 Al	5.96	1.371	1.428	1.469	1.491
150	3 Al + 0.1 Cu	8.05	1.398	1.467	1.517	1.544
150	3 Al + 0.2 Cu	9.26	1.404	1.477	1.532	1.561

TABLE 22. BACKSCATTER FACTORS $B_{air}(Q)$ AT THE ENTRANCE SURFACE OF A 15 cm THICK WATER PHANTOM FOR SQUARE CLINICAL BEAMS USED IN INTERVENTIONAL RADIOLOGY[a] (cont.)

			Water phantom thickness (cm)			
			15	15	15	15
			Field size (cm × cm)			
Tube voltage	Filtration (mm)	Half-value layer (mm Al)	10 × 10	15 × 15	20 × 20	25 × 25
150	3 Al + 0.3 Cu	10.10	1.403	1.479	1.536	1.567
150	3 Al + 0.6 Cu	11.60	1.392	1.473	1.532	1.566
150	3 Al + 0.9 Cu	12.50	1.381	1.462	1.523	1.558

[a] The estimated combined standard uncertainty is 0.5%.

Appendix IV

SUMMARY OF PAEDIATRIC DOSE DATA

Recent paediatric DRL data for planar (Table 23) and CT (Table 24) imaging are given. Other sources of paediatric DRL data can be found in the literature [10, 203–205]. A number of other articles involving paediatric dose can also be found in the literature [26, 135, 206–211].

TABLE 23. COMPARISON OF PUBLISHED DIAGNOSTIC REFERENCE LEVELS FOR RADIOLOGICAL EXAMINATIONS

Examination	Age	K_i or K_e (mGy)				P_{KA} (mGy·cm²)				
		Austria K_i [193]	France K_e [194]	Ireland K_e [195]	United Kingdom K_e [196, 197]	Austria [193]	France [194]	Germany [198]	Netherlands [199]	United Kingdom [200]
Chest AP/PA	Newborn	0.05	0.08	—	0.05	17	10	5	15	—
	1 year	0.06	0.08	0.057	0.05	23	20	15	20	—
	5 years	0.07	0.1	0.053	0.07	26	50	25	50	—
	10 years	0.09	0.2	0.066	0.12	37	70	35	—	—
	15 years	0.11	—	0.088	—	73	—	—	—	—
Chest LAT	5 years	—	0.2	—	—	—	60	40	—	—
	10 years	—	0.3	—	—	—	80	60	—	—
Head AP/PA	Newborn	0.35	—	—		150	—	—	—	—
	1 year	0.6	—	—	0.8	250	—	200	—	—
	5 years	0.75	—	—	1.1	350	—	300	—	—
	10 years	0.9	—	—	1.1	450	—	—	—	—
	15 years	1	—	—	1.1	500	—	—	—	—

TABLE 23. COMPARISON OF PUBLISHED DIAGNOSTIC REFERENCE LEVELS FOR RADIOLOGICAL EXAMINATIONS (cont.)

Examination	Age	K_i or K_e (mGy)				P_{KA} (mGy·cm²)				
		Austria K_i [193]	France K_e [194]	Ireland K_e [195]	United Kingdom K_e [196, 197]	Austria [193]	France [194]	Germany [198]	Netherlands [199]	United Kingdom [200]
Head LAT	Newborn	0.3	—	—	—	100	—	—	—	—
	1 year	0.4	—	—	1.5	200	—	200	—	—
	5 years	0.5	—	—	0.8	250	—	250	—	—
	10 years	0.55	—	—	0.8	300	—	—	—	—
	15 years	0.6	—	—	0.8	350	—	—	—	—
Pelvis AP/PA	Newborn	—	—	—	—	—	—	—	—	—
	1 year	—	0.2	0.265	—	—	30	—	—	—
	5 years	—	0.9	0.475	—	—	200	150	—	—
	10 years	—	1.5	0.807	—	—	400	250	—	—
	15 years	—	—	0.892	—	—	—	—	—	—

TABLE 23. COMPARISON OF PUBLISHED DIAGNOSTIC REFERENCE LEVELS FOR RADIOLOGICAL EXAMINATIONS (cont.)

Examination	Age	K_i or K_e (mGy)				P_{KA} (mGy·cm²)				
		Austria K_i [193]	France K_e [194]	Ireland K_e [195]	United Kingdom K_e [196, 197]	Austria [193]	France [194]	Germany [198]	Netherlands [199]	United Kingdom [200]
Abdomen AP/PA	Newborn	0.2	—	—	—	60	—	—	15	—
	1 year	0.3	—	0.33	0.4	90	—	200	100	—
	5 years	0.4	1	0.752	0.5	200	300	250	250	—
	10 years	0.75	1.5	—	0.8	500	700	350	—	—
	15 years	1	—	—	—	700	—	—	—	—
Micturating cystourethrogram	Newborn	—	—	—	—	500	—	100	300	100
	1 year	—	—	—	—	700	—	200	700	300
	5 years	—	—	—	—	1200	—	300	800	300
	10 years	—	—	—	—	2000	—	600	—	400
	15 years	—	—	—	—	—	—	—	—	900

TABLE 23. COMPARISON OF PUBLISHED DIAGNOSTIC REFERENCE LEVELS FOR RADIOLOGICAL EXAMINATIONS (cont.)

Examination	Age	K_i or K_e (mGy)				P_{KA} (mGy·cm²)				
		Austria K_i [193]	France K_e [194]	Ireland K_e [195]	United Kingdom K_e [196, 197]	Austria [193]	France [194]	Germany [198]	Netherlands [199]	United Kingdom [200]
Barium meal	Newborn	—	—	—	—	—	—	—	—	100
	1 year	—	—	—	—	—	—	—	—	200
	5 years	—	—	—	—	—	—	—	—	200
	10 years	—	—	—	—	—	—	—	—	700
	15 years	—	—	—	—	—	—	—	—	2000
Barium swallow	Newborn	—	—	—	—	—	—	—	—	200
	1 year	—	—	—	—	—	—	—	—	400
	5 years	—	—	—	—	—	—	—	—	500
	10 years	—	—	—	—	—	—	—	—	1800
	15 years	—	—	—	—	—	—	—	—	3000

Note: AP: anteroposterior; LAT: lateral; PA: posteroanterior.

TABLE 24. COMPARISON OF PUBLISHED DIAGNOSTIC REFERENCE LEVELS FOR COMPUTED TOMOGRAPHY EXAMINATIONS

Examination	Age	C_{VOL} (mGy)					P_{KL} (mGy·cm)					
		France [194]	Germany [198]	Netherlands [199]	Switzerland [201]	United Kingdom [202]	Austria [193]	France [194]	Germany [198]	Netherlands [199]	Switzerland [201]	United Kingdom [202]
Head/brain (16 cm phantom)	Newborn	—	27	20	27	—	300	—	300	240	290	—
	1 year	30	33	25	33	30	400	420	400	300	390	270
	5 years	40	40	35	40	45	600	600	500	420	520	470
	10 years	50	50	50	50	50	750	900	650	600	710	620
	15 years	—	60	—	50	—	900	—	850	—	920	—
Facial bones (16 cm phantom)	Newborn	—	9	—	9	—	—	—	70	—	70	—
	1 year	25	11	—	11	—	—	200	95	—	95	—
	5 years	25	13	—	13	—	—	275	125	—	125	—
	10 years	25	17	—	17	—	—	300	180	—	180	—
	15 years	—	20	—	20	—	—	—	230	—	230	—

TABLE 24. COMPARISON OF PUBLISHED DIAGNOSTIC REFERENCE LEVELS FOR COMPUTED TOMOGRAPHY EXAMINATIONS (cont.)

Examination	Age	C_{VOL} (mGy)					P_{KL} (mGy·cm)					
		France [194]	Germany [198]	Netherlands [199]	Switzerland [201]	United Kingdom [202]	Austria [193]	France [194]	Germany [198]	Netherlands [199]	Switzerland [201]	United Kingdom [202]
Chest/thorax (32 cm phantom)	Newborn	—	1.5	—	1	—	80	—	20	—	12	—
	1 year	3	2	—	1.7	6	100	30	30	—	28	100
	5 years	4	3.5	—	2.7	6,5	150	65	65	—	55	115
	10 years	5	5	—	4.3	10	180	140	115	—	105	185
	15 years	—	8	—	6.8	—	200	—	230	—	205	—
Abdomen (32 cm phantom)	Newborn	—	2.5	—	1.5	—	—	—	45	—	27	—
	1 year	4	3.5	—	2.5	—	—	80	85	—	70	—
	5 years	5	6	—	4	—	—	120	165	—	125	—
	10 years	7	8	—	6.5	—	—	245	250	—	240	—
	15 years	—	13	—	10	—	—	—	500	—	500	—

TABLE 24. COMPARISON OF PUBLISHED DIAGNOSTIC REFERENCE LEVELS FOR COMPUTED TOMOGRAPHY EXAMINATIONS (cont.)

Examination	Age	C_{VOL} (mGy)					P_{KL} (mGy·cm)					
		France [194]	Germany [198]	Netherlands [199]	Switzerland [201]	United Kingdom [202]	Austria [193]	France [194]	Germany [198]	Netherlands [199]	Switzerland [201]	United Kingdom [202]
Lumbar spine (32 cm phantom)	Newborn	—	—	—	3.7	—	—	—	—	—	42	—
	1 year	—	—	—	6.5	—	—	—	—	—	85	—
	5 years	—	—	—	10	—	—	—	—	—	135	—
	10 years	—	—	—	16	—	—	—	—	—	215	—
	15 years	—	—	—	26	—	—	—	—	—	380	—

REFERENCES

[1] NATIONAL RESEARCH COUNCIL OF THE NATIONAL ACADEMIES, Health Risks from Exposure to Low Levels of Ionizing Radiation; BEIR VII Phase 2, Committee to Assess Health Risks from Exposure to Low Levels of Ionizing Radiation, National Academies Press, Washington, DC (2006).

[2] INTERNATIONAL ATOMIC ENERGY AGENCY, Clinical Training of Medical Physicists Specializing in Diagnostic Radiology, Training Course Series No. 47, IAEA, Vienna (2011).

[3] INTERNATIONAL ATOMIC ENERGY AGENCY, Dosimetry in Diagnostic Radiology: An International Code of Practice, Technical Reports Series No. 457, IAEA, Vienna (2007).

[4] INTERNATIONAL ATOMIC ENERGY AGENCY, Radiation Protection and Safety of Radiation Sources: International Basic Safety Standards — Interim Edition, IAEA Safety Standards Series No. GSR Part 3 (Interim), IAEA, Vienna (2011).

[5] INTERNATIONAL ATOMIC ENERGY AGENCY, Diagnostic Radiology Physics: A Handbook for Teachers and Students, IAEA, Vienna (2013).

[6] INTERNATIONAL ELECTROTECHNICAL COMMISSION, Medical Electrical Equipment — Dosimeters with Ionization Chambers and/or Semi-conductor Detectors as Used in X ray Diagnostic Imaging, IEC-61674, IEC, Geneva (1997).

[7] INTERNATIONAL ELECTROTECHNICAL COMMISSION, Medical Diagnostic X-ray Equipment — Radiation Conditions for Use in the Determination of Characteristics, IEC-61267, IEC, Geneva (2005).

[8] MARTIN, C.J., An evaluation of semiconductor and ionization chamber detectors for diagnostic x-ray dosimetry measurements, Phys. Med. Biol. **52** (2007) 4465–4480.

[9] INTERNATIONAL ELECTROTECHNICAL COMMISSION, Medical Electrical Equipment — Part 2-43: Particular Requirements for the Safety of X-ray Equipment for Interventional Procedures, IEC 60601-2-43, IEC, Geneva (2000).

[10] KILJUNEN, T., JÄRVINEN, H., SAVOLAINEN, S., Diagnostic reference levels for thorax X-ray examinations of paediatric patients, Br. J. Radiol. **80** (2007) 452–459.

[11] INSTITUTE OF PHYSICS AND ENGINEERING IN MEDICINE, The Commissioning and Routine Testing of Mammographic X-ray Systems, 3rd edn, Rep. 59, IPEM, York, UK (2004).

[12] INTERNATIONAL COMMISSION ON RADIOLOGICAL PROTECTION, Radiological Protection and Safety in Medicine, Publication 73, Pergamon Press, Oxford and New York (1997).

[13] NATIONAL RADIOLOGICAL PROTECTION BOARD, Documents of the NRPB, Vol. 10, National Radiological Protection Board, College of Radiographers and Royal College of Radiologists, NRPB, Chilton, UK (1999).

[14] NATIONAL COUNCIL ON RADIATION PROTECTION AND MEASUREMENTS, Ionizing Radiation Exposure of the Population of the United States, NCRP Rep. 160, NCRP, Bethesda, MD (2009).

[15] INTERNATIONAL ATOMIC ENERGY AGENCY, Implementation of the International Code of Practice on Dosimetry in Diagnostic Radiology (TRS 457): Review of Test Results, IAEA Human Health Reports No. 4, IAEA, Vienna (2011).

[16] INTERNATIONAL ATOMIC ENERGY AGENCY, Status of Computed Tomography Dosimetry for Wide Cone Beam Scanners, IAEA Human Health Reports No. 5, IAEA, Vienna (2011).

[17] DIXON, R.L., A new look at CT dose measurement: beyond CTDI, Med. Phys. **30** (2003) 1272–1280.

[18] DIXON, R.L., Restructuring CT dosimetry — a realistic strategy for the future requiem for the pencil chamber, Med. Phys. **33** (2006) 3973–3976.

[19] BOONE, J.M., The trouble with CTD100, Med. Phys. **34** (2007) 1364–1371.

[20] INTERNATIONAL COMMISSION ON RADIOLOGICAL PROTECTION, Radiological Protection in Medicine, Publication 105, Elsevier (2007).

[21] JÄRVINEN, H., et al., Patient doses in paediatric CT: feasibility of setting diagnostic reference levels, Radiat. Prot. Dosim. **147** (2011) 142–146.

[22] EUROPEAN COMMISSION, European Guidelines on Quality Criteria for Computed Tomography, EC Working Document, EUR 16262 EN, European Commission, Brussels (1998).

[23] BILLINGER, J., NOWOTNY, R., HOMOLKA, P., Diagnostic reference levels in pediatric radiology in Austria, Eur. Radiol. **20** (2010) 1572–1579.

[24] CHAPPLE, C.L., BROADHEAD, D.A., FAULKNER, K., A phantom based method for deriving typical patient doses from measurements of dose-area product on populations of patients, Br. J. Radiol. **68** (1995) 1083–1086.

[25] MARTIN, C.J., FARQUHAR, B., STOCKDALE, E., MACDONALD, S., A study of the relationship between patient dose and size in paediatric radiology, Br. J. Radiol. **67** (1994) 864–871.

[26] NATIONAL RADIOLOGICAL PROTECTION BOARD, Reference Doses and Patient Size in Paediatric Radiology, NRPB Rep. R318, Chilton, UK (2000).

[27] INTERNATIONAL ELECTROTECHNICAL COMMISSION, Medical Electrical Equipment — Part 2-44: Particular Requirements for the Safety of X-ray Equipment for Computed Tomography, IEC-60601-2-44-Ed.2.1 (incl. amendment 1), IEC, Geneva (2002).

[28] STRAUSS, K.J., GOSKE, M.J., FRUSH, D.P., BUTLER, P.F., MORRISON, G., Image gently vendor summit: working together for better estimates of pediatric radiation dose from CT, AJR Am. J. Roentgenol. **192** (2009) 1169–1175.

[29] AMERICAN ASSOCIATION OF PHYSICISTS IN MEDICINE, Size-specific Dose Estimates (SSDE) in Paediatric and Adult Body CT Examinations, Rep. 204, AAPM, New York (2011).

[30] NATIONAL COUNCIL ON RADIATION PROTECTION AND MEASUREMENTS, Radiation Dose Management for Fluoroscopically-guided Interventional Medical Procedures, NCRP Rep. 168, NCRP, Bethesda, MD (2010).

[31] LINET, M.S., KIM, K.P., RAJARAMAN, P., Children's exposure to diagnostic medical radiation and cancer risk: epidemiologic and dosimetric considerations, Pediatr. Radiol. **39** Suppl 1. (2009) S4–26.

[32] UNITED NATIONS, Hereditary Effects of Radiation, Scientific Committee on the Effects of Atomic Radiation (UNSCEAR), UN, New York (2001).

[33] INTERNATIONAL COMMISSION ON RADIOLOGICAL PROTECTION, The 2007 Recommendations of the International Commission on Radiological Protection, Publication 103, Elsevier (2008).

[34] BRENNER, D.J., Effective dose: a flawed concept that could and should be replaced, Br. J. Radiol. **81** (2008) 521–523.

[35] HARRISON, J.D., STREFFER, C., The ICRP protection quantities, equivalent and effective dose: their basis and application, Radiat. Prot. Dosim. **127** (2007) 12–18.

[36] MARTIN, C.J., Effective dose: how should it be applied to medical exposures? Br. J. Radiol. **80** (2007) 639–647.

[37] DIETZE, G., HARRISON, J.D., MENZEL, H.G., Effective dose: a flawed concept that could and should be replaced. Comments on a paper by D J Brenner (Br J Radiol 2008;81:521–523), Br. J. Radiol. **82** (2009) 348–351; Authors' reply, 350–351.

[38] INTERNATIONAL COMMISSION ON RADIATION UNITS AND MEASUREMENTS, Patient Dosimetry for X Rays Used in Medical Imaging, ICRU Rep. 74, ICRU, Bethesda, MD (2006).

[39] INTERNATIONAL COMMISSION ON RADIOLOGICAL PROTECTION, Reference Man: Anatomical, Physiological and Metabolic Characteristics, Publication 23, Pergamon Press, Oxford and New York (1975).

[40] INTERNATIONAL COMMISSION ON RADIOLOGICAL PROTECTION, Basic Anatomical and Physiological Data for Use in Radiological Protection: Reference Values, Publication 89, Elsevier (2002).

[41] INTERNATIONAL COMMISSION ON RADIATION UNITS AND MEASUREMENTS, Tissue Substitutes in Radiation Dosimetry and Measurement, ICRU Rep. 44, ICRU, Bethesda, MD (1989).

[42] WHITE, D.R., The formulation of tissue substitute materials using basic interaction data, Phys. Med. Biol. **22** (1977) 889–899.

[43] WHITE, D.R., MARTIN, R.J., DARLISON, R., Epoxy resin based tissue substitutes, Br. J. Radiol. **50** (1977) 814–821.

[44] VARCHENA, V., GUBATOVA, D., SIDORIN, V., KALNITSKY, S., Children's heterogeneous phantoms and their application in roentgenology, Radiat. Prot. Dosim. **49** (1993) 77–78.

[45] The Consortium of Computational Human Phantoms, http://www.virtualphantoms.org/phantoms.htm

[46] INTERNATIONAL COMMISSION ON RADIOLOGICAL PROTECTION, Adult Reference Computational Phantoms, Publication 110, Elsevier (2009).

[47] LEE, C., BOLCH, W.E., Age-dependent organ and effective dose coefficients for external photons: a comparison of stylized and voxel-based paediatric phantoms, Phys. Med. Biol. **51** (2006) 4663–4688.

[48] LEE, C., WILLIAMS, J.L., BOLCH, W.E., Whole-body voxel phantoms of paediatric patients — UF Series B, Phys. Med. Biol. **51** (2006) 4649–4661.

[49] ZANKL, M., et al., The construction of computer tomographic phantoms and their application in radiology and radiation protection, Radiat. Environ. Biophys. **27** (1988) 153–164.

[50] TAPIOVAARA, M., SIISKONEN, T., PCXMC — A PC-based Monte Carlo Program for Calculating Patient Doses in Medical X-ray Examinations, STUK — Radiation and Nuclear Safety Authority, Rep. STUK-A231, Helsinki (2008), http://www.stuk.fi/pcxmc/

[51] IMPACT, ImPACT CT Dosimetry Calculator, Imaging Performance Assessment of CT Scanners, St. George's Hospital (2002), www.impactscan.org

[52] STAMM, G., NAGEL, H.D., CT-Expo. Medizinische Hochschule Hannover Abt. Experimentelle Radiologie (2001), http://www.mh-hannover.de/1604.html

[53] HART, D., WALL, B.F., HILLIER, M.C., SHRIMPTON, P.C., Frequency and Collective Dose for Medical and Dental X-ray Examinations in the UK, 2008, Health Protection Agency, Rep. HPA-CRCE-012, Chilton, UK (2010).

[54] TAPIOVAARA, M., LAKKISTO, M., SERVOMAA, A., PCXMC: A PC-based Monte Carlo Program for Calculating Patient Doses in Medical X-ray Examinations, STUK (Finnish Centre for Radiation and Nuclear Safety), Rep. STUK-A139, Helsinki (1997).

[55] ROSENSTEIN, M., WARNER, G.G., BECK, T.J., Handbook of Selected Organ Doses for Projections Common in Pediatric Radiology, Bureau of Radiological Health, Rep., HEW Publication (FDA), Rockville, MD (1979).

[56] HART, D., JONES, D.G., WALL, B.F., Normalised Organ Doses for Paediatric X-ray Examinations Calculated Using Monte Carlo Techniques, National Radiological Protection Board, Rep. NRPB-SR279, Chilton, UK (1996).

[57] HART, D., JONES, D.G., WALL, B.F., Coefficients for Estimating Effective Doses from Paediatric X-ray examination, Her Majesty's Stationery Office, Rep. NRPB-R279, London (1996).

[58] ZANKL, M., PETOUSSI, N., VEIT, R., FENDEL, H., "Organ doses for a child in diagnostic radiology: comparison of a realistic and a MIRD-type phantom", Optimization of Image Quality and Patient Exposure in Diagnostic Radiology, BIR Report 20 (MOORES, B.M., WALL, B.F., ERISKAT, H., SCHIBILLA, H., Eds), British Institute of Radiology, London (1989) 196–198.

[59] ZANKL, M., PANZER, N., DREXLER, G., Tomographic Anthropomorphic Models Part II: Organ Doses from Tomographic Examinations in Paediatric Radiology, GSF-Bericht 30/93, Institut für Strahlenschutz, Neuherberg, Germany (1993).

[60] TURNER, A.C., et al., The feasibility of patient size-corrected, scanner-independent organ dose estimates for abdominal CT exams, Med. Phys. **38** (2011) 820–829.

[61] STRAUSS, K.J., KASTE, S.C., ALARA in pediatric interventional and fluoroscopic imaging: striving to keep radiation doses as low as possible during fluoroscopy of pediatric patients — a white paper executive summary, J. Am. Coll. Radiol. **3** (2006) 686–688.

[62] STRAUSS, K.J., KASTE, S.C., The ALARA concept in pediatric interventional and fluoroscopic imaging: striving to keep radiation doses as low as possible during fluoroscopy of pediatric patients — a white paper executive summary, AJR Am. J. Roentgenol. **187** (2006) 818–819.

[63] BARNES, G.T., "Specification of diagnostic x-ray imaging equipment and the bid process", Specification, Acceptance Testing and Quality Control of Diagnostic X-ray Imaging Equipment (BARNES, G.T., FREY, C.D., Eds), American Association of Physicists in Medicine, New York (1991) 10–30.

[64] GRAY, J.E., MORIN, R.L., Purchasing medical imaging equipment, Radiology **171** (1989) 9–16.

[65] HENDEE, W.R., ROSSI, R.P., Performance specifications for diagnostic X-ray equipment, Radiology **120** (1976) 409–412.

[66] ROSSI, R.P., "Identification of clinical needs (roentgenography)", The Selection and Performance Evaluation of Radiologic Equipment (HENDEE, W.R., Ed.), Williams and Wilkins, Baltimore, MD (1985) 9–12.

[67] ROSSI, R.P., HENDEE, W.R., The exchange of information between the purchaser and supplier of radiologic imaging equipment, Proc. SPIE **96** (1976) 385–388.

[68] STRAUSS, K.J., Interventional suite and equipment management: cradle to grave, Pediatr. Radiol. **36** Suppl. 2 (2006) 221–236.

[69] BHATNAGAR, J.P., RAO, G.U., Kilovoltage calibration of diagnostic roentgen ray generators, Acta Radiol. Ther. Phys. Biol. **9** (1970) 555–566.

[70] HARRISON, R.M., FORSTER, E., Performance characteristics of X-ray tubes and generators, Radiography **50** (1984) 245–248.

[71] RAUCH, P.L., "Performance characteristics of diagnostic x-ray generators", Acceptance Testing of Radiological Imaging Equipment (Proc. AAPM Symp. No. 1), (LIN, P.J.P., KRIZ, R.J., RAUCH, P.L., STRAUSS, K.J., ROSSI, R.P., Eds), American Association of Physicists in Medicine, New York (1982) 126–156.

[72] ROSSI, R.P., "Acceptance testing of radiographic x-ray generators", Acceptance Testing of Radiological Imaging Equipment (Proc. AAPM Symp. No. 1), (LIN, P.J.P., KRIZ, R.J., RAUCH, P.L., STRAUSS, K.J., ROSSI, R.P., Eds), American Institute of Physics, New York (1982) 110–125.

[73] ROSSI, R.P., LIN, P.J.P., RAUCH, P.L., STRAUSS, K.J., Performance Specifications and Acceptance Testing for X-ray Generators and Automatic Exposure Control Devices, AAPM Rep. No. 14, American Institute of Physics, New York (1985).

[74] STRAUSS, K.J., "Radiographic equipment and components: technology overview and quality improvement", Syllabus: A Categorical Course in Physics-technology Update and Quality Improvement of Diagnostic X-ray Imaging Equipment (GOULD, R.G., BOONE, J.M., Eds), Radiological Society of North America, Oak Brook, IL (1996) 21–48.

[75] AMIS, E.S., JR., et al., American College of Radiology white paper on radiation dose in medicine, J. Am. Coll. Radiol. **4** (2007) 272–284.

[76] STRAUSS, K.J., KASTE, S.C., The ALARA (as low as reasonably achievable) concept in pediatric interventional and fluoroscopic imaging: striving to keep radiation doses as low as possible during fluoroscopy of pediatric patients — a white paper executive summary, Pediatr. Radiol. **36** Suppl. 2 (2006) 110–112.

[77] GRAY, J.E., "Acceptance testing of diagnostic x-ray imaging equipment: considerations and rationale", Specification, Acceptance Testing and Quality Control of Diagnostic X-ray Imaging Equipment (SIEBERT, J.A., BARNES, G.T., GOULD, R.G., Eds), American Association of Physicists in Medicine, New York (1991) 1–9.

[78] ROSSI, R.P., "Acceptance testing (roentgenography)", The Selection and Performance Evaluation of Radiologic Equipment (HENDEE, W.R., Ed.), Williams and Wilkins, Baltimore, MD (1985) 98–130.

[79] STRAUSS, K.J., "Interventional equipment acquisition process: cradle to grave", Intravascular Brachytherapy Fluoroscopically Guided Interventions (BALTER, S., CHAN, R.C., SHOPE, T.B., Eds), Medical Physics Publishing, Madison, WI (2002) 797–848.

[80] HENDEE, W.R., An opportunity for radiology, Radiology **238** (2006) 389–394.

[81] CHRISTIE, J., Performance specifications from the radiologist's perspective, Proc. SPIE **70** (1975) 242–243.

[82] VYBORNY, C.J., "Image quality: the radiologist's perspective", Specification, Acceptance Testing and Quality Control of Diagnostic X-ray Imaging Equipment, AAPM Monograph No. 20, AAPM 1991 (SIEBERT, J.A., BARNES, G.T., GOULD, R.G., Eds), American Institute of Physics, New York (1994) 145–172.

[83] BURNS, C., Using computed digital radiography effectively, Semin. Radiol. Technol. **1** (1993) 24–36.

[84] KRUPINSKI, E.A., et al., Digital radiography image quality: image processing and display, J. Am. Coll. Radiol. **4** (2007) 389–400.

[85] WILLIAMS, M.B., et al., Digital radiography image quality: image acquisition, J. Am. Coll. Radiol. **4** (2007) 371–388.

[86] STRAUSS, K.J., "Cardiac catheterization equipment requirements: Pediatric catheterization laboratory considerations", Categorical Course in Diagnostic Radiology Physics: Cardiac Catheterization Imaging, Radiological Society of North America, Oak Brook, IL (1998) 105–119.

[87] LEE, D.L., CHEUNG, L.K., JEROMIN, L.S., New digital detector for projection radiography, Proc. SPIE **2432** (1995) 237–249.

[88] ROWLANDS, J.A., YORKSTON, J., "Flat panel detectors for digital radiography", Handbook of Medical Imaging, Vol. 1, Physics and Psychophysics (BEUTEL, J., KUNDEL, H.L., VAN METTER, R.L., Eds), SPIE — The International Society for Optical Engineering, Bellingham, WA (2000) 223–328.

[89] SEIBERT, J.A., Tradeoffs between image quality and dose, Pediatr. Radiol. **34** Suppl. 3 (2004) S183–195, discussion S234–241.

[90] SEIBERT, J.A., Flat-panel detectors: how much better are they? Pediatr. Radiol. **36** Suppl. 2 (2006) 173–181.

[91] DAVIES, A.G., COWEN, A.R., KENGYELICS, S.M., BURY, R.F., BRUIJNS, T.J., Threshold contrast detail detectability measurement of the fluoroscopic image quality of a dynamic solid-state digital x-ray image detector, Med. Phys. **28** (2001) 11–15.

[92] MORIN, R.L., SEIBERT, J.A., Considerations for selecting a digital radiography system, J. Am. Coll. Radiol. **2** (2005) 287–290.

[93] BUSHBERG, J.T., SEIBERT, J.A., LEIDHOLDT, E.M.J., BOONE, J.M., The Essential Physics of Medical Imaging, 2nd edn, Williams and Wilkins, Baltimore, MD (2002).

[94] HADLEY, J.L., AGOLA, J., WONG, P., Potential impact of the American College of Radiology appropriateness criteria on CT for trauma, AJR Am. J. Roentgenol. **186** (2006) 937–942.

[95] HUFTON, A.P., RUSSELL, J.G., The use of carbon fibre material in table tops, cassette fronts and grid covers: magnitude of possible dose reduction, Br. J. Radiol. **59** (1986) 157–163.

[96] GEISER, W.R., HUDA, W., GKANATSIOS, N.A., Effect of patient support pads on image quality and dose in fluoroscopy, Med. Phys. **24** (1997) 377–382.

[97] McCOLLOUGH, C.H., The AAPM/RSNA physics tutorial for residents. X-ray production, Radiographics **17** (1997) 967–984.

[98] NOCE, J.P., Diagnostic X-ray fundamentals: the tube, Biomed. Instrum. Technol. **30** (1996) 293–295.

[99] ZINK, F.E., X-ray tubes, Radiographics **17** (1997) 1259–1268.

[100] AMMAN, E., WIEDE, G., "Generators and tubes in interventional radiology", Syllabus: A Categorical Course in Physics-physical and Technical Aspects of Angiography and Interventional Radiology (BALTER, S., SHOPE, T.B., Eds), Radiological Society of North America, Oak Brook, IL (1995) 59–74.

[101] PLEWES, D.B., VOGELSTEIN, E., Grid controlled x-ray tube switching time: implications for rapid exposure control, Med. Phys. **11** (1984) 693–696.

[102] TROUT, E.D., The protective housing for a diagnostic x-ray tube, Radiology **87** (1966) 75–81.

[103] STRAUSS, K.J., Pediatric interventional radiography equipment: safety considerations, Pediatr. Radiol. **36** Suppl. 2 (2006) 126–135.

[104] ABLOW, R.C., JAFFE, C.C., ORPHANOUDAKIS, S.C., MARKOWITZ, R.I., ROSENFIELD, N.S., Fluoroscopic dose reduction using a digital television noise-reduction device, Radiology **148** (1983) 313–315.

[105] ATKINS, H.L., FAIRCHILD, R.G., ROBERTSON, J.S., GREENBERG, D., Effect of absorption edge filters on diagnostic x-ray spectra, Radiology **115** (1975) 431–437.

[106] BALTER, S., Managing radiation in the fluoroscopic environment, Philips Medical Systems (1995) 1–15.

[107] BURGESS, A.E., Physical measurements of heavy metal filter performance, Med. Phys. **12** (1985) 225–228.

[108] CAMPBELL, J.M., KUNTZLER, C.M., NIKESCH, W., Exposure reduction using yttrium filters in a cardiac catheterization unit, Cathet. Cardiovasc. Diagn. **12** (1986) 202–204.

[109] DEN BOER, A., DE FEYTER, P.J., HUMMEL, W.A., KEANE, D., ROELANDT, J.R., Reduction of radiation exposure while maintaining high-quality fluoroscopic images during interventional cardiology using novel x-ray tube technology with extra beam filtering, Circulation **89** (1994) 2710–2714.

[110] GAGNE, R.M., QUINN, P.W., "X-ray spectral considerations in fluoroscopy", Syllabus: A Categorical Course in Physics-physical and Technical Aspects of Angiography and Interventional Radiology (BALTER, S., SHOPE, T.B., Eds), Radiological Society of North America, Oak Brook, IL (1995) 49–58.

[111] GAGNE, R.M., QUINN, P.W., JENNINGS, R.J., Comparison of beam-hardening and K-edge filters for imaging barium and iodine during fluoroscopy, Med. Phys. **21** (1994) 107–121.

[112] JANGLAND, L., AXELSSON, B., Niobium filters for dose reduction in pediatric radiology, Acta Radiol. **31** (1990) 540–541.

[113] ORT, M.G., GREGG, E.C., PILLAI, K.M., RAO, P.S., Radiographic quality, tube potential, and patient dose, Med. Phys. **6** (1979) 134–136.

[114] ROSSI, R.P., HARNISCH, B., HENDEE, W.R., Reduction of radiation exposure in radiography of the chest, Radiology **144** (1982) 909–914.

[115] THIERENS, H., KUNNEN, M., VAN DER PLAETSEN, A., SEGAERT, O., Evaluation of the use of a niobium filter for patient dose reduction in chest radiography, Br. J. Radiol. **64** (1991) 334–340.

[116] VILLAGRAN, J.E., HOBBS, B.B., TAYLOR, K.W., Reduction of patient exposure by use of heavy elements as radiation filters in diagnostic radiology, Radiology **127** (1978) 249–254.

[117] WESENBERG, R.L., AMUNDSON, G.M., MUELLER, D.L., COUPLAND, S.G., Ultra-low-dose routine pediatric radiography utilizing a rare-earth filter, Can. Assoc. Radiol. J. **38** (1987) 158–164.

[118] WILLIAMSON, B.D., VAN DOORN, T., The efficacy of K-edge filters in diagnostic radiology, Australas. Phys. Eng. Sci. Med. **17** (1994) 162–174.

[119] BOONE, J.M., SEIBERT, J.A., A comparison of mono- and poly-energetic x-ray beam performance for radiographic and fluoroscopic imaging, Med. Phys. **21** (1994) 1853–1863.

[120] BURGESS, A.E., Contrast effects of a gadolinium filter, Med. Phys. **8** (1981) 203–209.

[121] JOHNSON, M.A., BURGESS, A.E., Clinical use of a gadolinium filter in pediatric radiography, Pediatr. Radiol. **10** (1981) 229–232.

[122] MOTZ, J.W., DANOS, M., Image information content and patient exposure, Med. Phys. **5** (1978) 8–22.

[123] TAPIOVAARA, M.J., SANDBORG, M., DANCE, D.R., A search for improved technique factors in paediatric fluoroscopy, Phys. Med. Biol. **44** (1999) 537–559.

[124] INTERNATIONAL ELECTROTECHNICAL COMMISSION, Dose Area Product Meters, IEC-60580, 2nd edn, IEC, Geneva (2000).

[125] CHUNG, T., KIRKS, D.R., "Techniques", Practical Pediatric Imaging (KIRKS, D.R., GRISCOM, N.T., Eds), Lippincott-Raven, Philadelphia, PA (1998) 1–63.

[126] HU, H., Multi-slice helical CT: scan and reconstruction, Med. Phys. **26** (1999) 5–18.

[127] McCOLLOUGH, C.H., ZINK, F.E., Performance evaluation of a multi-slice CT system, Med. Phys. **26** (1999) 2223–2230.

[128] MORI, S., et al., Physical performance evaluation of a 256-slice CT-scanner for four-dimensional imaging, Med. Phys. **31** (2004) 1348–1356.

[129] NAGEL, H.D. (Ed.), Radiation Exposure in Computed Tomography: Fundamentals, Influencing Parameters, Dose Assessment, Optimisation, Scanner Data, Terminology, 4th edn, CTB Publications, Hamburg (2002).

[130] FLOHR, T.G., et al., First performance evaluation of a dual-source CT (DSCT) system, Eur. Radiol. **16** (2006) 256–268.

[131] CENTRE FOR EVIDENCE-BASED PURCHASING, CT scanner clinical applications software comparison. Comparative specifications, CEP 08024, NHS PASA (2009), http://nhscep.useconnect.co.uk/CEPProducts/Catalogue.aspx

[132] HENDEE, W.R., ROSSI, R.P., The exchange of information between the purchaser and supplier of radiologic imaging equipment, Proc. SPIE **96** (1976) 385–388.

[133] WILLIS, C.E., Strategies for dose reduction in ordinary radiographic examinations using CR and DR, Pediatr. Radiol. **34** Suppl. 3 (2004) S196–200, discussion S234–241.

[134] SANDBORG, M., DANCE, D.R., CARLSSON, G.A., PERSLIDEN, J., TAPIOVAARA, M.J., A Monte Carlo study of grid performance in diagnostic radiology: task-dependent optimization for digital imaging, Phys. Med. Biol. **39** (1994) 1659–1676.

[135] WARD, V.L., et al., Pediatric radiation exposure and effective dose reduction during voiding cystourethrography, Radiology **249** (2008) 1002–1009.

[136] LIN, P.J., The operation logic of automatic dose control of fluoroscopy system in conjunction with spectral shaping filters, Med. Phys. **34** (2007) 3169–3172.

[137] ROSSI, R.P., WESENBERG, R.L., HENDEE, W.R., A variable aperture fluoroscopic unit for reduced patient exposure, Radiology **129** (1978) 799–802.

[138] RUDIN, S., BEDNAREK, D.R., "Spatial shaping of the beam: collimation, grids, equalization filters, and region-of-interest fluoroscopy", Syllabus: A Categorical Course in Physics-physical and Technical Aspects of Angiography and Interventional Radiology (BALTER, S., SHOPE, T.B., Eds), Radiological Society of North America, Oak Brook, IL (1995) 75–86.

[139] RUDIN, S., BEDNAREK, D.R., MILLER, J.A., Dose reduction during fluoroscopic placement of feeding tubes, Radiology **178** (1991) 647–651.

[140] AUFRICHTIG, R., XUE, P., THOMAS, C.W., GILMORE, G.C., WILSON, D.L., Perceptual comparison of pulsed and continuous fluoroscopy, Med. Phys. **21** (1994) 245–256.

[141] RAUCH, P.L., The "30-30-30 rule", a practical guide to setting the detector input exposure rate for a fluoroscopic imager, Med. Phys. **37** (2010) 3123.

[142] McNITT-GRAY, M.F., AAPM/RSNA physics tutorial for residents: topics in CT. Radiation dose in CT, Radiographics **22** (2002) 1541–1553.

[143] KLEINMAN, P.L., STRAUSS, K.J., ZURAKOWSKI, D., BUCKLEY, K.S., TAYLOR, G.A., Patient size measured on CT images as a function of age at a tertiary care children's hospital, AJR Am. J. Roentgenol. **194** (2010) 1611–1619.

[144] CHENG, Z., et al., Low-dose prospective ECG-triggering dual-source CT angiography in infants and children with complex congenital heart disease: first experience, Eur. Radiol. **20** (2010) 2503–2511.

[145] CRAWLEY, M.T., BOOTH, A., WAINWRIGHT, A., A practical approach to the first iteration in the optimization of radiation dose and image quality in CT: estimates of the collective dose savings achieved, Br. J. Radiol. **74** (2001) 607–614.

[146] HUDA, W., Dose and image quality in CT, Pediatr. Radiol. **32** (2002) 709–713, discussion 751–754.

[147] HUDA, W., SCALZETTI, E.M., LEVIN, G., Technique factors and image quality as functions of patient weight at abdominal CT, Radiology **217** (2000) 430–435.

[148] LUCAYA, J., et al., Low-dose high-resolution CT of the chest in children and young adults: dose, cooperation, artifact incidence, and image quality, AJR Am. J. Roentgenol. **175** (2000) 985–992.

[149] YU, L., LI, H., FLETCHER, J.G., McCOLLOUGH, C.H., Automatic selection of tube potential for radiation dose reduction in CT: a general strategy, Med. Phys. **37** (2010) 234–243.

[150] O'DANIEL, J.C., STEVENS, D.M., CODY, D.D., Reducing radiation exposure from survey CT scans, AJR Am. J. Roentgenol. **185** (2005) 509–515.

[151] BRISSE, H.J., et al., Automatic exposure control in multichannel CT with tube current modulation to achieve a constant level of image noise: experimental assessment on pediatric phantoms, Med. Phys. **34** (2007) 3018–3033.

[152] UDAYASANKAR, U.K., et al., Low-dose nonenhanced head CT protocol for follow-up evaluation of children with ventriculoperitoneal shunt: reduction of radiation and effect on image quality, AJNR Am. J. Neuroradiol. **29** (2008) 802–806.

[153] HUDA, W., OGDEN, K.M., KHORASANI, M.R., Effect of dose metrics and radiation risk models when optimizing CT x-ray tube voltage, Phys. Med. Biol. **53** (2008) 4719–4732.

[154] ADDY, J.W., Increased filtration due to tungsten deposits inside the envelopes of x-ray tubes, Br. J. Radiol. **51** (1978) 397.

[155] McDANIEL, D.L., COHEN, G., WAGNER, L.K., ROBINSON, L.H., Relative dose efficiencies of antiscatter grids and air gaps in pediatric radiography, Med. Phys. **11** (1984) 508–512.

[156] THOMPSON, T.T., A Practical Approach to Modern Imaging Equipment, 2nd edn, Little Brown, Boston, MA (1985).

[157] GRAY, J.E., SWEE, R.G., The elimination of grids during intensified fluoroscopy and photofluoro spot imaging, Radiology **144** (1982) 426–429.

[158] RUDIN, S., BEDNAREK, D.R., Minimizing radiation dose to patient and staff during fluoroscopic, nasoenteral tube insertions, Br. J. Radiol. **65** (1992) 162–166.

[159] KALRA, M.K., et al., Strategies for CT radiation dose optimization, Radiology **230** (2004) 619–628.

[160] INTERNATIONAL ATOMIC ENERGY AGENCY, Applying Radiation Safety Standards in Diagnostic Radiology and Interventional Procedures Using X Rays, Safety Reports Series No. 39, IAEA, Vienna (2006).

[161] INTERNATIONAL ATOMIC ENERGY AGENCY, Radiation Protection in Paediatric Radiology, Safety Reports Series No. 71, IAEA, Vienna (2012).

[162] STRAUSS, K.J., et al., Image gently: Ten steps you can take to optimize image quality and lower CT dose for pediatric patients, AJR Am. J. Roentgenol. **194** (2010) 868–873.

[163] MILLER, D.L., et al., Clinical radiation management for fluoroscopically guided interventional procedures, Radiology **257** (2010) 321–332.

[164] TZEDAKIS, A., et al., Influence of z overscanning on normalized effective doses calculated for pediatric patients undergoing multidetector CT examinations, Med. Phys. **34** (2007) 1163–1175.

[165] TZEDAKIS, A., PERISINAKIS, K., RAISSAKI, M., DAMILAKIS, J., The effect of z overscanning on radiation burden of pediatric patients undergoing head CT with multidetector scanners: a Monte Carlo study, Med. Phys. **33** (2006) 2472–2478.

[166] DONNELLY, L.F., et al., Minimizing radiation dose for pediatric body applications of single-detector helical CT: strategies at a large Children's Hospital, AJR Am. J. Roentgenol. **176** (2001) 303–306.

[167] DA COSTA E SILVA, E.J., DA SILVA, G.A., Eliminating unenhanced CT when evaluating abdominal neoplasms in children, AJR Am. J. Roentgenol. **189** (2007) 1211–1214.

[168] FRANKLIN, M.F., Comparison of weight and height relations in boys from 4 countries, Am. J. Clin. Nutr. **70** (1999) 157S–162S.

[169] LINDSKOUG, B.A., The Reference Man in diagnostic radiology dosimetry, Br. J. Radiol. **65** (1992) 431–437.

[170] BOHMANN, I., Ermittlung der Durchstrahlungsdurchmesser bei Säuglingen, Kindern und Jugendlichen zur Aufstellung von Belichtungswerten in der Röntgendiagnostik und Abschätzung der Organdosiswerte bei typischen Röntgenuntersuchungen, GSF-Bericht 16/90, Gesellschaft für Strahlen und Umweltforschung, Neuherberg, Germany (1990).

[171] BRITISH STANDARDS INSTITUTE, Body Measurements of Boys and Girls from Birth up to 16.9 Years, Rep. BS7231 Part 1, London (1990).

[172] FREEMAN, J.V., et al., Cross sectional stature and weight reference curves for the UK, 1990, Arch. Dis. Child. **73** (1995) 17–24.

[173] GREGORY, J.R., et al., National Diet and Nutrition Survey, Children Aged 1½ to 4½ Years, Office of Population Censuses and Surveys London, Stationery Office (1995).

[174] CENTRE FOR DISEASE CONTROL AND PREVENTION, 2000 CDC Growth Charts for the United States: Methods and Development, Vital and Health Statistics, Department of Health and Human Services, Rep. (PHS) 2002-1696, Hyattsville, MD (2002).

[175] VARCHENA, V., Pediatric phantoms, Pediatr. Radiol. **32** (2002) 280–284.

[176] WILLIAMS, G., ZANKL, M., ABMAYR, W., VEIT, R., DREXLER, G., The calculation of dose from external photon exposures using reference and realistic human phantoms and Monte Carlo methods, Phys. Med. Biol. **31** (1986) 449–452.

[177] INTERNATIONAL COMMISSION ON RADIATION UNITS AND MEASUREMENTS, Photon, Electron, Proton and Neutron Interaction Data for Body Tissues, ICRU Rep. 46, ICRU, Bethesda, MD (1991).

[178] HUBBELL, J.H., SELTZER, S.M., Tables of X-ray Mass Attenuation Coefficients and Mass Energy-absorption Coefficients from 1 keV to 20 MeV for Elements Z = 1 to 92 and 48 Additional Substances of Dosimetric Interest, National Institute of Standards and Technology, Rep. NISTIR 5632, Gaithersburg, MD (1995).

[179] NOWOTNY, R., HÖFER, A., A computer code for the calculation of diagnostic x-ray spectra, Fortschr. Roentgenstr. Geb. Bildgebenden Verfahr. **142** (1985) 685–689.

[180] PETOUSSI-HENSS, N., ZANKL, M., DREXLER, G., PANZER, W., REGULLA, D., Calculation of backscatter factors for diagnostic radiology using Monte Carlo methods, Phys. Med. Biol. **43** (1998) 2237–2250.

[181] CHICA, U., ANGUIANO, M., LALLENA, A.M., Study of the formalism used to determine the absorbed dose for low-energy x-ray beams, Phys. Med. Biol. **53** (2008) 6963–6977.

[182] CHICA, U., FLOREZ, G., ANGUIANO, M., LALLENA, A.M., A simple analytical expression to calculate the backscatter factor for low energy X-ray beams, Phys. Med. **27** (2010) 75–80.

[183] KIM, J., HILL, R., CLARIDGE MACKONIS, E., KUNCIC, Z., An investigation of backscatter factors for kilovoltage x-rays: a comparison between Monte Carlo simulations and Gafchromic EBT film measurements, Phys. Med. Biol. **55** (2010) 783–797.

[184] OMRANE, L.B., VERHAEGEN, F., CHAHED, N., MTIMET, S., An investigation of entrance surface dose calculations for diagnostic radiology using Monte Carlo simulations and radiotherapy dosimetry formalisms, Phys. Med. Biol. **48** (2003) 1809–1824.

[185] BENMAKHLOUF, H., BOUCHARD, H., FRANSSON, A., ANDREO, P., Backscatter factors and mass energy-absorption coefficient ratios for diagnostic radiology dosimetry, Phys. Med. Biol. **56** (2011) 7179–7204.

[186] SALVAT, F., FERNÁNDEZ-VAREA, J.M., SEMPAU, J., PENELOPE, a code system for Monte Carlo simulation of electron and photon transport, OECD Nuclear Energy Agency, Issy-les-Moulineaux, France (2010).

[187] HUBBELL, J.H., SELTZER, S.M., Tables of X-ray Mass Attenuation Coefficients and Mass Energy-absorption Coefficients (version 1.4), National Institute of Standards and Technology, Gaithersburgh, MD (2004), http://physics.nist.gov/xaamdi

[188] ANDREO, P., NAHUM, A.E., Stopping-power ratio for a photon spectrum as a weighted sum of the values for monoenergetic photon beams, Phys. Med. Biol. **30** (1985) 1055–1065.

[189] KNIGHT, R.T., Absorbed dose conversion factors for therapeutic kilovoltage and megavoltage x-ray beams calculated by the Monte Carlo method, PhD Thesis, London Univ. (1996).

[190] POLUDNIOWSKI, G., LANDRY, G., DEBLOIS, F., EVANS, P.M., VERHAEGEN, F., SpekCalc: a program to calculate photon spectra from tungsten anode x-ray tubes, Phys. Med. Biol. **54** (2009) N433–438.

[191] JOINT COMMITTEE FOR GUIDES IN METROLOGY (WG1), Evaluation of Measurement Data — Guide to the Expression of Uncertainty in Measurement (GUM), Rep. 100:2008, BIPM, Sèvres (2008).

[192] ANDREO, P., BURNS, D.T., SALVAT, F., On the uncertainties of photon mass energy-absorption coefficients and their ratios for radiation dosimetry, Phys. Med. Biol. **57** (2012) 2117–2136.

[193] BUNDESMINISTERIUM FÜR GESUNDHEIT, Medizinische Strahlenschutzverordnung (2010), http://www.ris.bka.gv.at/GeltendeFassung.wxe?Abfrage=Bundesnormen&Gesetzesnummer=20003681

[194] INSTITUT DE RADIOPROTECTION ET DE SÛRETÉ NUCLÉAIRE, Les niveaux de référence diagnostiques en radiologie (2011), http://nrd.irsn.fr/index.php?page=radiologie

[195] MEDICAL COUNCIL, Diagnostic Reference Levels (2004), http://www.medicalcouncil.ie/About-Us/Legislation/Medical-Ionising-Radiation/Diagnostic-Referance-Levels-03-12-2004.pdf

[196] HART, D., WALL, B.F., SHRIMPTON, P.C., BUNGAY, D.R., DANCE, D.R., Reference Doses and Patient Size in Paediatric Radiology, National Radiological Protection Board, Rep. NRPB-R-318, Chilton, UK (2000).

[197] HART, D., WALL, B.F., SHRIMPTON, P.C., DANCE, D.R., The establishment of reference doses in paediatric radiology as a function of patient size, Radiat. Prot. Dosim. **90** (2000) 235–238.

[198] BUNDESAMT FÜR STRAHLENSCHUTZ, Bekanntmachung der aktualisierten diagnostischen Referenzwerte für diagnostische und interventionelle Röntgenuntersuchungen, Bundesanzeiger **111** (2010) 2594–2596.

[199] NEDERLANDSE COMMISSIE VOOR STRALINGSDOSIMETRIE, Diagnostische referentieniveaus in Nederland (2012), http://www.stralingsdosimetrie.nl/assets/files/ncs_report/NCS%20Rapport%2021%20DRN%20juni%202012.pdf

[200] HART, D., HILLIER, M.C., SHRIMPTON, P.C., Doses to Patients from Radiographic and Fluoroscopic X-ray Imaging Procedures in the UK — 2010 Review, Rep. HPA-CRCE-034, HPA, Chilton, UK (2012), http://www.hpa.org.uk/webc/HPAwebFile/HPAweb_C/1317134577210

[201] BUNDESAMT FÜR GESUNDHEIT BAG, Diagnostische Referenzwerte in der Computertomographie (2010), http://www.bag.admin.ch/themen/strahlung/10463/10958/

[202] SHRIMPTON, P.C., HILLIER, M.C., LEWIS, M.A., DUNN, M., Doses from Computed Tomography (CT) Examinations in the UK — 2003 Review, National Radiological Protection Board, Rep. NRPB-W67, Chilton, UK (2005), http://www.hpa.org.uk/webc/HPAwebFile/HPAweb_C/1194947420292

[203] BORISOVA, R., INGILIZOVA, C., VASSILEVA, J., Patient dosimetry in paediatric diagnostic radiology, Radiat. Prot. Dosim. **129** (2008) 155–159.

[204] ONNASCH, D.G., SCHRODER, F.K., FISCHER, G., KRAMER, H.H., Diagnostic reference levels and effective dose in paediatric cardiac catheterization, Br. J. Radiol. **80** (2007) 177–185.

[205] SONAWANE, A.U., SUNIL KUMAR, J.V., SINGH, M., PRADHAN, A.S., Suggested diagnostic reference levels for paediatric X-ray examinations in India, Radiat. Prot. Dosim. **147** (2010) 423–428.

[206] EUROPEAN COMMISSION, European Guidelines on Quality Criteria for Diagnostic Radiographic Images in Paediatrics, Rep. EUR 16261 EN, European Commission, Luxembourg (1996).

[207] MUHOGORA, W.E., et al., Paediatric CT examinations in 19 developing countries: frequency and radiation dose, Radiat. Prot. Dosim. **140** (2010) 49–58.

[208] SMANS, K., et al., Results of a European survey on patient doses in paediatric radiology, Radiat. Prot. Dosim. **129** (2008) 204–210.

[209] THOMAS, K.E., WANG, B., Age-specific effective doses for pediatric MSCT examinations at a large children's hospital using DLP conversion coefficients: a simple estimation method, Pediatr. Radiol. **38** (2008) 645–656.

[210] VANO, E., et al., Paediatric entrance doses from exposure index in computed radiography, Phys. Med. Biol. **53** (2008) 3365–3380.

[211] VERDUN, F.R., et al., Management of patient dose and image noise in routine pediatric CT abdominal examinations, Eur. Radiol. **14** (2004) 835–841.

Annex

DOSIMETRY WORK-SHEETS

This Annex contains examples of several paediatric general radiography dosimetry work-sheets.

K_i phantom:
Paediatric abdomen 1

Determination of incident air kerma using paediatric phantoms

User: _____ Date: _____

Hospital or clinic name: _____

1. X ray equipment

X ray unit and model: _____ Room No.: _____

Imaging using screen-film combination Imaging using digital image receptor

Screen-film combination: _____ Image receptor model: _____

Film processor model: _____

Developer and fixer (brand name): _____

2. Dosimeter and phantom

Dosimeter model: _____ Serial No.: _____ Date of calibration: _____

Calibration coefficient[1] N_{K,Q_0}: _____ □ mGy/nC □ mGy/reading

Reference conditions: Half-value layer (mm Al): _____ Field size: _____

Pressure P_0 (kPa): _____ Temperature T_0 (ºC): ___

Phantom material and thickness: _____

3. Exposure conditions

□ AEC □ Manual AEC setting: _____ mA setting: _____ Tube voltage (kV): _____

Manual or (if available) post-exposure mAs: _____

Table (horizontal) or wall (vertical) Bucky: _____

Distance d_{FTD} of Bucky from the X ray focus (mm): _____

Distance d_m of dosimeter from Bucky (mm): _____

Thickness d_p of phantom (mm): _____

4. Dosimeter reading and calculation of incident air kerma

Dosimeter reading (M_1, M_2, M_3): _____ Mean dosimeter reading $\bar{M}$: _____

Pressure P (kPa): ___ Temperature T (ºC): ___

$$k_{TP} = \left(\frac{273.2+T}{273.2+T_0}\right)\left(\frac{P_0}{P}\right) = \_\_\_\_\_^{2}$$

Half-value layer (from point 5 on next page) (mm Al) = ___ k_Q = _____

Calculated value of air kerma $K(d) = \bar{M} N_{K,Q_0} k_Q k_{TP}$ = _____ mGy

Calculated value of incident air kerma $K_i = K(d)\left(\frac{d_{FTD} - d_m}{d_{FTD} - d_p}\right)^2$ = _____ mGy

[1] This is the calibration coefficient for the whole dosimeter, including the detector and the measurement assembly. For systems with separate calibration coefficients for the detector and measurement assembly, the overall calibration coefficient is calculated as a product of the two separate calibration coefficients.

[2] For dosimeters with a semiconductor detector, $k_{TP} = 1$.

K_i phantom: Paediatric abdomen 2

5. Determination of half-value layer

Dosimeter readings should be obtained for filter thicknesses that bracket the half-value layer. The first and last readings M_{01} and M_{02} are made at zero filter thickness.

Filter thickness (mm Al)	Dosimeter reading (mGy)	Average dosimeter reading $\bar{M}$ at zero thickness
0.00		$(M_{01} + M_{02})/2$ = _____ mGy
0.00		Interpolated half-value layer (mm Al): _____

K_i tube: Output 1

Determination of X ray tube output

User: _____ Date: _____

Hospital or clinic name: _____

1. X ray equipment

X ray unit and model: _____ Room No.: _____

Imaging using screen-film combination

Screen-film combination: _____

Film processor model: _____

Developer and fixer (brand name): _____

Imaging using digital image receptor

Image receptor model: _____

2. Dosimeter

Dosimeter model: _____ Serial No.: _____ Date of calibration: ___

Calibration coefficient[3] N_{K,Q_0}: _____ □ mGy/nC □ mGy/reading

Reference conditions: Half-value layer (mm Al): _____ Field size: _____

Pressure P_0 (kPa): _____ Temperature T_0 (°C): ___

3. Exposure conditions

Distance d of dosimeter from tube focus (mm): ___

4. Dosimeter reading and X ray tube output calculation

Pressure (kPa): ___ Temperature (ºC): ___ $k_{TP} = \left(\frac{273.2+T}{273.2+T_0}\right)\left(\frac{P_0}{P}\right) =$ _____[4]

Tube voltage (kV)	Tube loading, P_{It} (mAs)	Dosimeter readings, M_1, M_2 and M_3	Mean dosimeter reading, $\bar{M}$	Half-value layer (mm Al)	k_Q	Calculated X ray tube output $Y(d)$ at distance d (mGy/mAs)

Note: X ray tube output $Y(d)$ is calculated as $Y(d) = \bar{M} N_{K,Q_0} k_Q k_{TP} / P_{It}$.

[3] This is the calibration coefficient for the whole dosimeter, including the detector and the measurement assembly. For systems with separate calibration coefficients for the detector and measurement assembly, the overall calibration coefficient is calculated as a product of the two calibration coefficients.

[4] For dosimeters with a semiconductor detector, $k_{TP} = 1$.

K_i tube:
Output 2

5. Determination of half-value layer

Dosimeter readings should be obtained for filter thicknesses that bracket the half-value layer. The first and last readings, M_{01} and M_{02}, are made at zero filter thickness.

Tube voltage (kV): _______

Filter thickness (mm Al)	Dosimeter reading (mGy)	Average dosimeter reading $\bar{M}$ at zero thickness
0.00		$(M_{01} + M_{02})/2 =$ _______ mGy
0.00		Interpolated half-value layer (mm Al): ____

Tube voltage (kV): _______

Filter thickness (mm Al)	Dosimeter reading (mGy)	Average dosimeter reading $\bar{M}$ at zero thickness
0.00		$(M_{01} + M_{02})/2 =$ _______ mGy
0.00		Interpolated half-value layer (mm Al): ____

Tube voltage (kV): _______

Filter thickness (mm Al)	Dosimeter reading (mGy)	Average dosimeter reading $\bar{M}$ at zero thickness
0.00		$(M_{01} + M_{02})/2 =$ _______ mGy
0.00		Interpolated half-value layer (mm Al): ____

Data collection sheet for indirect assessment of incident air kerma and entrance surface air kerma

User: _____ Date: _____

Hospital or clinic name: _____

1. X ray equipment

X ray unit and model: _____ Room No.: _____

Imaging using screen-film combination

Screen-film combination: _____

Film processor model: _____

Examination: _____

Imaging using digital image receptor

Image receptor model: _____

Developer and fixer (brand name): _____

Filtration: _____ Grid: _____

2. Collected data

Tube focus to tabletop distance d_{FTD} (mm): _____ (if constant) Age group: _____

Patient age	Patient height (cm)	Patient weight (kg)	Tube voltage (kV)	Tube loading (mAs)	One or other of:		Field size (mm × mm)
					Patient thickness, t_P (mm)	Tube focus to patient surface distance, d_{FSD} (mm)	

Calculations:

(1) The value of $Y(d)$ is interpolated from measured values of tube output

(2) Incident air kerma

$$K_i = Y(d)P_{It}\left(\frac{d}{d_{FTD} - t_p}\right)^2 \text{ or } K_i = Y(d)P_{It}\left(\frac{d}{d_{FSD}}\right)^2 = \_\_\_\_ \text{ mGy}$$

(3) Entrance surface air kerma

$K_e = K_i B = \_\_\_\_$ mGy

K_i paediatric patient: Clinical general radiography sheet

Hospital/clinic: _____ Room/X ray tube: _____

Examination and projection: thorax / abdomen / neonatal thorax and abdomen (circle one)

Paediatric age group: 0–1 month / 1 month–1 year / >1–5 years / >5–10 years (circle one)

Focus to detector distance (if constant) (mm): _____

	Examination date (dd-mm-yy)	Date of birth (dd-mm-yy)	Height (cm)	Weight (kg)	kV	mAs	Focus skin distance (mm)	Patient thickness (mm)	Sex (M/F)	Field size (mm × mm)
e.g.	09-05-09	09-05-02	130	33	65	8	1090	105	M	100 × 120
1										
2										
3										
4										
5										
6										
7										
8										
9										
10										
11										
12										
13										
14										
15										

Additional technique information:

$\dot{K}_e$ phantom:
Paediatric fluoro 1

Paediatric fluoroscopy dosimetry data sheets

Determination of entrance surface air kerma rate for a fluoroscopy installation

User: _____ Date: _____ Under couch □ Over couch □ C-arm □

Hospital or clinic name: _____

1. X ray equipment

X ray unit and model: _____ Room No.: _____

Image intensifier model: _____ Anti-scatter grid: □ Yes □ No

2. Dosimeter and phantom

Dosimeter model: _____ Serial No.: _____ Date of calibration: _____

Calibration coefficient[5] N_{K,Q_0}: _____ □ mGy/nC □ mGy/reading

Reference conditions: Half-value layer (mm Al): _____ Pressure P_0 (kPa): _____ Temperature T_0 (ºC): _____

Phantom construction:

Water Polymethyl methacrylate Phantom thickness (mm): _____

3. Exposure conditions for phantom

Focus to intensifier distance (mm): _____ Focus to chamber distance (mm): _____

Ambient conditions: Pressure P (kPa): _____ Temperature T (ºC): _____ k_{TP} = _____

[5] This is the calibration coefficient for the whole dosimeter, including the detector and the measurement assembly. For systems with separate calibration coefficients for the detector and measurement assembly, the overall calibration coefficient is calculated as a product of the two separate calibration coefficients.

$\dot{K}_e$ phantom:
Paediatric fluoro 2

4. Dosimeter reading and calculation of entrance surface air kerma rate

Selected option	Tube voltage (kV)	Tube current (mA)	Filtration (mm Al)	Manual or auto mode setting[a]	Field size (mm × mm)	Dosimeter readings, $\dot{M}_1, \dot{M}_2, \dot{M}_3$ (mGy/min)	Mean dosimeter reading, $\bar{\dot{M}}$ (mGy/min)	k_Q	Entrance surface air kerma rate, $\dot{K}_e$ [b] (mGy/min)

[a]Enter M (manual) or auto mode details.

[b]For a water phantom, use formula: $\dot{K}_e = \bar{\dot{M}} N_{K,Q_0} k_Q k_{TP}$, where $k_{TP} = \left(\frac{273.2+T}{273.2+T_0}\right)\left(\frac{P_0}{P}\right)$.

For a polymethyl methacrylate phantom, use formula: $\dot{K}_e = \bar{\dot{M}} N_{K,Q_0} k_Q k_{TP} \frac{B_w}{B_{PMMA}}$, where $k_{TP} = \left(\frac{273.2+T}{273.2+T_0}\right)\left(\frac{P_0}{P}\right)$; k_{TP} = 1 for systems with automatic temperature and pressure corrections, and for semiconductor dosimeters.

P_{KA} paediatric patient: Fluoro 1

Determination of air kerma area product

User: _____ Date: _____

Hospital or clinic name: _____

1. X ray equipment

X ray unit and model: _____ Room No.:_____

Image intensifier model: _____

Anti-scatter grid: □ Yes □ No Grid ratio:_____

2. Kerma area product meter

Kerma area product model: _____ Serial No.: ____ Calibration date: _____

Calibration coefficient N_{P_{KA},Q_0}: _____ □ Gy·cm^2/C □ Gy·cm^2/reading

Reference conditions: Beam quality: _____ Half-value layer (mm Al): _____

Pressure P_0 (kPa): _____ Temperature T_0 (°C): ____

3. Kerma area product reading and calculation of air kerma area product

Ambient conditions: Pressure P (kPa): ____ Temperature T (°C): ____ k_{TP} = ____

Examination details	Patient date of birth (dd-mm-yy)	Patient height (cm)	Patient weight (kg)	Tube voltage (kV)	Automatic brightness control setting	Kerma area product meter reading, M	k_Q	Air kerma area product, P_{KA}[a] (Gy·cm^2)	Fluoroscopy time (s)

$P_{KA} = MN_{P_{KA},Q_0} k_Q k_{TP}$, where $k_{TP} = \left(\frac{273.2+T}{273.2+T_0}\right)\left(\frac{P_0}{P}\right)$.

P_{KA} paediatric patient: Clinical fluoro sheet

Hospital/clinic: _____ Room: _____

Age group: 0–1 month / 1 month–1 year / >1–5 years / >5–10 years (circle one)

Examination type(s): micturating cystourethrogram / contrast swallow / contrast enema (circle one)

	Examination date (dd-mm-yy)	Patient date of birth (dd-mm-yy)	Sex (M/F)	Patient height (cm)	Patient weight (kg)	Tube voltage (kV)	Protocols used (automatic exposure control/automatic brightness control mode, etc.)	Kerma area product meter reading, *M*	Fluoroscopy time (s)
e.g.	01-03-09	05-12-01		134	32	80	'Low' dose rate, 0.2 mm Cu	89 mGy·cm^2	90
1									
2									
3									
4									
5									
6									
7									
8									
9									
10									
11									
12									
13									
14									
15									

Phantom: CT 1

Paediatric computed tomography dosimetry data sheets

Measurement of $C_{a,100}$, $C_{PMMA,100,c}$, $C_{PMMA,100,p}$ and calculation of C_W

User: _____ Date: _____

Hospital or clinic name: _____

1. X ray equipment

Computed tomography scanner model: _____ Room No.: _____

2. Ionization chamber, electrometer and phantom

Dosimeter model: _____ Serial No.: _____ Calibration date: _____

Calibration coefficient N_{P_{KL},Q_0}[6]: _____ □ mGy·cm/nC □ mGy·cm/reading

Reference conditions: Beam quality: _____ Half-value layer (mm Al): _____

Pressure P_0 (kPa): ___ Temperature T_0 (°C): ___

Manufacturer of phantom: _____ Serial No.: _____

Conditions during measurement:

Pressure (kPa): ___ Temperature (°C): ___ $k_{TP} = \left(\frac{273.2+T}{273.2+T_0}\right)\left(\frac{P_0}{P}\right) =$ _____

[6] This is the calibration coefficient for the whole dosimeter, including the detector and the measurement assembly. For systems with separate calibration coefficients for the detector and measurement assembly, the overall calibration coefficient is calculated as a product of the two separate calibration coefficients.

Phantom: CT 2

3. Computed tomography air kerma index $C_{a,100}$

Scanner settings (tube voltage, beam filter, etc.)	Nominal slice thickness, T (mm)	Number of slices (in 1 rot), N	Tube loading (1 rot), P_{It} (mAs)	Dosimeter readings, M_1, M_2, M_3	Mean dosimeter reading, $\bar{M}$	Calculated value of $C_{a,100}$ (mGy)	Calculated value of ${}_nC_{a,100}$ (mGy/mAs)

Note: The computed tomography air kerma index is calculated using[7]: $C_{a,100} = \frac{10}{N \cdot T} M N_{P_{KL},Q_0} k_Q k_{TP}$; ${}_nC_{a,100} = \frac{C_{a,100}}{P_{It}}$.

[7] The factor of ten in the formulas for $C_{a,100}$, $C_{PMMA,100,c}$ and $C_{PMMA,100,p}$ takes account of the use of a dosimeter calibration in milligray centimetres and a slice thickness specified in millimetres.

Phantom: CT 3

4. Computed tomography air kerma indices $C_{PMMA,100,c}$, $C_{PMMA,100,p}$ and C_W for the standard paediatric body phantom (16 cm adult head phantom)

Scanner settings (tube voltage, beam filter, etc.)	Nominal slice thickness, T (mm)	Number of slices (in 1 rot), N	Tube loading (1 rot), P_{It} (mAs)	Position	Dosimeter readings, M_1, M_2, M_3[a]	Mean $\bar{M}_c$ or $\bar{M}_p$	Calculated value of $C_{PMMA,100,c}$ (mGy)	Calculated value of $C_{PMMA,100,p}$ (mGy)	Calculated value of C_W (mGy)	Calculated value of ${}_nC_W$ (mGy/mAs)
				C						
				P1						
				P2						
				P3						
				P4						
				C						
				P1						
				P2						
				P3						
				P4						
				C						
				P1						
				P2						
				P3						
				P4						

Note: $\bar{M}_c$ is the mean of the three readings[a] in the central chamber bore C. $\bar{M}_p$ is the mean of the 12 readings in the peripheral bores (three readings[a] in each of the bores P1, P2, P3 and P4). The computed tomography air kerma indices are calculated using: $C_{PMMA,100,c} = \frac{10}{N \cdot T} \bar{M}_c N_{P_{KL},Q_0} k_Q k_{TP}$; $C_{PMMA,100,p} = \frac{10}{N \cdot T} \bar{M}_p N_{P_{KL},Q_0} k_Q k_{TP}$; $C_W = \frac{1}{3}(C_{PMMA,100,c} + 2C_{PMMA,100,p})$; and ${}_nC_W = \frac{C_W}{P_{It}}$.

[a]Three sets of readings required for initial reading; thereafter, only one set required.

Phantom: CT 4

Estimation of $P_{KL,CT}$ for computed tomography patient exposures

User: _____ Date: _____

Hospital or clinic name: _____

1. X ray equipment

Computed tomography scanner model: _____ ${}_nC_W$ taken from above table using appropriate kV and $N{\cdot}T$ values Room No.: _____

Examination details	Patient age	Patient height (cm)	Patient weight (kg)	Scanner settings (tube voltage, beam filter, etc.)	Tube loading P_{It} or $P_{It,eff}$ (circle that used) (mAs)	Acquisition slice setting $N{\cdot}T$ (e.g. 4 × 5 mm) (mm)	Couch movement per rotation, I (=$N{\cdot}T$ pitch) (mm)	Scan length, L (cm)	Total tube loading $P_{It,tot}$ for scan series (mAs)	Displayed value of C_{VOL} (mGy)	Displayed value of $P_{KL,CT}$ (mGy·cm)

Note: C_{VOL} is calculated using $C_{VOL} = {}_nC_W P_{It}(N{\cdot}T/I)$ or $C_{VOL} = {}_nC_W\ P_{It,eff}$ and $P_{KL,CT}$ is calculated using $P_{KL,CT} = {}_nC_W\, N{\cdot}T\, P_{It,tot}$ or $P_{KL,CT} = C_{VOL}\, L$.

Paediatric patient:
Clinical CT sheet

Hospital/clinic: _____ Scanner details: _____

Examination: head/thorax (for infection/tumours) / abdomen and pelvis (for tumours)

Paediatric age group: 0–1 month / 1 month–1 year / >1–5 years / >5–10 years (circle one)

	Patient details			Please fill in as many of these columns as possible that are displayed on the computed tomography scanner console. Total mAs recorded includes/excludes scanogram (delete as appropriate)												Scanner displayed values	
Examination date (dd-mm-yy)	Date of birth (dd-mm-yy)	Height (cm)	Weight (kg)	kV	mA	mAs per rotation	Effective mAs	Rotation time (s)	Total mAs	Total scan time (s)	Dose modulation used (Y/N)	Scan length (range) (mm)	Filter mode (head, body; small/ medium/ large)	Acquisition slice setting (e.g. 4 × 5 mm) (mm)	Pitch or increment	Total dose length product (mGy·cm)	Mean computed tomography dose index (mGy)

Phantom: CT 1
Patient: CT 6

Scanogram/topogram information for average protocol. If two projections are done routinely, please note both sets of factors.

Projection	kV	mA	Typical scan length (mm)	Slice width (mm)	Total mAs (just scanogram)
AP	120	50	240	2 × 1	240

No. of scanograms/topograms per examination: _____

GLOSSARY

automatic exposure control. A mode of operation of an X ray machine by which the tube loading is automatically controlled and terminated when a preset radiation exposure to the imaging receptor is reached. The tube potential may or may not be automatically controlled.

backscatter factor. The ratio of the entrance surface air kerma to the incident air kerma.

calibration. A set of operations that establish the relationship between values of quantities indicated by the instrument under reference conditions and the corresponding values realized by standards.

diagnostic reference level. A level used in medical imaging to indicate whether, in routine conditions, the dose to the patient or the amount of radiopharmaceuticals administered in a specified radiological procedure is unusually high or unusually low for that procedure.

dosimeter.

diagnostic. Equipment which uses ionization chambers and/or semiconductor detectors for the measurement of air kerma. Air kerma length and/or air kerma rate in the beam of an X ray machine used for diagnostic medical radiological examinations.

thermoluminescent. A detector made of a material that emits visible light when heated after irradiation. The amount of light emitted is dependent upon the radiation exposure.

effective dose. The sum over all of the organs and tissues of the body of the product of the equivalent dose H_T to the organ or tissue and a tissue weighting factor w_T for that organ or tissue. Thus: $E = \sum_T w_T H_T$

entrance surface air kerma. The air kerma at a point in a plane corresponding to the entrance surface of a specified object, e.g. a patient's breast or a standard phantom. The radiation incident on the object and the backscatter radiation are included.

entrance surface dose. Absorbed dose in air, including the contribution from backscatter. This is assessed at a point on the entrance surface of a specified object.

exposure parameters. The settings of X ray tube voltage (kV), tube current (mA), exposure time (s), source to image distance and use of a grid.

imaging device. A device used for imaging body anatomy. The X ray devices are assumed in this code of practice.

incident air kerma. The air kerma measured free-in-air (without backscatter) at a point in a plane corresponding to the entrance surface of a specified object. e.g. a patient's breast or a standard phantom.

influence quantity. Any external quantity that affects the result of the measurement (e.g. ambient temperature, pressure, humidity, radiation quality).

intrinsic error. The deviation of the measured value (i.e. the indicated value corrected to reference conditions) from the conventional true value of the measurand when the measuring instrument is subjected to a specified reference radiation under specified reference conditions.
***relative*.** Ratio of intrinsic error to the conventional true value.

ionization chamber. A detector filled with a suitable gas, in which an electric field (insufficient to induce gas multiplication) is provided for the collection of charges associated with the ions and the electrons produced in the sensitive volume of the detector by the ionizing radiation. Note: The ionization chamber includes the sensitive volume, the collecting and polarizing electrodes, the guard electrode (if any), the chamber wall, the parts of the insulator adjacent to the sensitive volume and any necessary buildup caps to ensure electron equilibrium.

kerma area product. Product of the area of a cross-section of a radiation beam and the average value of a kerma related quantity over that cross-section. This quantity is available clinically either by direct measurement with a kerma area product meter or by the calculator and display on a kerma area product indicator.

medical exposure. Exposure incurred by patients for the purposes of medical or dental diagnosis or treatment; by carers and comforters; and by volunteers subject to exposure as part of a programme of biomedical research.
Note: A patient is an individual who is a recipient of services of health care professionals and/or their agents that are directed at: (i) health promotion; (ii) prevention of illness and injury; (iii) monitoring health; (iv) maintaining

health; and (v) medical treatment of diseases, disorders and injuries in order to achieve a cure or, failing that, optimum comfort and function. Some asymptomatic individuals are included.

optical density. The degree of blackening of processed X ray or photographic film. It is numerically equal to the decadal logarithm of the ratio of light incident on the film to that transmitted through the film.

patient dose (exposure). A generic term used for a variety of quantities applied to a patient or group of patients. The quantities are related and include absorbed dose, incident air kerma and entrance surface air kerma.

phantom. Used to absorb and/or scatter radiation equivalently to a patient and, hence, to estimate radiation doses and test imaging systems without actually exposing a patient. It may be an anthropomorphic or a physical test object.

polymethylmethacrylate. A polymer plastic commercially available as Perspex or Lucite.

radiation effect.

***stochastic*.** A radiation effect generally occurring without a threshold level of dose, the probability of which is proportional to the dose and the severity of which is independent of the dose.

radiation quality. A measure of the penetrating power of an X ray beam, usually characterized by a statement of the tube potential and the half-value layer.

radiation tissue effect. A radiation effect for which generally a threshold level of dose exists above which the severity of the effect is greater for a higher dose.

reading. The uncorrected indication of the dosimeter corrected to atmospheric reference conditions.

tissue equivalent material. Material which absorbs and scatters a specified ionizing radiation to the same degree as a particular biological tissue.

tissue weighting factor (w_T). A dimensionless factor used to weight the equivalent dose in a tissue or organ.

tube current–exposure time product (mAs). The product of X ray tube current (mA) and the exposure time (s).

tube loading. The tube current–exposure time product that applies during a particular exposure.

uncertainty budget. The uncertainty budget is an organized way to present and mathematically process the effects on a measurement from a range of elements.

X ray tube. Vacuum tube designed to produce X rays by bombardment of the anode by a beam of electrons accelerated through a potential difference.

X ray tube voltage. Potential difference applied between the cathode and anode of an X ray tube. Note: The X ray tube voltage may vary as a function of time.

X ray unit. An assembly comprising a high voltage supply; an X ray tube with its protective housing and high voltage electrical connections.

CONTRIBUTORS TO DRAFTING AND REVIEW

Almén, A.	Sahlgrenska University Hospital, Sweden
Andreo, P.	Stockholm University and Karolinska University Hospital, Sweden
Benmakhlouf, H.	Stockholm University and Karolinska University Hospital, Sweden
Chapple, C.-L.	Newcastle upon Tyne Hospitals Foundation Trust, United Kingdom
Delis, H.	International Atomic Energy Agency
Fransson, A.	Karolinska University Hospital, Sweden
Homolka, P.	Medical University of Vienna, Austria
Järvinen, H.	Radiation and Nuclear Safety Authority, Finland
Le Heron, J.	International Atomic Energy Agency
Martin, C.	Gartnavel Royal Hospital, United Kingdom
McLean, I.D.	International Atomic Energy Agency
Sandborg, M.	Linköpings University, Sweden
Shrimpton, P.	Health Protection Agency, United Kingdom
Strauss, K.	University of Cincinnati, United States of America
Tapiovaara, M.	Radiation and Nuclear Safety Authority, Finland
Van der Putten, W.	International Atomic Energy Agency
Verdun, F.	Centre Hospitalier Universitaire Vaudois, Switzerland
Wambani, J.	Kenyatta National Hospital, Kenya

Consultants Meetings

Vienna, Austria: 10–12 February 2010, 13–15 December 2010, 29 March–1 April 2011

IAEA
International Atomic Energy Agency

No. 23

ORDERING LOCALLY

In the following countries, IAEA priced publications may be purchased from the sources listed below or from major local booksellers.

Orders for unpriced publications should be made directly to the IAEA. The contact details are given at the end of this list.

AUSTRALIA
DA Information Services
648 Whitehorse Road, Mitcham, VIC 3132, AUSTRALIA
Telephone: +61 3 9210 7777 • Fax: +61 3 9210 7788
Email: books@dadirect.com.au • Web site: http://www.dadirect.com.au

BELGIUM
Jean de Lannoy
Avenue du Roi 202, 1190 Brussels, BELGIUM
Telephone: +32 2 5384 308 • Fax: +32 2 5380 841
Email: jean.de.lannoy@euronet.be • Web site: http://www.jean-de-lannoy.be

CANADA
Renouf Publishing Co. Ltd.
5369 Canotek Road, Ottawa, ON K1J 9J3, CANADA
Telephone: +1 613 745 2665 • Fax: +1 643 745 7660
Email: order@renoufbooks.com • Web site: http://www.renoufbooks.com

Bernan Associates
4501 Forbes Blvd., Suite 200, Lanham, MD 20706-4391, USA
Telephone: +1 800 865 3457 • Fax: +1 800 865 3450
Email: orders@bernan.com • Web site: http://www.bernan.com

CZECH REPUBLIC
Suweco CZ, spol. S.r.o.
Klecakova 347, 180 21 Prague 9, CZECH REPUBLIC
Telephone: +420 242 459 202 • Fax: +420 242 459 203
Email: nakup@suweco.cz • Web site: http://www.suweco.cz

FINLAND
Akateeminen Kirjakauppa
PO Box 128 (Keskuskatu 1), 00101 Helsinki, FINLAND
Telephone: +358 9 121 41 • Fax: +358 9 121 4450
Email: akatilaus@akateeminen.com • Web site: http://www.akateeminen.com

FRANCE
Form-Edit
5 rue Janssen, PO Box 25, 75921 Paris CEDEX, FRANCE
Telephone: +33 1 42 01 49 49 • Fax: +33 1 42 01 90 90
Email: fabien.boucard@formedit.fr • Web site: http://www.formedit.fr

Lavoisier SAS
14 rue de Provigny, 94236 Cachan CEDEX, FRANCE
Telephone: +33 1 47 40 67 00 • Fax: +33 1 47 40 67 02
Email: livres@lavoisier.fr • Web site: http://www.lavoisier.fr

L'Appel du livre
99 rue de Charonne, 75011 Paris, FRANCE
Telephone: +33 1 43 07 50 80 • Fax: +33 1 43 07 50 80
Email: livres@appeldulivre.fr • Web site: http://www.appeldulivre.fr

GERMANY
Goethe Buchhandlung Teubig GmbH
Schweitzer Fachinformationen
Willstätterstrasse 15, 40549 Düsseldorf, GERMANY
Telephone: +49 (0) 211 49 8740 • Fax: +49 (0) 211 49 87428
Email: s.dehaan@schweitzer-online.de • Web site: http://www.goethebuch.de

HUNGARY
Librotade Ltd., Book Import
PF 126, 1656 Budapest, HUNGARY
Telephone: +36 1 257 7777 • Fax: +36 1 257 7472
Email: books@librotade.hu • Web site: http://www.librotade.hu

INDIA

Allied Publishers
1st Floor, Dubash House, 15, J.N. Heredi Marg, Ballard Estate, Mumbai 400001, INDIA
Telephone: +91 22 2261 7926/27 • Fax: +91 22 2261 7928
Email: alliedpl@vsnl.com • Web site: http://www.alliedpublishers.com

Bookwell
3/79 Nirankari, Delhi 110009, INDIA
Telephone: +91 11 2760 1283/4536
Email: bkwell@nde.vsnl.net.in • Web site: http://www.bookwellindia.com

ITALY

Libreria Scientifica "AEIOU"
Via Vincenzo Maria Coronelli 6, 20146 Milan, ITALY
Telephone: +39 02 48 95 45 52 • Fax: +39 02 48 95 45 48
Email: info@libreriaaeiou.eu • Web site: http://www.libreriaaeiou.eu

JAPAN

Maruzen Co., Ltd.
1-9-18 Kaigan, Minato-ku, Tokyo 105-0022, JAPAN
Telephone: +81 3 6367 6047 • Fax: +81 3 6367 6160
Email: journal@maruzen.co.jp • Web site: http://maruzen.co.jp

NETHERLANDS

Martinus Nijhoff International
Koraalrood 50, Postbus 1853, 2700 CZ Zoetermeer, NETHERLANDS
Telephone: +31 793 684 400 • Fax: +31 793 615 698
Email: info@nijhoff.nl • Web site: http://www.nijhoff.nl

Swets Information Services Ltd.
PO Box 26, 2300 AA Leiden
Dellaertweg 9b, 2316 WZ Leiden, NETHERLANDS
Telephone: +31 88 4679 387 • Fax: +31 88 4679 388
Email: tbeysens@nl.swets.com • Web site: http://www.swets.com

SLOVENIA

Cankarjeva Zalozba dd
Kopitarjeva 2, 1515 Ljubljana, SLOVENIA
Telephone: +386 1 432 31 44 • Fax: +386 1 230 14 35
Email: import.books@cankarjeva-z.si • Web site: http://www.mladinska.com/cankarjeva_zalozba

SPAIN

Diaz de Santos, S.A.
Librerias Bookshop • Departamento de pedidos
Calle Albasanz 2, esquina Hermanos Garcia Noblejas 21, 28037 Madrid, SPAIN
Telephone: +34 917 43 48 90 • Fax: +34 917 43 4023
Email: compras@diazdesantos.es • Web site: http://www.diazdesantos.es

UNITED KINGDOM

The Stationery Office Ltd. (TSO)
PO Box 29, Norwich, Norfolk, NR3 1PD, UNITED KINGDOM
Telephone: +44 870 600 5552
Email (orders): books.orders@tso.co.uk • (enquiries): book.enquiries@tso.co.uk • Web site: http://www.tso.co.uk

UNITED STATES OF AMERICA

Bernan Associates
4501 Forbes Blvd., Suite 200, Lanham, MD 20706-4391, USA
Telephone: +1 800 865 3457 • Fax: +1 800 865 3450
Email: orders@bernan.com • Web site: http://www.bernan.com

Renouf Publishing Co. Ltd.
812 Proctor Avenue, Ogdensburg, NY 13669, USA
Telephone: +1 888 551 7470 • Fax: +1 888 551 7471
Email: orders@renoufbooks.com • Web site: http://www.renoufbooks.com

United Nations
300 East 42nd Street, IN-919J, New York, NY 1001, USA
Telephone: +1 212 963 8302 • Fax: 1 212 963 3489
Email: publications@un.org • Web site: http://www.unp.un.org

Orders for both priced and unpriced publications may be addressed directly to:

IAEA Publishing Section, Marketing and Sales Unit, International Atomic Energy Agency
Vienna International Centre, PO Box 100, 1400 Vienna, Austria
Telephone: +43 1 2600 22529 or 22488 • Fax: +43 1 2600 29302
Email: sales.publications@iaea.org • Web site: http://www.iaea.org/books

13-38901

IMPLEMENTATION OF THE INTERNATIONAL CODE OF PRACTICE ON DOSIMETRY IN DIAGNOSTIC RADIOLOGY (TRS 457): REVIEW OF TEST RESULTS
IAEA Human Health Reports No. 4
STI/PUB/1498 (129 pp.; 2011)
ISBN 978–92–0–114010–4 Price: €58.00

DOSIMETRY IN DIAGNOSTIC RADIOLOGY: AN INTERNATIONAL CODE OF PRACTICE
Technical Reports Series No. 457
STI/DOC/010/457 (359 pp.; 2007)
ISBN 92–0–115406–2 Price: €75.00

RADIATION PROTECTION IN PAEDIATRIC RADIOLOGY
Safety Reports Series No. 71
STI/PUB/1543 (111 pp.; 2013)
ISBN 978–92–0–125710–9 Price: €38.00

Concern about the radiation dose to children from diagnostic radiology examinations stems from the observation that children can receive doses in excess of those delivered to adults, in part due to the digital nature of image receptors that may give no warning to the operator of the dose to the patient. This concern should be extended to the broad range of paediatric diagnostic radiological procedures responsible for radiation dose in children, especially as factors including increased radiosensitivity and the longer life expectancy of children increase the associated radiation risk. Dosimetry for paediatric patients undergoing diagnostic radiology requires special consideration in addition to the general dosimetric methodologies used for adult patients. This publication informs health professionals about standardized methodologies to determine paediatric dose for all major modalities, such as general radiography, fluoroscopy and computed tomography.

IAEA HUMAN HEALTH SERIES

INTERNATIONAL ATOMIC ENERGY AGENCY
VIENNA
ISBN 978–92–0–141910–1
ISSN 2075–3772